# AN EVALUATION OF THE LATE QUATERNARY DISPLACEMENTS AND SEISMIC HAZARD ASSOCIATED WITH THE HOPE AND KAKAPO FAULTS, AMURI DISTRICT, NORTH CANTERBURY.

---

A thesis

submitted in partial fulfilment

of the requirements for the Degree

of

Master of Science in Engineering Geology

in the

University of Canterbury

by

H.A. Cowan

---

University of Canterbury

1989

*"For some time before the shock the inmates of Dyers accommodation house were aroused by loud rumbling sounds as of thunder and at the first shake they rushed out. The scene was almost indescribable. The house was rattling and shaking as if built of reeds, and every moment it seemed as if it would collapse utterly. The mountains appeared to be bending to and fro, nodding to each other; the whole earth was in movement whilst stones and rocks, some of immense size, were rushing down the mountain sides, striking each other and leaving long trains of fire. All the phenomena we have described point to some great convulsion of nature about the centre of this island, it being noticeable that the shock was much slighter the further north it travelled."*

Letter from W.T. Burley to The Editor, Canterbury Times, September 14th, 1888. Dyers Accommodation House was located at the western entrance to Otira Gorge.

FRONTISPIECE: Oblique view looking east along the trace of the Hope Fault at Glynn Wye Station, Hope River at left. Note the right-lateral offset on the scrub covered western face of the Late Pleistocene, Glynn Wye Advance terminal moraine and the broad zone of normal faulting forming Poplars Graben to the north and south of the main fault trace.

# ABSTRACT

The Amuri Earthquake of September 1, 1888 (magnitude M = 6.5 to 6.8) occurred on the Hope River Segment of the Hope Fault west of Hanmer Plains. The earthquake was felt strongly in North Canterbury and North Westland and caused considerable property damage and landsliding in the Lower Hope Valley. However, damage reports and the spatial distribution of felt intensities emphasize extreme variations in seismic effects over short distances, probably due to topographic focusing and local ground conditions.

Significant variations in lateral fault displacement occurred at secondary fault segment boundaries (side-steps and bends in the fault trace) during the 1888 earthquake. This historical spatial variation in lateral slip is matched by the Late Quaternary geomorphic distribution of slip on the Hope River Segment of the Hope Fault. Trenching studies at two sites on the Hope Fault have also identified evidence for five pre-historic earthquakes of similar magnitude to the 1888 earthquake and an average recurrence interval of 134 ±27 years between events.

Magnitude estimates for the 1888 earthquake are combined with a strong ground motion attenuation expression to provide an estimate of potential ground accelerations in Amuri District during future earthquakes on the Hope River Segment of the Hope Fault. The predicted acceleration response on bedrock sites within 20 km of the epicentral region is between 0.23 g and 0.34 g.

The close match between the historic, inferred pre-historic and geomorphic distribution of lateral slip indicates that secondary fault segmentation exerts a strong structural control on rupture

propagation and the expression of fault displacement at the surface. In basement rocks at depth the spatial variations in slip are inferred to be distributed within zones of pervasive cataclastic shear, on either side of the fault segment boundaries. The large variations in surface displacement across fault segment boundaries means that one must know the geometry of the fault in order to evaluate slip-rates calculated from individual locations.

The average Late Quaternary slip-rate on the Hope Fault at Glynn Wye Station is between 15.5 mm/yr and 18.25 mm/yr and the rate on the subsidiary Kakapo Fault is between 5.0 mm/yr and 7.5 mm/yr. These rates have been determined from sites which are relatively free of structural complication.

TABLE OF CONTENTS

LIST OF TABLES

LIST OF FIGURES

## LIST OF STEREOPAIRS

## LIST OF SHEETS IN MAP POCKET

MAP 1 Faulting Related Landforms and Late Quaternary Structure of the Lower Hope Valley.

MAP 2 Late Quaternary Geomorphology of the Lower Hope Valley.

MAP 3 Detailed Geomorphology of the Late Quaternary Offsets, Kakapo Fault: Dismal Valley.

MAP 4 Detailed Geomorphology and Structure of the Glynn Wye Moraine Complex.

TRENCH LOG No. 1 Hope Fault 300 m west of Manuka Creek, State Highway 7.

TRENCH LOG No. 2 Hope Fault in Raupo Swamp 300 m east of Horseshoe Lake, State Highway 7.

LIST OF APPENDICES

# ACKNOWLEDGEMENTS

This work was funded by a University of Canterbury research grant and benefited greatly from the advice, assistance and thoughtful encouragement of numerous people in the broad inter-disciplinary field of Late Quaternary studies.

Firstly, I would like to thank my advisors, Dr Jarg Pettinga, Mrs Jocelyn Campbell and Dr John Berrill for their consistent interest and involvement in the project throughout the year.

Dr Neville Moar and Dr Matt McGlone provided invaluable analyses of pollen spectra from Late Pleistocene and Late Holocene sites respectively, and Mr R. Patel identified wood samples at very short notice.

Dr Phil Tonkin provided encouragement at a critical stage in the study and his advice on soil genesis and radiocarbon dating is greatly appreciated. I would also like to thank Mr Trevor Chinn, Dr Kelvin Berryman, Dr Nigel Newman and Prof. Harold Wellman for useful and interesting discussions. Dr Mary Savina expressed great enthusiasm for this study and her advice in the field and during the editing process was a tremendous help.

I am grateful to Mr John Shearer of "The Poplars", and Mr Graham Hewitt of "Glenhope" for access to their properties and their helpful advice.

I would especially like to thank Mr Cliff Cox of "Glynn Wye" for providing accommodation throughout the study and for excellent logistic support; a UH07 excavator and dewatering equipment during the trenching study, and at other times a horse, "Kahlua" who, together with Eva (the doberman), made my stay at Glynn Wye even more enjoyable.

Many people joined me in the field at various times and their company was always a pleasure. Special thanks go to Dr Jarg Pettinga, Mrs Joc Campbell, Mr Chris Thornley, Mr Jim McLean, Mr Paul Horrey and Mr David Barrell for assistance with trench logging, surveying and other fieldwork under difficult and occasionally unpleasant conditions.

The late Mr Archie Sutherland did the trench excavation work and Mrs Mary Sutherland fed hungry mouths. Their involvement assisted greatly with the smooth running of the site investigations.

I am grateful to Earth Deformation Section, DSIR for provision of the low altitude, high resolution aerial photographs. The N.Z. Seismological Observatory, Wellington, kindly provided an historical seismicity catalogue. Radiocarbon Dating was performed by the Institute of Nuclear Sciences, Lower Hutt and I would like to thank Nicola Redvers-Higgins for her helpful comments concerning the interpretation of corrected age radiocarbon dates.

Lee Leonard did a superb job in draughting all of the maps and figures at very short notice and Mr Albert Downing assisted greatly with the photographic reproduction. Sincere thanks also to Tracy Robinson for assistance with word processing and printing.

My special thanks to Jeanine Keller for consistent help and encouragement at all stages during this study.

Finally, I would like to express gratitude to previous workers in the Lower Hope Valley all of whom have contributed to a growing understanding of the geomorphic history of the area. Special credit must go to Mr Alexander McKay, Professor F.W. Hutton, Mr Edgar Jones and several newspaper journalists who documented carefully the effects of the 1888 Amuri Earthquake.

# CHAPTER 1 INTRODUCTION

## 1.1 Fundamental aims of this study

On September 1, 1888 a large earthquake caused ground rupture, landsliding and severe damage to buildings in the Lower Hope Valley of the Amuri District, North Canterbury. It was felt strongly in North Westland and elsewhere in North Canterbury including Christchurch, where part of the cathedral spire broke off.

The earthquake occurred on the Hope Fault, a member of the Marlborough Transform System, which itself comprises part of the Australian-Pacific plate boundary. This event remains one of the most strongly felt earthquakes within the North Canterbury Region since post-European settlement.

A greater understanding of the past rate of activity on the segment of the Hope Fault which ruptured in 1888 will be valuable in evaluating potential future seismic hazard within the region.

The aims of this study are firstly, to gain an improved understanding of past rates of movement on the segment of the Hope Fault ruptured during the 1888 earthquake; and secondly, to obtain data which may prove useful in assessing the future hazard potential of the Hope Fault in this area as well as a better understanding of the geometric and kinematic character of this segment.

## 1.2 Description of the study area setting

### 1.2.1 Regional Tectonic Setting and Geological Structure

New Zealand is located across the active Australian-Pacific plate boundary. Relative oblique convergent movement of 40 mm/yr to 60 mm/yr between these plates is accommodated within a zone of deformation ranging from 70 to 350 km wide and characterised by: (i) shallow to intermediate depth earthquakes (12-60 km); (ii) volcanic activity; and (iii) active faulting and folding (e.g. Walcott 1978; 1984; Hatherton 1980).

The configuration of the present-day plate boundary zone derives from an accelerating change in the direction of motion between the plates due to a south-westward shift in the position of the pole of plate rotation, from about 10 million years ago (Walcott 1984). The direction of motion changed from strike-slip parallel to the plate boundary in Mid Cenozoic time to oblique-slip during the Upper Cenozoic with a compressional component that has increased to a rate of between 10-20 mm/yr today (Walcott 1979). Shortening in the continental crust across the boundary along the Alpine Fault has resulted in uplift forming the Southern Alps, and the Marlborough mountains. A 10° to 50° clockwise rotation of parts of eastern North Island and north-eastern Marlborough may also have occurred (Walcott et.al. 1981).

The major tectonic elements of the plate boundary include the subduction zone that extends southward from the Tonga-Kermadec Trench to the Hikurangi Trench (off the east coast of the North Island), and a transform zone that extends northward from the mid-oceanic rise around the Antarctic Plate boundary to the Alpine Fault (on the west side of the Southern Alps) (Walcott 1984) (Figure 1.1). Oblique subduction of the

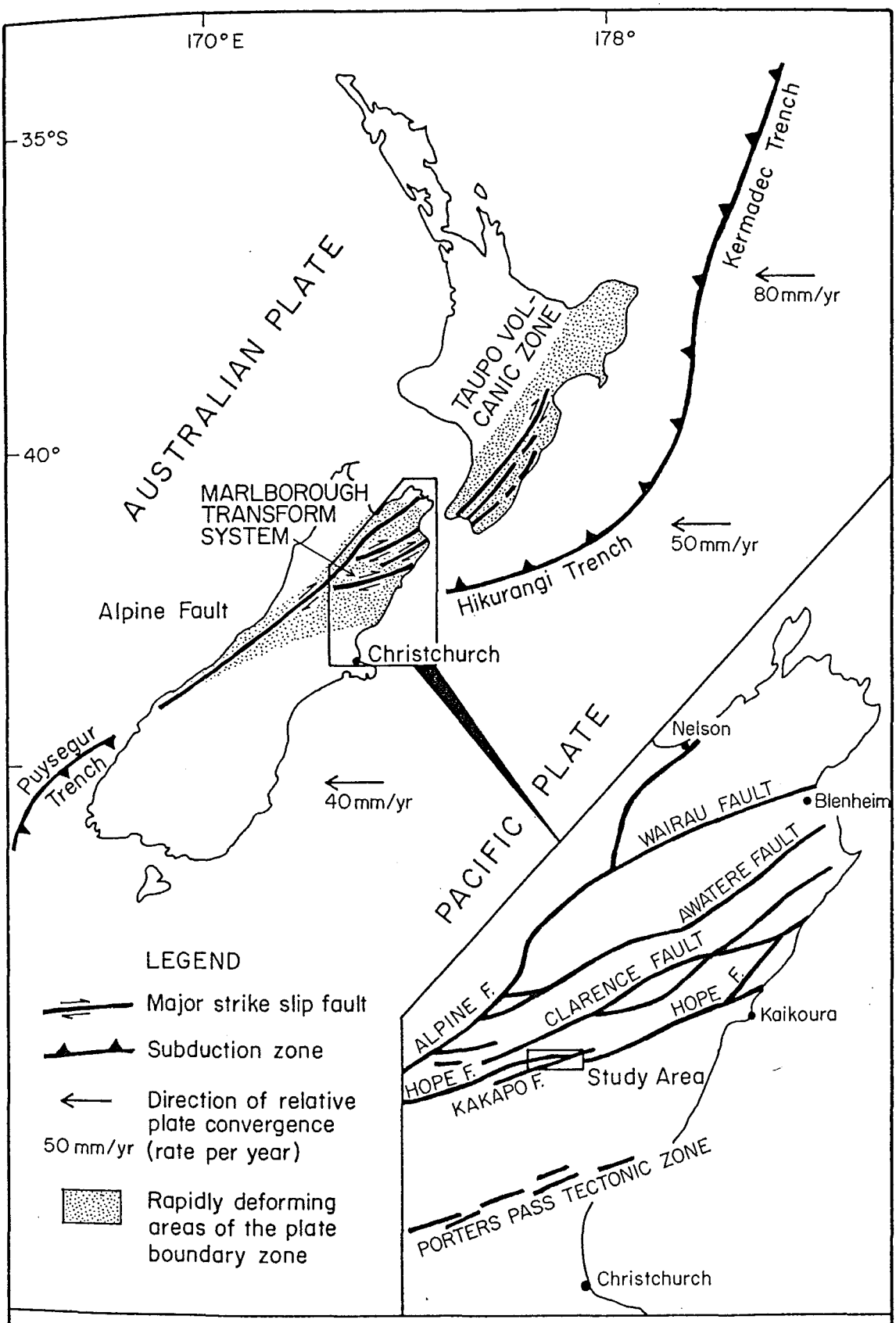


Figure 1·1 New Zealand's Plate Tectonic Setting and Location of Study Area (adapted from Walcott, 1984)

oceanic crustal Australian Plate occurs beneath the continental rocks of Fiordland, forming the Puysegur Trench south-west of Fiordland (Walcott 1984).

A complex transition between plate boundary subduction and the Marlborough Transform System occurs in central New Zealand. A broadly SW-NE trending transpressional* system of faults splays from the Alpine Fault to accommodate the oblique relative motion and shear between the plates (Walcott 1984) (Figure 1.1). The Hope and subsidiary Kakapo Faults, discussed in this study, are elements of this transform system and have been considered to represent the southern boundary of the rapidly deforming transpressional plate boundary zone (e.g Freund 1971).

South-east of the Hope Fault Late Cenozoic deformation is more diffuse and structures are less persistent, but a highly active zone of inter-connected wrench faults and actively growing sigmoidal anticlines in Cenozoic cover occurs between Porter's Pass and Waipara area bounding the northern Canterbury Plains 30 km north-west of Christchurch. This fault zone is informally referred to as the Porter's Pass Tectonic Zone (Campbell & Yousif in press) and is considered to represent the juvenile stages of a future through-going strike-slip fault, reflecting southward propagation of the Marlborough Transform System.

*Harland (1971) terms a combination of transcurrence and extension transtension, and a combination of transcurrence and compression transpression.

### 1.2.2 Regional Geomorphology and The Hope Fault Zone

The landscape of north Canterbury and southern Marlborough is dominated by fault bounded mountain ranges of Torlesse Supergroup basement, quartzofeldspathic greywacke and argillite; and basins containing extensive Quaternary fluvial and glacio-fluvial deposits and in the south, remnants of a once continuous Cenozoic cover (Suggate et.al. 1978).

Over much of its 240 km length the Hope Fault occupies fault-controlled valleys and forms a prominent lineament in the landscape, which extends with a strike of 075°, from the Alpine Fault in the Taramakau River area to the east coast of the South Island at Hapuku north of Kaikoura (Figure 1.2).

The Hope Fault is expressed as a complex, narrow, and sinuous surface trace comprising a succession of segments which step over from one to the next in a consistent right-lateral sense.

The main fault branches at both ends into numerous splays through which the lateral movement is dissipated (Freund 1971). The strike-slip movement along the segmented fault zone has resulted in the development of pull-apart basins, the largest and most complex of which is the 11 km long Hanmer Basin (Clayton 1966; Freund 1971). The Hope Fault consists of two principal segments: (i) a segment extending from Hanmer Basin eastward to Kaikoura; and (ii) the fault west of Hanmer Basin, which ruptured during the 1888 earthquake and which is referred to in this study as the Hope River Segment of the Hope Fault. The large scale fault segments are themselves segmented on a smaller scale. These secondary segments and the structure of associated segment boundaries are discussed later in this study.

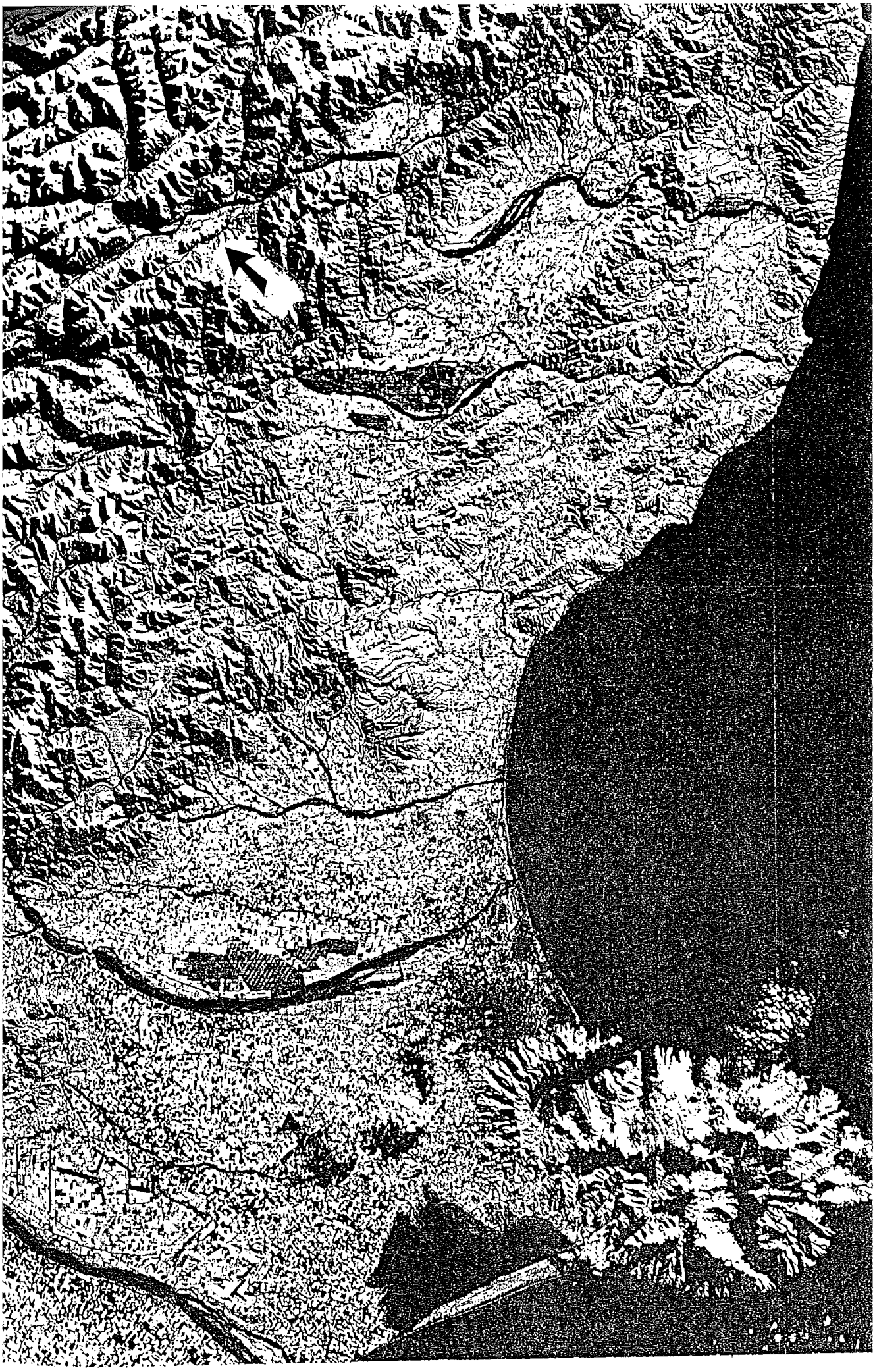

Figure 1.2 Landsat photograph of North Canterbury
Study area indicated by the arrow. From Ellis et.al.(1978)

## 1.3 Criteria for selecting this study

1. At the time of the earthquake in 1888, the Lower Hope Valley was being settled by pastoralists. A number of homesteads in the area were seriously damaged by the earthquake, which received wide media coverage as well as attracting the interest of early New Zealand geologists.

   For this reason the earthquake was well documented, but the information is scattered among various scientific articles, newspaper reports, and biographical accounts.

   Recently, a number of authors have referred to, or discussed the 1888 earthquake in the context of magnitude, length of surface rupture and maximum felt intensities, but there is little consensus. For example current estimates of magnitude range from 6.5-6.75 (Dibble et.al. 1980) to 7.3 (Smith & Berryman 1986); and similarly for rupture length where the following estimates have been made: 13km-43km (Wood 1984), 50km (Berryman 1984), ~150km (Knuepfer 1984).

   The scattered records of this important historic event are an essential and valuable source of information about the likely magnitude, length of surface rupture, the spatial distribution of various seismic effects and the attenuation of strong ground motion for this and future events.

2. The 1888 earthquake was most severely felt in the Lower Hope Valley and was accompanied by right-lateral displacements of up to 2.6 metres on the Hope Fault surface trace at Glynn Wye Station. At Glynn Wye Station evidence for Late Quaternary lateral and vertical displacements is preserved in the form of offsets on glacial deposits

and river degradation terraces, making this locality particularly useful for the analysis of past activity on the Hope Fault.

Since the first of these features was recognised (35 years ago), many geologists working in the area have recorded additional sites of measureable offsets and re-interpreted earlier ones. There has been very little consensus on the size and age of important Late Pleistocene (>10 000 years before present) and Holocene (<10 000 years before present) offsets and the rates of displacement which they imply. Most geologists have studied the Glynn Wye Station locality either only at a reconnaissance level, or as a small component of larger studies of the entire Hope Fault Zone, or even within the entire Marlborough Transform System (Freund 1971; Knuepfer 1984).

A detailed study of the Late Quaternary faulting at Glynn Wye is now warranted, in order to clarify the size, style and relative rates of previous displacements in the area which experienced surface rupture during the 1888 earthquake and in previous events.

## 1.4 Specific study objectives

1. To produce appropriate engineering geological maps and cross-sections at various scales, of the Hope and Kakapo Faults in the Lower Hope Valley. The aim of these maps is to establish faulting and ground deformation styles and the relationships between faulting and the Late Quaternary deposits.

2. To conduct detailed exposure logging and sampling of backhoe trenches excavated across, or adjacent to the Hope Fault at selected

localities. Particular emphasis was placed on obtaining organic material suitable for absolute radiocarbon dating to clarify fault displacement history.

3. To provide a comprehensive historical review of the 1888 earthquake, involving collation and summarizing of information from scientific articles, contemporary press reports, and biographical sources. This review places particular emphasis on on clarifying the epicenter, magnitude, surface rupture length, and attenuation of strong ground motion with increasing epicentral distance.

4. To conduct a seismotectonic hazard evaluation of the Hope and Kakapo Faults in the Lower Hope Valley, with a view to developing an engineering geological model of characteristic earthquake events (rupture length, isoseismal intensity patterns, and local magnitude), and thereby predicting likely risks to the Amuri District, North Canterbury.

## 1.5 Description of the study area

This thesis is an account of reconnaisance and detailed fieldwork carried out on the Hope and Kakapo Faults. Fieldwork was undertaken on 83 days throughout 1988. The study area is centred on Glynn Wye Station, a large (over 26 000 hectares) high-country farm situated in the Lower Hope Valley of the Amuri District, North Canterbury, 35 kilometres west of Hanmer Springs. Fieldwork was also conducted on Poplars Station and Glenhope Station between the Hope-Boyle River junction to the west and Manuka Creek to the east.

Access is from State Highway 7, but permission for entry must be gained from the owners of respective properties. All of the detailed study sites are well exposed and accessible by two-wheeled drive vehicles followed by short walks. Gumboots are advisable!

## 1.6 Thesis organisation

Chapter 2 provides an introduction to neotectonic studies and an outline of previous work on the Hope and Kakapo Faults in the Lower Hope Valley. This is followed by a brief description of the methodology and approach to the analysis of fault displacement history adopted in this study. Chapter 3 describes the geology and glacial geomorphology of the Lower Hope Valley and sets out the field relationships between Late Pleistocene glacial deposits and associated landforms. The Late Quaternary stratigraphy is reviewed in the context of age estimates for features offset by faulting, and the tectonic landforms associated with Late Quaternary displacements are introduced.

In Chapter 4 a detailed historical review of the 1888 Amuri earthquake is compiled from a comprehensive search of scientific articles, press reports and biographical sources. The regional felt intensities and inferred earthquake magnitude are revised and the surface rupture length, although remaining equivocal, is estimated on a "most probable" basis using the attenuation of high felt intensities and an interpretation of the earthquake rupture mechanics.

Chapter 5 provides firstly, a description and analysis of the Late Quaternary displacements on the Hope and Kakapo Faults. Secondly, the results of detailed site investigation at one locality on the Hope Fault (where it has been possible to recognise and tentatively date evidence

for four pre-historic - i.e. pre-1888 earthquakes) are provided. The displacement measurements from offset Late Quaternary surfaces are then combined with the results of this pre-historic record of faulting and the observations of displacement during the 1888 earthquake, to demonstrate repeated Late Quaternary displacement on the Hope River Segment of the Hope Fault accompanying earthquakes of similar magnitude, generating similar point-specific displacement.

Chapter 6 provides an introduction to the concepts and assumptions underlying seismic hazard analysis, and includes a review of existing estimates of seismic hazard within North Canterbury based on regional (historic instrumental) seismicity.

The new data from Chapters 4 and 5 of relevance to seismic hazard evaluation, are combined with an attenuation expression to infer the spatial distribution of strong motion in future moderate to large magnitude earthquakes on the Hope Fault.

Lastly, Chapter 7 lists in point form the major conclusions reached in this study and recommends areas of future study.

# CHAPTER 2 BACKGROUND AND METHODS

## 2.1 An introduction to neotectonic studies

The field of study known as "neotectonics" is the study of Late Cenozoic deformation; crustal movements which are recent enough to permit detailed analysis and an assessment of rates of change (e.g. Vita-Finzi 1986). The techniques of geology, geophysics and geodesy combined with historical records, can all help evaluate past, present and continuing trends in tectonic activity. Each discipline provides a different time-frame of reference for tectonic processes. Respective techniques may be integrated to obtain a better understanding of tectonic processes currently operating, but it is important to note that in any attempt to predict future crustal movements, it is imperative that the period of time analysed must be long enough to adequately sample a particular series of events, or changes in rates of events (Vita-Finzi 1986). The time ranges covered by the major sources of evidence relating to recent crustal movements are shown in Figure 2.1.

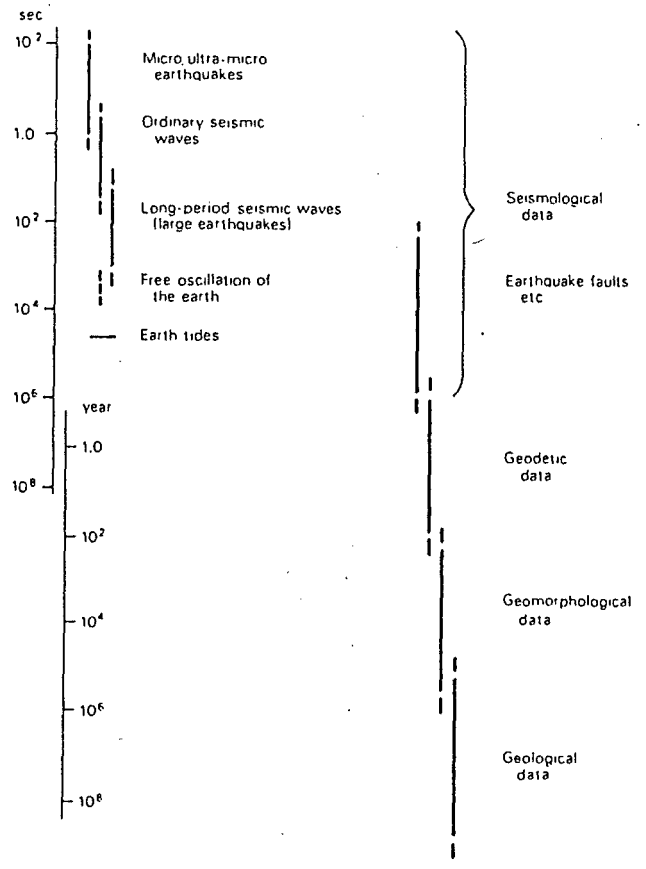


Figure 2.1 Sources of information on crustal movements. From Vita-Finzi (1986) after Kasahara (1981)

## 2.2 Sources of evidence of tectonic activity

### 2.2.1 Eye-Witness Reports:

Eye-witness reports, and the physical evidence of historical events have traditionally conditioned the public perception of "risk" . Apart from providing an indication of presently seismically active regions, such information may greatly aid the interpretation of prehistoric events. The description of processes that accompany deformation, (such as liquefaction, landsliding, or the size and distribution of displacements) can be used as clues to prehistoric events, which are often imperfectly recorded in the field evidence.

A problem with eye-witness accounts is that they are often the subject of colourful or fearful exaggeration, and they are rarely scientific. They may also be misinterpreted by others.

### 2.2.2 Historical Seismicity

Instrumentally recorded seismicity provides a valuable means of assessing the current frequency and distribution of seismic activity and provides insight into the nature of tectonic processes occurring within the seismic zones. Over a period of time, seismically hazardous zones may be identified on the basis of consistent activity, or by virtue of uncharacteristic inactivity in a region that is accumulating elastic energy (Kasahara 1981). This information may be used to develop a seismicity model for a region or regions, which describes the relative frequency of different magnitude earthquakes. The seismicity model may in turn be combined with an attenuation expression (which describes the

decay of strong ground motion with increasing epicentral distance) to evaluate the seismic hazard within a region for a time period of interest.

The limitations of historical seismicity become apparent when the time period of interest is greater than the historical record. In New Zealand this is only 140 years in most places. Without a paleoseismic history of regional activity to compare with the historical record, trends indicated by historical records may be misleading.

### 2.2.3 Geodetic Monitoring

Technological developments over the past 50 years, in the fields of geodesy and geophysics have enabled increasingly precise monitoring of crustal movements.

On a grand scale the record of ocean floor magnetic anomalies preserved by the cooling of oceanic crust during sea-floor spreading, permits assessments to be made of both the magnitude and direction of relative plate movement. Along a complex convergent plate boundary (e.g., the Australian-Pacific plate boundary through New Zealand) where deformation is diffuse across a wide zone, strain may be distributed in different ways and among different structural elements. First order geodetic surveying at successive intervals helps establish the overall rates at which strain is accumulating, by focusing attention on the total change over a specified time period (for a New Zealand application see Walcott 1979; Bibby 1981).

Precise monitoring of specific fault zones (near-field geodesy) may be carried out by repeat surveying of small-aperature trilateration arrays and repeat levelling of closely spaced permanent benchmarks. Such

methods provide long-term monitoring of horizontal and vertical movements respectively, and identify critical localities for further investigation (Sylvester 1986). Site specific studies may involve the use of instruments such as strain-meters and tilt-meters installed across faults or folds to obtain a continuous record of change. Measurements of current movement help to establish the reliability of long-term average rates, and identify any changes in the type of deformation occurring. Geodetic techniques have their shortcomings not least of which is the long time period required for results to be obtained (typically 30-100 years), and the inability to discriminate elastic strain (released in earthquakes) and anelastic strain (distributed aseismically).

### 2.2.4 Geological Evidence

The geological record encompasses the longest time range for evaluating crustal movements, but the resolution of the record diminishes with time due to the frequency and intensity of tectonic activity, and the rate of landscape changes. Landscape changes are also greatly influenced by climate; rates of landscape modification are very rapid in New Zealand, due to the humid temperate climate and strong orographic effects (e.g. Bull & Knuepfer 1987).

In the recent geological past, tectonic activity, and in particular large magnitude earthquakes (M >6.5), have been frequent enough to permit a wide range of related features to be preserved. Almost all shallow foci moderate to large magnitude earthquakes, are accompanied by ground rupture on surface fault traces and the effects of rupture will often display a "signature" that is characteristic of the style of the earthquake event.

For example, the effects of strike-slip faulting (of which the Hope Fault is an excellent example) will be recorded as linear valleys or mountain escarpments, offset streams, shutter ridges, sag ponds and pressure ridges (Figure 2.2).

Where a fault traverses features of different age (such as glacial moraines and river terraces), successive movements over time will be recorded as cumulative displacements on progressively older surfaces. The total tectonic movement of the fault over a measurable period of time can thus be determined, and expressed as an average known as the "slip-rate". Some of the earliest pioneering work in this field was carried out by Lensen (1964; 1968) in New Zealand on the Wairau Fault.

The slip-rate (expressed in mm/yr) is used as a basis for comparing the relative activity of faults, and reflects the average rate of strain energy release on a fault (Schwartz & Coppersmith 1986). This may be compared with rates of strain accumulation predicted from the oceanic record of sea-floor spreading, used in conjunction with geophysical and geodetic studies, to evaluate a stress-strain budget and the mechanisms of strain release (e.g. Bibby 1981).

Where a chronology of faulted landforms such as offset streams, alluvial fans, river terraces or uplifted marine benches can be established, rates of tectonic processes can be calculated from geomorphic evaluation and used to derive recurrence intervals for damaging earthquakes and ultimately long-term earthquake prediction (Bull 1984; Stevens 1974).

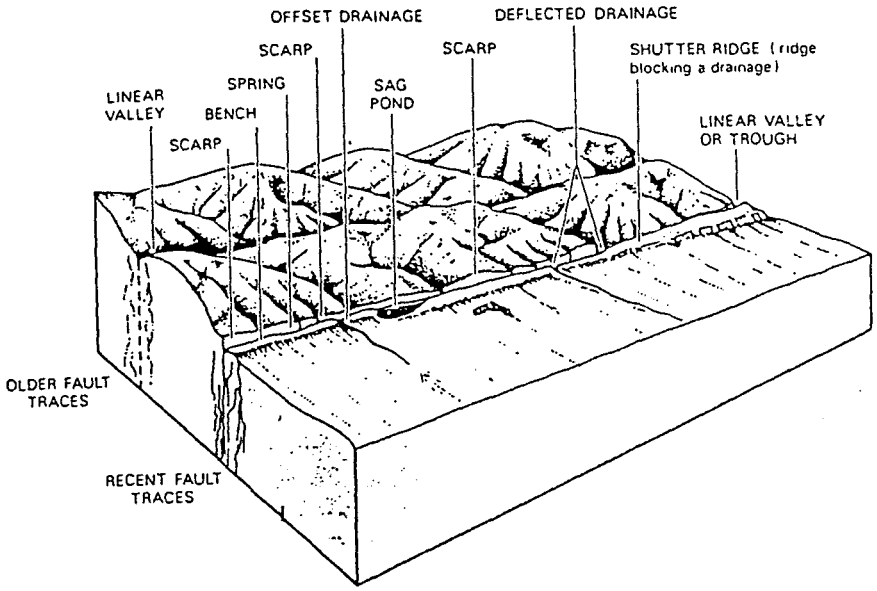


Figure 2.2 Assemblage of landforms associated with active strike-slip faulting. From Keller (1986)

Late Quaternary faulted landforms may contain organic materials such as wood or fossil shells, that enable absolute dates and minimum recurrence intervals to be calculated by means of $^{14}C$ radiometric methods. Inland areas (especially in mountainous terrain) dominated by colluvial/alluvial processes may lack organic materials in critical locations, and age estimations must then be made using relative dating or correlation techniques. Methods of relative dating include the use of soil development indices, rock weathering, and landform modification. Such techniques are more widely applicable than methods of absolute dating, but are imprecise and require adequate calibration (Pierce 1986).

## 2.5 Review of previous work on the Hope fault

Following the Amuri Earthquake of September 1, 1888 considerable attention was focused on the "remarkable line of depression" running from the Taramakau River in Westland, to the east coast at Kaikoura (McKay 1890). McKay appreciated that the 1888 earthquake had occurred along a pre-existing fracture; subsequently several previous earthquakes felt strongly in North Canterbury were reinterpreted and assigned epicenters in the Lake Sumner area (Hogben 1890; 1891).

No further original work on the Hope Fault was carried out until Cotton (1947) described the geomorphology of the Hope Fault and surrounding mountains, identified the Hanmer Plain as a basin of tectonic origin, and suggested the existence of two faults; a predominantly dip-slip fault east of Hanmer, retaining the name Kaikoura Fault (given by McKay (1902)), and a dominantly strike-slip fault west of Hanmer, to which he gave the name Hope Fault. His emphasis, however, was very much on vertical tectonics.

It was not until air-photo coverage became widely available, and Wellman (1953) described offsets of tens to hundreds of metres across Pleistocene glacial deposits and Holocene river terraces, that the predominantly strike-slip nature of both faults became apparent. The name Hope Fault has since been adopted, to describe the entire 240 km fault zone.

During the 1960's, mapping for the New Zealand Geological Survey's 1:250 000 series identified many additional features of the Hope Fault, the active Kakapo and Hanmer Faults, and the splaying of the Hope Fault at both ends (Lensen 1963; Gregg 1964; Warren 1967).

Suggate (1965), and Clayton (1965, 1968), described the Late

Pleistocene glacial history of the Hope River area, based primarily on air-photo interpretation of landforms, deposits and regional correlation with glacial sequences in the Waimakariri Valley and North Westland.

Clayton (1966) also drew attention to the development of "tectonic depressions" and compressional buckling along the Hope Fault, which he ascribed to the effect of strike-slip faulting between en-echelon fault strands. Clayton recognised that this style of secondary structure was developed at a range of scale lengths, of which the most spectacular is the Hanmer Basin.

Freund (1971), working on the gross geometry and structure of the fault zone, inferred a total 19km offset across the Hope Fault and 1.6km across the Kakapo Fault. This was based on the distribution of contrasting lithologies in the Torlesse basement rocks. He described semi-quantitatively the accommodation of gross offset towards the Alpine Fault, in terms of partitioning among numerous splays, and proposed a series of models to account for rhomboid horst and graben development along the fault zone. In recent years, the Hope River-Hanmer section of the fault has featured prominently in international studies of pull-apart basin development (e.g. Aydin & Nur 1982; Mann et.al. 1983), but these represent only a reinterpretation of Freund's and Clayton's work and, with the exception of a very recent gravity survey of the Hanmer Basin (Anderson 1987), no new data have been obtained.

As part of a much larger study of the Marlborough Transform System, Knuepfer (1984) concentrated on documenting and dating the Late Quaternary fault offsets, with the aim of determining slip rates and temporal variations in slip rate over time-spans of $10^3$ -$10^4$years. He proposed a tentative horizontal slip-rate of between 30-50mm/year for Late Pleistocene-mid Holocene activity on the Hope Fault, reducing to

approximately 4mm/year during the late Holocene. This estimate of slip exceeds the rates obtained (in the same study) from the sum of slip across the other major faults in the Marlborough Transform System. The upper bound estimate for the Hope Fault also exceeds the long-term average crustal plate convergence rate predicted from sea-floor spreading (Walcott 1978). Almost all of the slip-rates estimated in this study were derived from features dated using relative-absolute techniques, such as greywacke-sandstone cobble weathering rinds and soil development indices. Although promising as dating tools in stony alluvial environments, both techniques are commonly subject to standard errors of up to 20% and 50% respectively.

At Glynn Wye Station in the Lower Hope Valley where faulted Late Quaternary and Holocene deposits are well preserved, the measurement and interpretation of important offsets has been a source of dispute and occasionally, confusion (Clayton 1968; Freund 1971; Suggate et.al. 1978; Hardy & Wellman 1984; Knuepfer 1984; Wellman 1985). Debate has variously focused on the direction in which fault displacements should be measured and the age of the faulted geomorphic surface.

## 2.6 Methodology

### 2.6.1 Mapping

An engineering geomorphological mapping programme was designed to document the Late Pleistocene and Holocene deposits as they affect interpretation of the faulting history. Mapping was conducted on a topographical map base at a scale 1:15 000, using enlargements of the 1:25 000 scale, NZMS 270 M32/A B C and D. The area mapped is located in

the Lower Hope Valley and Kakapo Brook between the Hope-Boyle River confluence to the west and Manuka Creek on State Highway 7, fourteen kilometres to the east (Maps 1 and 2 in map pocket).

Detailed maps of specific Late Quaternary fault displacements on the Hope and Kakapo Faults were prepared at a scale of 1:3000 and 1:2000, from enlargements of 1:15 000 and 1:10 500 low-altitude, high resolution vertical air photographs of Run GS (Geological Survey) 544/ 1-32 and GS 450/ 1-15 respectively.

It became evident during this study that air photographs at a number of scales and of different age were useful for the identification of different features at various localities. All detailed study of the Late Quaternary fault displacements was accomplished with the aid of enlarged, low-altitude air photographs. High altitude air photographs at a scale of 1:80 000 (Run 4037/ 57-60, NZ Aerial Mapping) were particularly useful for identifying certain Late Pleistocene glacial deposits, which despite their large size and prominence in the landscape are virtually invisible on the larger scale (1:25 000, Dept. of Lands & Information Run SN C5849) and (1:20 000, Dept. of Lands & Information Runs 2219/ 15-27 (Hope Fault); and 2220/ 19-28 (Kakapo Fault).

### 2.6.2 Measurement of Fault Displacements

Knuepfer (1984) discusses the basis for recognising and documenting Late Quaternary fault displacements, emphasising the relationship between processes associated with the formation of the offset landforms and the relative timing of the first preservation of fault displacements on the surfaces, after the abandonment of these surfaces by the agents which created them (ice or water).

In this study I have adopted his approach to the analysis of faulted moraines and stream terrace sequences and the measurement of fault displacements as stated in summary form below.

i) Displacements recorded by a glacial terminal moraine are inferred to be post-depositional (i.e. post-ice retreat from the terminus) because of the rapid rate of surface modification at these sites while the moraine is being constructed.

ii) The displacement of a stream terrace riser records the amount of slip across the lower terrace, because the age of abandonment of a terrace riser by a river is the same as the age of the terrace surface below it.

iii) The displacement of abandoned stream channels on a terrace surface is not presumed to record the total displacement on the terrace unless it can be established that the channels do not post-date the surface into which they are incised.

iv) Fault displacements on stream terraces were measured from the crest, mid-point, and toe of the riser above the terrace surface. The highest terrace riser in a sequence is denoted R1, and the terrace surface below this is denoted T1. The down-dropping riser to the next terrace level is denoted R2 and so on.

v) Displacements are quoted with an estimate of the associated measurement error which is introduced by poor exposure, or inferred modification of original topography. The errors represent an averaging of the confidence placed on each set of three measurements of the offset between riser crests, mid-point and toe, rounded to the nearest 0.5 m (Note: This departs from the previous work of Knuepfer (1984) which records measurements at a 0.1 m increment, but the differences involved are undetectable in the landscape).

Late Quaternary fault displacements were studied in detail at one locality on the Kakapo Fault and two localities on the Hope Fault. The displacements are right-lateral and dominantly strike-slip. They consist of offset Late Pleistocene glacial moraine, fluvio-glacial outwash, and Late Pleistocene and Holocene river degradation terraces

Lateral displacements were measured directly where possible with a 100 m tape, stadia rod, and abney level, or with a Wild theodolite and electronic distance meter (EDM). At the Manuka Creek study site, vertical and lateral displacements on the Hope Fault were surveyed relative to precise level Bench Mark UB 68 (orthometric height above mean sea-level at Lyttleton = 419.6778 m).

Displacements were also measured from enlargements of vertical aerial photographs accurately scaled to precisely measured ground control. It became apparent in a review of previous work that a number of workers have used only the uncorrected general scale on air photographs of 1:25 000 to 1:80 000 to measure displacements of less than ± 100 m. The general photograph scale is unique to a single horizontal datum in the landscape and the large amount of relief in the study area requires

that ground control be established before displacements can be measured to a desired accuracy of less than 1% of the total displacement.

### 2.6.3 Slip Rate Estimates

The slip-rate is an expression of the average rate of fault displacement during a measurable period of time. It requires a knowledge of the age of the faulted landform and the size of the associated displacement. Both of these estimates will involve an uncertainty which must be accommodated by the slip-rate.

I follow Knuepfer's formula for calculating error limits on slip-rate estimates, which involves dividing the smallest estimate of displacement by the maximum estimate of age (a lower bound), and the greatest estimate of displacement by the minimum estimate of age (an upper bound). For example; Lateral displacement = 286 ±6 m

Age Estimate of the faulted landform = 17 000 ±1 000 years.

$$\text{A lower bound is } \frac{280 \text{ m}}{18\,000 \text{ yr}} = 15.6 \text{ mm/yr}$$

$$\text{An upper bound is } \frac{292 \text{ m}}{16\,000 \text{ yr}} = 18.2 \text{ mm/yr}$$

$$\text{The resultant slip-rate} = 16.8\,^{+1.4}_{-1.2} \text{ mm/yr}$$

This format is incorporated in tables and discussion presented in Chapter 5.

### 2.6.4 Radiocarbon Dates

All radiocarbon dates obtained in this study were processed by the Radiocarbon Dating Laboratory, Institute of Nuclear Sciences, Lower Hutt (Appendix 1). All radiocarbon ages quoted in this study and those quoted from Knuepfer (1984) are corrected radiocarbon ages (68% Confidence Interval) quoted in calendar years before present (in this study, years before 1950; for Knuepfer (1984), years before 1982). The corrected age uses the dendrochronological calibration curves of Stuiver and Pearson (1986) which represent the best currently available correction for fluctuations in atmospheric carbon during the last few thousand years.

# CHAPTER 3 GEOLOGY AND GLACIAL GEOMORPHOLOGY OF THE LOWER HOPE VALLEY

## 3.1 Introduction

At Glynn Wye Station in the Lower Hope Valley of Amuri District, latest-Quaternary glacial moraines and glacial and post-glacial stream terraces are well exposed due to an absence of forest cover. Successive Late Quaternary glaciations have left fluvioglacial deposits preserved at various levels up to 500 m above the modern Hope River floodplain (c.900 m a.s.l.). Ice cut surface remnants related to earlier Quaternary glaciations may be traced beyond this limit, to broadly accordant summits at 1600-1800 metres a.s.l..

Detailed mapping of Otiran glacial and post-glacial deposits and associated landforms at four localities traversed by the Hope or Kakapo faults has provided information on the latest-Quaternary displacement history. In order to evaluate correctly the rates of faulting displacement and the variations in the rate of displacement with time, field relationships and ages of these Otiran and post-glacial deposits must be known.

The following objectives are addressed in this chapter.

i) To provide a brief outline of the basement geology and Late Cenozoic regional structure and a detailed account of the Late Quaternary geology and geomorphic surfaces within the Lower Hope Valley. The emphasis is on landforms of the Otiran glaciation (between 70 000 yr BP and 14 000 yr BP) and of post-glacial time, because of their relevance to the study of Late Quaternary faulting. The Late Quaternary stratigraphic nomenclature of Clayton (1968) will be

used.

ii) To report new data on the distribution of latest last-glacial and early post-glacial landforms and deposits.

iii) To discuss the history of post-glacial down-cutting by the Hope River in the context of radiocarbon ages from former flood-plain levels.

iv) To revise the latest-Otiran stratigraphy , and to summarise the Late Quaternary history of the Lower Hope Valley

## 3.2 Basement Geology

### 3.2.1 Stratigraphy

Basement rocks of the Lower Hope Valley form part of a 10-20 km wide zone of tectonic melange, broken formation and thrust slices within the Torlesse terrane, a region of quartzo-feldspathic greywacke and mudstone of Permian and Mesozoic Torlesse age (Bradshaw & Andrews 1980, cf. Torlesse Supergroup (Suggate et.al. 1978). This zone, the Esk Head subterrane (Bradshaw and Andrews 1980), separates Permian-Late Triassic quartzo-feldspathic greywacke of the Rakaia subterrane on the west from latest Jurassic-Early Cretaceous, conglomeratic marginal marine facies of the Pahau subterrane to the east. Esk Head subterrane is distinguished from adjacent parts of the predominantly greywacke Torlesse terrane by a greater abundance of tectonic blocks and slivers of limestones, bedded chert-argillite, and basalt and associated basaltic sediments (Silberling et.al. 1988).

Mapping of basement stratigraphy and structure, however, was beyond the scope of this study and the reader is referred to the cited

references for an account of these topics, although much of the region still awaits detailed mapping.

The following section presents an overview of the structure.

### 3.2.2 Structure

Basement rock structure belong to at least three different categories corresponding to three different periods of deformation: Mesozoic, Late Cenozoic, and Late Quaternary.

Mesozoic structures within basement rocks are extremely complex and involve steeply-dipping anastomosing shears bounding intricately fault-slivered greywacke, basalt and bedded chert-argillite, interpreted as the product of deformation within a Pacific-facing Gondwana margin accretionary prism (e.g. Sporli (1978); Bradshaw et.al. (1980); MacKinnon (1983)).

Late Cenozoic basement structure is by contrast relatively simple; strata dip at high angles (60-80°) and strike northeast, closely paralleling the regional northeast trend of the active Hope and Kakapo faults. Gross offsets of conglomerates and coloured chert-argillite across the Hope Fault in the Lower Hope Valley and around Hanmer Basin have been used by Freund (1971) to infer a right-lateral strike-slip displacement of approximately 19 kilometers.

Late Quaternary basement structures are related to strike-slip displacements on the major faults. The dip of the Hope Fault is not clearly expressed at available exposures in the study area. Freund (1971) measured a dip of 80°N on the west bank of Kakapo Brook, but this was not located during this study. The surface expression of dip may be misleading, especially if inferred from the outline of the surface trace

across topography. Abrupt changes in strike are common along the Hope Fault and are accompanied by localised oblique-reverse and oblique-normal faulting patterns in the Late Quaternary cover. A single direct measurement of the dip on the Kakapo Fault (83°S) was obtained in a tributary stream of Kakapo Brook (Map 1 in map pocket).

Along the principal strand of the Hope Fault, cataclastic zones have developed, these comprise anastomosing domains of pervasive shear sub-parallel to the fault and up to hundreds of metres wide (Map 1). A similar cataclastic zone about 100 m wide occurs along the Kakapo Fault. These zones of pervasive shear are most spectacular between Gorge Stream and Manuka Creek, State Highway 7, where the Kakapo Fault converges with the Hope Fault as a series of discontinuous splays (Figure 3.1).

Secondary faulting produced by deformation of the block between the Hope and Kakapo Faults is exposed as normal displacement ridge rents (sackung), and inferred from mega-boudinaging marked by cross-cutting valleys (Map 1). Secondary structures on a still smaller scale are produced at constraining and releasing bends evident in the faulting of surficial deposits along the Hope Fault, but their effect in basement cannot be observed.

## 3.3 Late Quaternary Glacial Deposits

### 3.3.1 Summary of Previous Work

Gregg (1964) and Suggate (1965) recognised the deposits and landforms of four glacial advances in the Lower Hope Valley and correlated these with sequences previously described from the Canterbury Plains, and glacial chronologies in the Hurunui and Waimakariri catchments and North Westland

Figure 3.1. Looking south into an actively eroding gully formed in pervasively sheared Torlesse basement rock, 300 m up Manuka Creek from State Highway 7. The Hope and Kakapo Faults converge in this area (Map 1), and this site is located on the projected strike of one of several splays of the Kakapo Fault. The overlying c. 20 m thickness of oxidised outwash gravels are assigned to the Horseshoe Glaciation (see Map 2).

(Table 3.1). Clayton (1968) recognised five glacial advances in the Lower Hope Valley, (three within the last (Otiran) glaciation) and established a local glacial chronology for the Hope and Waiau valleys. All authors assigned landforms and deposits to respective formations or advances according to the down-valley position and size of terminal moraines, the extent and relative heights of associated outwash surfaces, and the degree of weathering of deposits and modification of original topography. Table 3.2 provides a summary of the general observations of the local Quaternary stratigraphy, made by previous workers. Essential differences between interpretations reached are highlighted. Recognition and interpretation of the latest-Otiran advance and retreat ice-limits, however, has been vague and equivocal in these previous studies and requires a fuller discussion now.

| Waiau Valleys | | Hurunui Valley (Powers, 1962) | Waimakariri Valley (Gage, 1961; Gage and Suggate, 1958, Suggate, 1965) | | West Coast (Gage, 1961; Gage and Suggate, 1958, Suggate, 1965) | |
|---|---|---|---|---|---|---|
| Hope Glaciation | Lewis Advance | Summer moraine, Low surface | Waimakariri Glaciation | Poulter advance | Otira Glaciation | Kumara-3 advance |
| | Glynnwye Advance | Sheppard moraine<br>Sisters moraine, Main surface | | Blackwater 2 advance | | 2 |
| | Glenhope Advance | Three Trees moraine | | Blackwater 1 advance | | Kumara-2 advance |
| | Leslie Hills Advance | High (Hitchin Hills) surface | | Otarama advance | | 1 |
| Horseshoe Glaciation | | | Woodstock Glaciation | | Waimea (Kumara-1) Glaciation | |
| Kakapo Glaciation | | | Avoca Glaciation | | Waimaunga (Hohonu) Glaciation | |

Table 3.1. Previous Correlations of the Late Pleistocene Glacial Chronology of the Lower Hope Valley with other South Island Chronologies. **From Clayton (1968)**

| Stages | Gregg ( 1964 ) Main Observations and Nomenclature | Suggate (1965) Main Observations and Nomenclature | Clayton (1968) Main Observations and Nomenclature | Kneupfer ( 1984 ) Main Observations and Nomenclature |
|---|---|---|---|---|
| Aranuian <14 000yr | Undifferentiated river alluvium. on Hope River floodplain. | Fans on latest Otiran surfaces, landslides, and terraces up to 45m above modern Hope River. | Fans on latest Otiran surfaces, landslides, and terraces up to 30-40m above the modern Hope River. | Fans on latest Otiran surfaces, landslides, and terraces west of Glynn Wye Moraine, up to 170m above modern Hope River. |
| Otiran 14-16 000 yr | St Bernard Formation (Gregg 1964) Fresh till or gravel correlatives of the Poulter Advance in the Waimakariri catchment. Terrace 45m above Hope River. N.W. of Poplars Station | St Bernard Formation, moraine and outwash surface correlatives west of Glynn Wye in Upper Hope Valley. | "Lewis Advance" of the Hope Glaciation. Terminal moraine at Lewis Pass and associated outwash surface 30-40m above the modern Hope River. $^{14}$C date of 13 309 ± 203 yr BP from bottomset lake beds near mouth of Doubtful River. Inferred lake to have ponded behind a dam of stagnant Glynn Wye Advance ice near the mouth of the Boyle River. Lake beds attributed to aggradation during Lewis Advance. | Glynn Wye terminal moraine dated by weathering rinds. Modal age=16630 ± 3230 yr BP Mean age =15390 ± 5100 yr BP. Terrace surface upstream from Glynn Wye moraine also dated. Modal age=7770 ± 1240 yr BP Mean age =8910 ± 2530 yr BP Late Otiran glacial lake may have ponded behind active glacier at Glynn Wye moraine terminus, not stagnant ice. Flood-plain level remained high until end of Otiran Glaciation. |
| Otiran 16-25 000 yr | Burnham Formation (Oborn & Suggate 1959) Slightly weathered glacial and peri-glacial outwash gravel correlatives of the Black-water Advance in the Waimakariri catchment. Terraces and moraine between 150-180m above west of Glynn Wye homestead, and in Dismal Valley. | Burnham Formation. Glynn Wye moraine and associated outwash, 3.2km west of Glynn Wye homestead, 170m above Hope River. Recessional moraine and outwash forming a surface 3km west of Glynn Wye moraine, 145m above Hope River. This surface merges with Glynn Wye surface downstream from Glynn Wye moraine. $^{14}$C date of 14 000 ± 220 years BP from clay on Glynn Wye surface buried by aggrading fan near Handysides Stream, State Highway 7. | "Glynn Wye Advance" of the Hope Glaciation. Terminal moraine 3.2km west of Glynn Wye homestead, 170m above the Hope River. Recessional moraine and outwash upstream from Glynn Wye moraine 145m above the Hope River. | Not recognised as a distinct period. Included in Glynn Wye Advance time range. |
| Otiran >25 000 yr | Not Recognised in the Lower Hope Valley | Not Recognised in Lower Hope Valley | "Glenhope Advance" of the Hope Glaciation. Terminal moraine and outwash 2km west of Glenhope Homestead, and and 1km south of Glynn Wye Homestead, 20-30m above Glynn Wye Advance surfaces. Terminal moraine also at Kakapo Brook in Dismal Valley. | Not referred to |
| Waimean c.140 000yr | Woodlands Formation (Oborn & Suggate 1959) Moderately-weathered and dissected gravel and till correlatives of the Woodstock Advance in the Waimakariri catchment. Gravels beneath ridge-top surface south and south-east of Horseshoe Lake, State Highway 7. | Woodlands Formation. Weathered gravel and moderately dissected surface south and S.E. of Horseshoe Lake, 90m above Glynn Wye outwash. | Horseshoe Glaciation. Same features as described by Gregg (1964) and Suggate (1965). | Not referred to |
| Waimaungan c.250 000 | Hororata Formation (Oborn & Suggate 1959) Strongly weathered and dissected gravel and till correlatives of the Avoca Advance in the Waimakariri catchment. Remnant surface forming summit of Mt Kakapo, 2.4km S.W. of Glynn Wye homestead. | Hororata Formation. Highest glacial surface in Lower Hope Valley, forming summit of Mt Kakapo, 2.4km S.W. of Glynn Wye homestead 240m above Glynn Wye outwash. | Kakapo Glaciation. Same features as described by Gregg (1964) and Suggate (1965). | Not referred to |

Notes: Ages of glacial periods within Stages have been taken from Fellows (1986), Suggate (1988) and Brown & Wilson (1988).

Table 3.2: Summary of the Main Observations and Conclusions of Previous Studies of the Late Quaternary Glacial and Post-Glacial Deposits and Associated Landforms in the Lower Hope Valley.

Clayton (1968) named three consecutive Otiran ice advances, Glenhope, Glynn Wye and Lewis respectively, after the geographic locations of terminal moraines and inferred maximum ice limits (Figure 3.2). He generally accepted Suggate's regional correlations, but re-interpreted the extent of the latest-Otiran glacial advance in the Hope catchment, for which Suggate had inferred an ice limit 2.4 km upstream from the Hope-Boyle river confluence (Figure 3.2). Clayton confined this advance to numerous minor glaciers in the upper catchments of tributary valleys, the largest of which produced terminal moraines at Lewis Pass.

Knuepfer (1984) used weathering rind development on morainic boulders and fluvial terrace gravels to date a number of geomorphic surfaces in the Lower Hope Valley, which are offset laterally by the Hope and Kakapo faults (a detailed discussion of these is presented in Chapter 4).

Knuepfer obtained an age estimate of 16 630 ±3230 yr BP for the Glynn Wye terminal moraine and 8910 ±2530 yr BP for a terrace surface upstream from the moraine (Table 3.2).

His date if valid, places the Glynn Wye Advance in the latest Otiran, whereas previous work suggested a correlation with older deposits in Canterbury and north Westland (Table 3.2).

Knuepfer preferred to recognise in the Hope Valley a "Late Otiran-1" advance between 18 000 and 14 000 yr BP, (encompassing Clayton's Glenhope and Glynn Wye age features), and a "Late Otiran-2" advance between 16 000 and 13 000 yr BP, which he did not distinguish from the Glynn Wye moraine and outwash. Instead, he suggested that the surface of the lake which occupied the Lower Boyle and Doubtful valleys at approximately 13 000 yr BP, was at the elevation of the main Glynn Wye terminal moraine and that an active glacier, not stagnant ice had formed the lake dam.

This interpretation was corroborated, he argued, by the $^{14}C$ date of

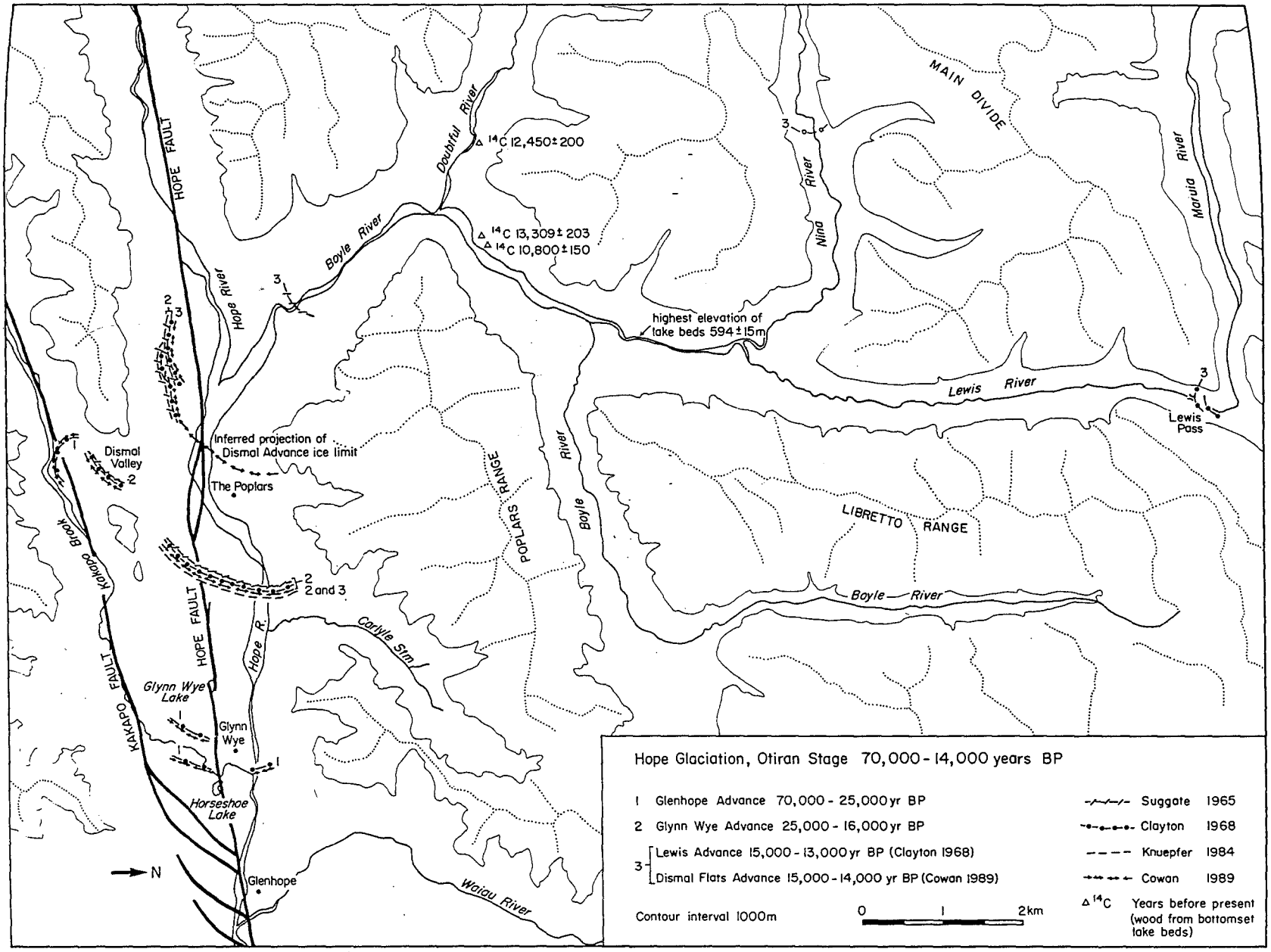


Fig 3·2: Late Pleistocene Ice Limits: Hope River Catchment

14 100 ±220 yr BP for aggradation downstream of the Glynn Wye moraine (Suggate 1965, see Table 3.2) indicating the presence of a glacier in the valley at that time. The post-glacial weathering rind age of between 7 000 and 10 000 yr BP which he (Knuepfer) obtained from stream terrace boulders 300 m upstream from Glynn Wye moraine and only 20-30 m below the moraine ridge crest, also indicated very recent deglaciation of the upper catchment.

Various other workers have speculated on the latest last-glacial down-valley ice-limits, the age and origin of the paleo-lake dam, and the timing and cause of lake in-filling. Burrows (1988) reports a $^{14}C$ date of 10 800 ±150 yr BP (NZ 6180) for wood obtained from the same lake-bed section sampled by Clayton (Table 3.2), but suggests that the date may be slightly young due to contamination by young carbon. Chinn (pers.comm. 1988) reports a date of 12 450 ±200 yr BP (NZ 5532A) from the bottomset lake beds, but in the Doubtful Valley 2 km upstream from the Doubtful-Boyle River confluence.

### 3.3.2 Pre-Otiran Deposits and Landforms

**i) Kakapo Glaciation** (Clayton 1968) (Table 3.2)

Inferred age:- (Waimaungan Stage, c.250 000 yr BP)

This glaciation derives its name from Mt Kakapo (853 m a.s.l.), a flat-topped ridge 2 km S.W. of Glynn Wye homestead and the highest surface on which rounded cobbles and boulders are recognised (Map 2 in map pocket). The Kakapo Surface is 270 m above Otiran surfaces and 440 m above the modern Hope River floodplain (Figure 3.3). No depositional

topography remains on this surface, and the remnant boulders are oxidised throughout.

ii) Horseshoe Glaciation (Clayton 1968) (Table 3.2)

Inferred age:- (Waimean Stage, c.140 000 yr BP)

Thirty to sixty metre thick gravels of the Horseshoe Glaciation underlie a prominent outwash surface south of Horseshoe Lake, from which the glaciation takes its name (Map 2). The Horseshoe outwash surface is 120 m above Otiran surfaces, and 270-300 m above the Hope River floodplain; it is variously preserved on both sides of the Hope River as terrace surface remnants or benches cut into the valley sides (Figure 3.4). The outwash gravels are oxidised throughout, but the surface (although buried by alluvial fans at the valley sides) is less dissected than the older Kakapo surface and retains much of its depositional topography.

### 3.3.3 Otiran (Hope) Glaciation Deposits and Landforms

#### i) Glenhope Advance

The Glenhope Advance is the earliest of the Hope Glaciation ice advances and encompasses a large, but poorly constrained time interval between 70 000 and 25 000 yr BP (Table 3.2). The advance is represented by a subdued (c.10 m relief) terminal moraine and associated outwash 150 m above the Hope River, 3.2 km west of Glenhope Station homestead and 800 m south of Glynn Wye Station homestead (Map 2 and Figure 3.5). An

Figure 3.3 View looking east along the Kakapo Glaciation surface (k) of Mt Kakapo. Hanmer Basin (hb) is visible in the distance. At left the Hope Fault (arrows) traverses the broad outwash surface of the Hope Glaciation, Glynn Wye Advance.

Figure 3.4 View looking south-east from the ridge between the Hope and Kakapo Faults. The broad bench (h) mantled by fan deposits is assigned to the Horseshoe Glaciation. The lower bench (gh) are capped by thin (<3m thick) outwash of the Hope Glaciation, Glenhope Advance. The Kakapo Fault forms a prominent trace across this surface, marked by a vegetation colour contrast due to ponded drainage on the south (down-thrown) side of the fault.
Kakapo Brook (foreground) is incised within a gorge on the upthrown side of the fault.


hb
k


h
gh

equivalent terminal moraine loop was formed by a subsidiary ice lobe in the Dismal Valley at Kakapo Brook.

Subsequent retreat of ice from these terminal positions resulted in the formation of a large lake behind the moraines, which accumulated at least an 80 m thickness of laminated silts, sands and fine gravels. These sediments now underlie younger Glynn Wye Advance outwash gravels and till, but crop out in streams, cliffs and road-cuttings between Glynn Wye Stream and Poplars Station, underlying younger Glynn Wye Advance outwash gravels and till (Figure 3.6).

There are no landforms of Glenhope age traversed by the Hope Fault in the study area, but the terminal moraine in Dismal Valley has been laterally displaced by the Kakapo Fault (see discussion in Chapter 4).

### ii) Glynn Wye Advance

The largest moraines and most extensive outwash surface in the Lower Hope Valley were formed during the Glynn Wye Advance, between 25 000 and 16 000 yr BP. The main terminal moraine and outwash surface are 180 m above the Hope River, 1 km south of the Hope Bridge on State Highway 7 (Figure 3.7 and Map 2). A subsidiary ice lobe constructed a second terminal moraine at the same altitude in Dismal Valley. Outwash from this ice lobe forms the main surface in Dismal Valley and has enveloped the Glenhope moraine at Kakapo Brook ( Map 2 ).

The Glynn Wye Advance outwash is up to 50-60 m thick and the outwash surface extends eastward from the moraine terminus to the southern margin of the Hanmer Plain, (where it is an average of 60 m above the Waiau River), then south through the Waiau Gorge to Culverden where it merges with the surface of the Amuri Plain.

Figure 3.5 View looking west from ridge top south of Horseshoe Lake. An example of Glenhope Advance terminal moraine (gh) mantling a basement rock high and enveloped by Glynn Wye Advance outwash (gy). Kakapo Brook is incised 80 m within a gorge (foreground). The Hope Fault (arrows) forms a bold trace across the Glynn Wye surface.

Figure 3.6 View looking south from State Highway 7, 300 m west of "The Poplars". Cliffs south of the Hope River (out of view) expose dark grey foreset delta gravels, sands and silts, inferred to have been deposited in a lake which occupied the Lower Hope Valley behind the Glenhope age terminal moraines during the "Glenhope Retreat". These sediments are overlain unconformably by an approximately 50 m thickness of light grey coloured outwash gravels, capped by till of the Glynn Wye Advance.


gh
gy

Upstream from the Glynn Wye moraine, there are three closely spaced recessional moraine loops across the entrance to Dismal Valley (Map 2). Related to the formation of these moraines are several meltwater channels and terraces which formerly extended from south to north across the Hope Valley behind Glynn Wye moraine but which are now bisected by the modern Hope River floodplain (Figure 3.8). These meltwater channels are 30 m above the latest last glacial outwash surface and moraine ridge (see section 3.3.3) and are most probably close in age to the main Glynn Wye moraine. However, Knuepfer (1984) calculated a Holocene weathering rind age of between 7 000 and 10 000 yr BP for boulders on a river terrace upstream from, and only 20-30 m below the crest of the Glynn Wye terminal moraine. He concluded that the flood-plain had remained at this level until early post-glacial times, before degrading to form river terraces at progressively lower levels between the Glynn Wye moraine and the modern Hope River. Evidently he was unaware of the existence of an outwash surface and moraine ridge to the west at Dismal Flats which are 30 m lower in altitude than his dated terrace (Figure 3.8) (Suggate 1965; Clayton 1968; see also Table 3.2 and Map 2). Detailed mapping carried out as part of this study indicates Knuepfer's terrace is a meltwater channel associated with one of the closely spaced recessional Glynn Wye moraines. A detailed discussion of this locality is presented in Chapter 4. The Holocene weathering rind age probably underestimates the age of this feature by between 37-60%.

I have not attempted weathering rind dating of deposits during this study, and a critical review of the application or calibration of this dating technique in the Hope Valley is beyond the scope of this discussion. The following comments, however, may be made about the anomalously young rind age for the Late Pleistocene meltwater terrace.

Figure 3.7 The Glynn Wye outwash surface extending eastward from the terminal moraine (arrows lower left). The Hope Fault forms a linear trace along the outwash surface and is marked also by a sag pond (s) and Lake Glynn Wye (lg) which has formed at a side-step in the fault (see discussion in Section 3.5). Glenhope Advance (gh) and Horseshoe Glaciation (h) surfaces are visible north-east of Lake Glynn Wye.



Figure 3.8 View looking west from the ridge between the Hope and Kakapo Faults, above the northern entrance to Dismal Valley, 1 km west of the main Glynn Wye Advance terminal moraine. In the foreground, kame terraces and moraine loops across the entrance to Dismal Valley and recessional from the Glynn Wye terminus. Beyond and 30 m lower in elevation is the Dismal Flats outwash surface (df) which extends westward to a subdued moraine ridge (m). Note also the Hope River (left) and Boyle River (right) confluence (centre right), and State Highway 7 (extreme centre right).


h
gh
la
s


m
df

i) The rind age may reflect a small sample size; Knuepfer does not list sample sizes, but stated difficulty in obtaining a suitable number of rinds.

ii) The rind age may be correct for the rinds sampled, and reflect exhumation of boulders due to deflation of loess, or heavy ground-shaking in repeated earthquakes.

iii) The rind age may reflect inherent inaccuracy of the rind calibration curves (Chinn 1981; Whitehouse et.al. 1984) in the Hope Valley or for surfaces of Late Pleistocene age generally. Of these latter two possibilities the second is more likely. One of Knuepfer's Late Holocene rind ages at Manuka Creek, State Highway 7 has been calibrated by a $^{14}C$ date during this study and is within the standard error of ±20% stated for the method (see Chapter 4).

### iii) Lewis Advance

West of the main Glynn Wye Advance moraine and associated recessional moraine loops, and 30 m lower in elevation an outwash surface forming Dismal Flats extends westward to a terminal moraine located along the northern edge of Dismal Flats, 600 m a.s.l. ( 145 m above the Hope River) (Map 2 and Figures 3.8 and 3.9 ). The moraine consists of several grass covered ridges which are difficult to see on aerial photographs and from lower levels at a distance, but in detail the moraine surface has up to 5 m relief and is scattered with boulders up to 2 m in diameter.

The outwash forming Dismal Flats is approximately 20 m thick and overlies silts, sands and gravels deposited in a lake which formed behind the Glynn Wye moraines during the ice retreat from the terminus (Figure 3.10 and 3.11). The Dismal Flats surface merges with the Glynn Wye

Figure 3.9. View north-east across the Dismal Flats Advance moraine ridge (arrow). The west face of Glynn Wye Advance terminal moraine is visible (upper extreme right). Terrace surfaces at lower levels (centre left) are post-glacial.

Advance outwash surface a few kilometres downstream from the Glynn Wye Advance moraine, and was mapped by Suggate (1965) and Clayton (1965) as recessional from Glynn Wye Advance.

In this study the moraine and its associated outwash surface are believed to represent the latest-Otiran advance ice limits in the Hope Valley (Figure 3.2). Terrace surfaces at a lower level and ascribed to this (Lewis) Advance by Clayton (1968), are reinterpreted as post-glacial degradational river terraces (Map 2).

An absolute age for the latest-Otiran (Lewis) advance is not available, but a minimum age may be inferred from the $^{14}C$ age of 14 000 ±220 between the outwash surface and a locally aggrading fan (see Suggate (1965), Table 3.2). It seems likely that ice had retreated from the Hope Valley by 13 309 ±203 yr BP when another lake began to form behind the Dismal Flats moraines in the Lower Hope, Boyle, and Doubtful valleys. Radiocarbon dates of 13 309 ±203, 12 450 ±200 and 10 800 ±150 yr BP from bottomset beds of this lake near the mouth of the Doubtful River (Figures 3.2 and 3.12 ), indicate the lake may have occupied the Lower Boyle and Hope valleys until 12 000 yr BP or later. Knuepfer (1984) suggested that the lake surface was at the level of the main Glynn Wye Advance terminal moraine (620-640 m a.s.l.), and that the lake had been dammed by an active glacier at the Glynn Wye terminus.

I support Knuepfer's observation that the lake extended further down-valley than the mouth of the Boyle River, but suggest that the lake level (as inferred from the highest elevation of lake beds in the Lewis and Lower Hope valleys) was between 590 and 600 m a.s.l., and was dammed behind the Dismal Flats terminal moraine ridge, extending north-south from Dismal Flats to Poplars Station (Figure 3.2).

Clayton (1968) recognised a surface below the level of the lake,

Figure 3.10. View looking south-east across the Boyle River (foreground) and Hope River (centre left), from State Highway 7. Dismal Flats Advance outwash capped by till forms the terrace surface 145 m above the Hope River. The Hope Fault is indicated ( arrows) trending 085° across several large landslides which have occurred in the terrace deposits.

Figure 3.11 Laminated lake silts exposed in a gully eroded into the Dismal Flats (Grid Ref: M32/612438). The lake beds grade upward (over 0.3-0.6 m) into fine to medium gravel ( max. c.30 mm). The gravels are 15 m thick but show only a slight coarsening upward trend. Scattered larger boulders (max. c.400 mm) are restricted to within 4 m of the outwash surface. Dismal Flats Advance till is located only 100 m west of this exposure.

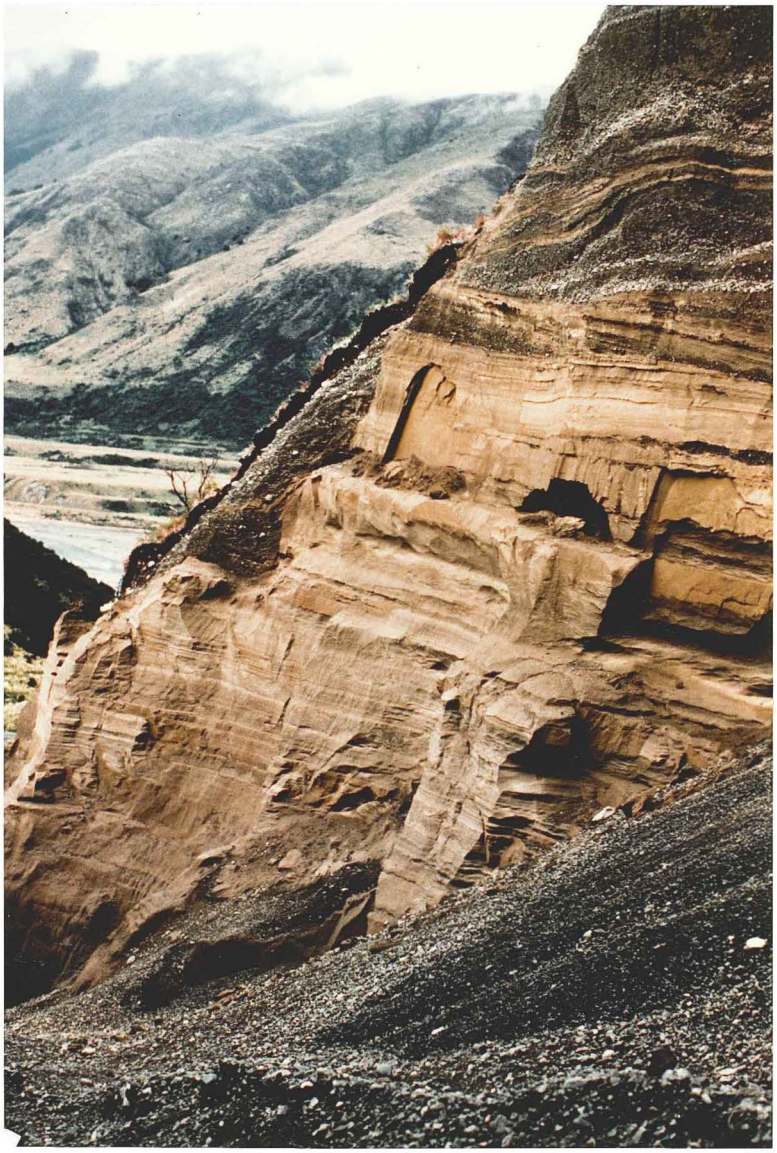

30-45 m above the modern Hope River which he attributed to outwash aggradation from a glacier terminus at Lewis Pass, during a latest-Otiran advance. He interpreted the lake as being dammed behind stagnant ice of the Glynn Wye Advance and the foreset lake beds in the Boyle River as the product of aggradation downstream from advancing latest-Otiran ice at Lewis Pass. Other workers have cited this as corroborative evidence for a younger-than-14 000 yr BP end to the Otiran Glaciation (e.g. Mabin 1983).

During this study field checks were made of available exposures beneath Clayton's Lewis Advance surface, along State Highway 7 west of The Poplars and between the confluence of the Hope and Boyle Rivers (Map 2). I found at all localities the Lewis surface is underlain by a thin (2-4 m) cap of degradational river gravels deposited on an eroded surface cut into lake beds (Figure 3.13 and 3.14). The lake sediments vary in attitude and texture from flat-lying or gently dipping coarse silts and sands incorporating fine gravel filled channels, to fine to medium gravels (average clast size 70 mm) in a coarse sandy matrix deposited as foreset beds dipping 20-25°E (Figure 3.15). These lake beds are not compacted and I believe that they are down-valley correlatives of the lake beds exposed along the Boyle and Doubtful rivers.

The moraine ridge remained an effective barrier to the lake waters until breached by streams and rivers eroding headward from the eastern (downstream) side, their competence increased by the reduced upstream sediment yield. If glaciers remained active at this time then they were probably restricted to the upper catchments of tributary valleys.

I see no justification for attributing this aggradation to a glacial advance; there is no evidence of any systematic textural changes within the lake sediments which might indicate a progressively more proximal

Figure 3.12 View of the west bank of the Boyle River from State Highway 7, 400 m upstream from the Boyle-Doubtful River confluence (out of view to left). This is the section from which Clayton (1968) and Burrows (1988) report $^{14}C$ dates of 13 309 ±203 yr BP, and 10 800 ±150 yr BP respectively for wood obtained within bottomset beds of the late-Otiran-early-Aranuian age lake in the Lower Hope and Boyle Valleys. The section is largely obscured by scree, but gravel foreset beds are visible at centre right (arrow).

Figure 3.13 Dark brown coloured laminated lake sediments overlain unconformably by a 2 m thick cap of river gravels, 30 m above the active Hope River floodplain and 1.7 km west of the Hope-Boyle River confluence.

sediment source, and the aggradation could equally be attributed to glacial retreat with an increase in flood-plain area exposed to fluvial erosion.

The Lewis Advance is therefore something of a misnomer, at least in the Lower Hope Valley where there is no clear evidence for an associated outwash surface. There is no denying that a sizeable terminal moraine exists at Lewis Pass, but I suggest that this may be near-equal in age with the Dismal Flats moraine, and that glacier retreat from the Hope Valley terminus to Lewis Pass could have been extremely rapid. The Main Divide at the head of the Hope, Doubtful and Lewis valleys is only 1600-1800 m a.s.l.. Broadly accordant summits bound almost all of the glacier catchment area. A small increase in the altitude of the permanent snowline (concurrent with warming) could suddenly reduce snow accumulation greatly, accelerate ablation, and cause the glacier to withdraw (as separate ice lobes), into the headwaters of tributary valleys. Sediment would continue to be deposited rapidly in the lake formed behind the down-valley terminal moraine, and need not be attributed to a glacial advance. The available evidence in the Hope Valley is indicative of a final ice retreat before 13 309 ±203. This is consistent with (but not proof of) an age of about 14 000 yr BP for the end of the Otiran Glaciation (Suggate 1965; Suggate 1988, see Table 3.2).

### 3.3.4 Revision of Late Otiran Stratigraphic Nomenclature

Clayton's nomenclature for the Otiran glacial sequence in the Lower Hope Valley has been used in this study, and his interpretation of the distribution of Glenhope Advance and most Glynn Wye Advance landforms is accepted.

Figure 3.14 View looking west from the crest of the west face of the Glynn Wye moraine, along the 20-30 m high Hope Fault scarp in Poplars Graben to the Hope-Boyle River confluence. The locations of Figures 3.13 and 3.15 are indicated.

Figure 3.15 Gravel foreset beds dipping 25°E exposed in the west bank of the Hope River 1.7 km upstream from the Hope-Boyle River confluence. The foreset beds are overlain unconformably by a 1-1.5 m thick cap of river gravels.

The latest-Otiran glacial advance and terminal ice limits, however, are reinterpreted. If the latest-Otiran advance is to be recognised according to the down-valley position of a terminal moraine and associated outwash surface, it should be called the Dismal Advance after Dismal Flats, Glynn Wye Station. The absolute age of the sizeable moraines at Lewis Pass (which are younger than those at Dismal Flats) is unknown, but I suggest that these may be only a few centuries younger than the Dismal Flats moraine and represent a late phase of the same advance.

## 3.4 Post-Glacial Deposits and Landforms

### 3.4.1 Fans

Post-glacial alluvial and debris-flow fans below steep eroding mountain slopes have buried Late Pleistocene landforms and deposits along all valley sides in the study area (Map 2).

Three kilometers west of Dismal Flats in a streambank at the head of a large gully eroded into the latest last-glacial outwash surface, fan gravels overlie a 0.4-0.5 m thick silt layer containing abundant charcoal and burnt wood above a degradational (post-glacial?) gravel lag on the outwash surface (Map 2 & Figure 3.16). The fan soil exhibits a well developed podsolic E Horizon indicating a minimum age for the fan of >1000-2000 years (P. Tonkin pers.comm.). A sample of the burnt wood was identified as Phyllocladus sp. (probably P. alpina) (R. Patel, pers. comm.). The charcoal and the surrounding silt layer were sampled for $^{14}C$ dating and pollen analysis, and submitted to Institute of Nuclear

Figure 3.16 Exposure in a gully eroded into Dismal Flats (Grid Ref: M32/593440). The section shows cross-bedded Dismal Flats outwash gravels (ow) overlain unconformably by a flat-lying, 0.5-0.7 m thick gravel lag (gl) which in turn is overlain by a 0.7 m thick silt layer (z) containing abundant charcoal and burnt wood (Phyllocladus sp.). The silt layer is overlain unconformably by angular fan debris (fd) on which a soil with a prominent podsolic E Horizon has developed (arrow).


fd
z
gl
ow

Sciences, Lower Hutt, for $^{14}C$ dating; the pollen samples to Dr N.T. Moar, Botany Division, D.S.I.R.; results will be reported shortly.

### 3.4.2 River Terraces

The oldest post-glacial terrace surface is approximately 145 m above the Hope River, at or just below the level of the latest last-glacial outwash surface at Dismal Flats. Degradational river terraces have been formed in glacial outwash, post-glacial lake sediments and bedrock. The broadest terraces occur WNW of Poplars Station, north of State Highway 7; these were attributed by Clayton (1968) to aggradation during the Lewis Advance. Other degradational river terraces are located in the Dismal Valley where they are offset by the Kakapo Fault, and east of Horseshoe Lake where they are traversed and offset by the Hope Fault.

## 3.5 Landforms Related to Active Faulting

The Hope Fault traverses glacial and post-glacial landforms in the Lower Hope Valley and forms an impressive surface trace across the Glynn Wye terminal moraine and along the outwash surface west of Glynn Wye homestead (frontispiece). Repeated Late Quaternary displacements on the Hope Fault have laterally offset these features, and the Glynn Wye terminal moraine presently records a cumulative displacement of nearly 300 m.

Localised but persistent side-steps and changes in the trend of the fault trace form zones of relative subsidence or uplift according to whether the direction of fault movement in successive earthquakes, produces an extensional or compressional jog (at side-steps) or a

releasing or constraining bend (at a change in fault trend) (Figure 3.17).

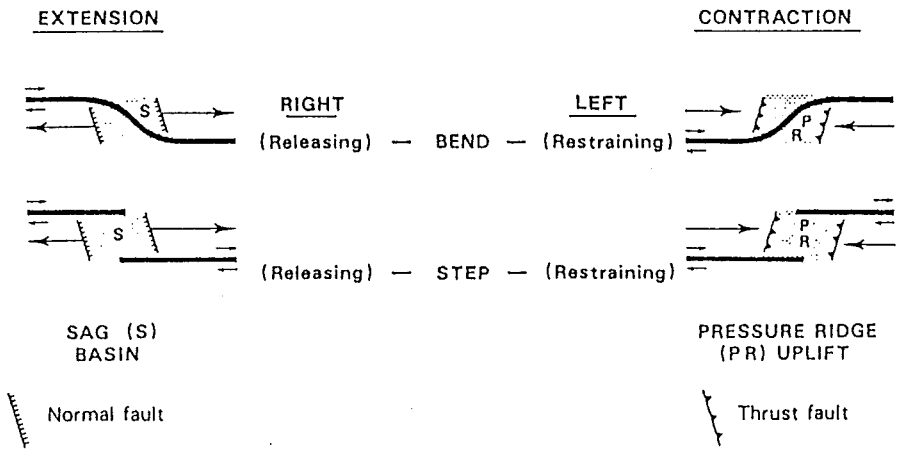


Figure 3.17 The relationship between strike-slip fault geometry and the development of compressional and extensional fault jogs and releasing and restraining fault bends. The example shown is for right-lateral faulting. From Keller (1986).

The most spectacular of these is the Poplars Graben (Clayton 1966; Freund 1971), a 800 to 900 m wide zone of extension, listric-normal faulting and subsidence beneath the meltwater terraces and recessional moraines developed at a releasing bend immediately to the west of the Glynn Wye terminal moraine (frontispiece).

Another is Lake Glynn Wye 1.5 km west of Glynn Wye homestead, which occupies a fault-bounded depression formed in the Glynn Wye outwash surface (Figure 3.18). The Lake Gynn Wye Graben is an extensional fault jog and was associated with intense and pervasive ground deformation and subsidence during the 1888 earthquake, and a sudden change in the amount of lateral displacement in that event (see Chapter 4). To the east of both Poplars and Lake Glynn Wye Graben, anticlinal ridges up to 20 m high have developed where the fault resumes its regional trend forming a constraining bend dominated locally by oblique-reverse and thrust

Figure 3.18 View looking north-west across Lake Glynn Wye, a large sag pond occupying the deepest part of Lake Glynn Wye Graben formed in the Glynn Wye outwash surface, 1.8 km west of Glynn Wye homestead. The graben has formed due to extensional faulting and subsidence at a right-lateral jog in the Hope Fault (see also Map 1). On the far side of the lake the Hope Fault forms a prominent double scarp (covered in matagouri) up to 25 m high (upper right).

faulting (Figure 3.19 and Figure 5.6 in Chapter 5). Horseshoe Lake, on State Highway 7 east of Glynn Wye homestead is traversed by the Hope Fault and is impounded behind an earthquake generated landslide (Figure 3.20). The valley to the east of the lake was formerly occupied by Kakakpo Brook and a braid of the Hope River and its geomorphic history is intimately associated with activity on the Hope Fault. The history of this locality is dicussed in detail in Chapter 5.

In addition to Horseshoe Lake other large and small slope failures are evident along this section of the Hope Fault, many of which occurred during the Sept. 1 1888, Amuri Earthquake and were subsequently mapped by Mr Alexander McKay, Assistant Geologist of the N.Z. Geological Survey (Figure 4.3 in Chapter 4).

Other spectacular landslides in glacial outwash and lake sediments have occurred along the Hope Fault are located at the northern edge of Dismal Flats (Figure 3.21), and SE of The Poplars (Map 2).

### 3.6 Post-Glacial Downcutting by the Hope River

If 12 000 yr BP is adopted for the onset of lake drainage and river degradation, a datum at approximately 145 m above the present level of the Hope River is established for the initial post-glacial floodplain level.

One kilometre east of Horseshoe Lake near Manuka Creek (Map 2), the highest of three terraces formed between 10-17 m above the modern Hope River are traversed and laterally offset by the Hope Fault. During a trenching study at this site (see Chapter 4) wood was obtained from overbank silts inferred to have been deposited during the formation of the +17 m terrace. The wood was dated at 3482 ±77 yr BP (NZ 7591,

Figure 3.19 An example of reverse (probably oblique-reverse) faulting exposed in lake sediments in Glynn Wye Stream (Grid Ref. M32/690454), 300 m north of a constraining bend on the Hope Fault (see also Map 1) to the east of Lake Glynn Wye. Note the back-thrust at top left of photograph.


100mm

Appendix 1). Surfaces between this level and the modern Hope River floodplain are latest Holocence in age.

South-west of Hope Bridge (Map 2) a large landslide in Glynn Wye Advance outwash gravels and underlying Glenhope age lake sediments has buried a formerly vegetated river terrace, 3.0-3.3 m above the modern Hope River. Knuepfer (1984) lists a calibrated radiocarbon age of 778 ±60 yr BP for wood buried by the landslide.

With these three well-constrained former flood-plain levels during post-glacial time, it is possible to describe a crude average down-cutting curve for the Hope River (Figure 3.22). The limited data available indicate an exponential decrease in the average rate of river down-cutting during post-glacial time. This trend reflects river adjustment from a base-level controlled by Late Pleistocene river aggradation, to a base-level controlled by the long-term rate of relative uplift at the Hope Fault and subsidence in Hanmer Basin. Similar trends in post-glacial river adjustment have been observed at other rivers in Marlborough and North Westland, where post-glacial down-cutting and tectonic data are available (Knuepfer 1984; Bull & Knuepfer 1987). In areas with more complete data rates of down-cutting were initially slow in early post-glacial time, but increased to a maximum at about 6 000 yr BP during a mid-Holocene climatic optimum, before slowing to a rate which approximates long-term tectonic uplift (Appendix 2).

In the Lower Hope Valley subsidence within the Hanmer Basin probably exerts the greatest control on Hope River down-cutting. The late-Otiran outwash surface which appears to be a composite of Glynn Wye Advance and Dismal Advance outwash is approximately 60 m above the Waiau River on the south side of Hanmer Plain. If an age of between 12 000 and 15 000 yr BP is assumed for the end of river aggradation at that level, then a

Figure 3.20 View north-west of Horseshoe Lake on State Highway 7 (centre right), impounded to the east behind a landslide (out of view). The Hope Fault traverses the northern shore of Horseshoe Lake (arrows); Glynn Wye Station buildings are visible on degradational river terrace beyond Kakapo Brook.



Figure 3.21 View WNW across the Dismal Flats outwash surface and moraine ridge, showing large landslides which have occurred along the trace of the Hope Fault at the northern edge of Dismal Flats.

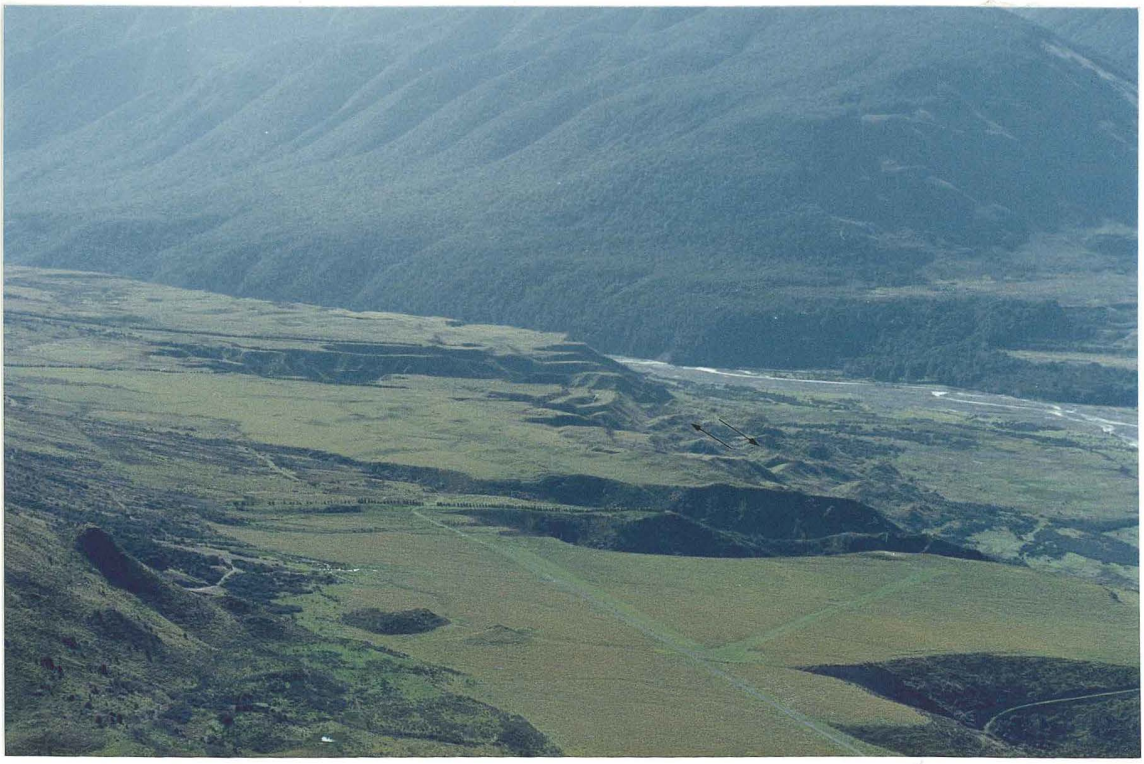

subsidence rate of between 4 and 5 m/kyr is indicated (1 kyr=1000 yr). The uplift rate at the Hope Fault (where determined from Late Holocene fault displacements, see Chapter 4) is only 0.71 m/kyr; whereas the rate of river down-cutting (during the period 0 to 3 500 yr BP) was approximately 4.8 m/kyr (Figure 3.22). At present the Hope River appears to be cutting a broad terrace, and high flows throughout the latter half of 1988 resulted in extensive lateral bank erosion along the reach at Poplars Station, upstream from Hope Bridge, State Highway 7 (J. Shearer pers.comm.).

## 3.7 Summary of the Late Quaternary History of the Lower Hope Valley

During three successive stadials of the Otiran (Hope) Glaciation (between 70 000 and 14 000 yr BP), ice of the Hope, Doubtful and Boyle valley glaciers coalesced to form a large valley-glacier occupying the Hope and Dismal valleys at Glynn Wye and Poplars stations (Figure 3.2).

The Glenhope Advance (between 70 000 and 25 000 yr BP) reached a maximum terminal ice limit at 550 metres a.s.l., north and south of Glynn Wye homestead. A subsidiary lobe of ice penetrated Dismal Valley as far as Kakapo Brook, forming a terminal moraine loop around the south-western side of that valley. Rivers of meltwater distributed till from the ice termini, creating an outwash surface which extended eastward to the Hanmer and Culverden Basins.

When the Glenhope glacier retreated during a slight warming interval (between 25 000 and 22 000 yr BP) a large lake formed behind the main terminal moraine, and occupied the Lower Hope and Boyle valleys. Sediment delivered to the lake by rivers and streams was held in storage, thus increasing the competency of rivers downstream from the lake.

Down-cutting commenced and headward erosion eventually breached the moraine dam, lowering and possibly draining the lake.

Ice again occupied the Hope Valley during the penultimate Glynn Wye Advance (between 22 000 and 16 000 yr BP). At the peak of this advance the glacier overrode Glenhope lake sediments to reach a main terminal ice limit in the Hope Valley at 640 m a.s.l., opposite Poplars Station. A subsidiary lobe of ice formed a terminus at the same altitude half-way into Dismal Valley. Glynn Wye Advance outwash flooded around the earlier Glenhope moraine loop in Dismal Valley, and in the Hope Valley a 50-60 m thickness of outwash accumulated, constructing an extensive surface to the east of the terminal moraine, 20 metres below the level of the Glenhope outwash surface. This surface also extended eastward to the Hanmer and Culverden extended eastward to the Hanmer and Culverden basins.

Between 18 000 and 16 000 yr BP the ice terminus oscillated about its maximum position, but formed three closely spaced recessional moraines and meltwater terraces behind the main Glynn Wye terminal moraine.

During a consistent ice retreat, possibly between 16 000 and 15 000 yr BP, a lake again occupied a large glacier-carved depression behind the terminal moraines. The cycle of sediment entrapment, increased downstream-downcutting, and probable lake drainage commenced, but was interrupted by the latest-Otiran, Dismal Advance (between 15 000 and 14 000 yr BP) which infilled the lake and reached an eastern ice limit in the Hope Valley, at about 600 m a.s.l. between Dismal Flats and Poplars Station. An approximately 20 m thickness of outwash accumulated during this last major pulse of glaciation, forming the surface of Dismal Flats which merged with the Glynn Wye surface a few kilometres downstream.

At the end of the Hope Glaciation (c.14 000 yr BP), ice withdrew

# Average rate of post-glacial down-cutting by the Hope River

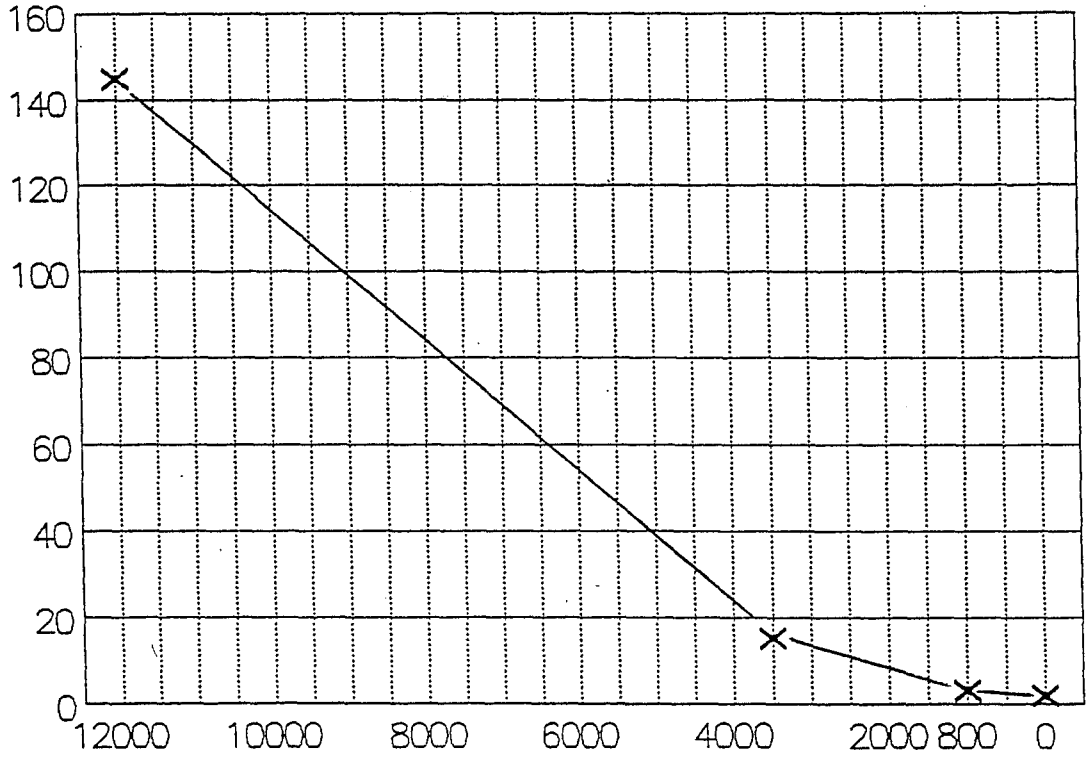


Figure 3.22

rapidly and by about 13 500 yr BP, another lake had formed behind the Dismal Advance terminal moraine. This lake accumulated approximately 50 metres of sediment. Radiocarbon dates of 13 309 ±203, 12 450 ±200 and 10 800 ±150 yr BP, from wood obtained within the bottomset lake beds indicate that the lake may have persisted until 11 000 or 12 000 yr B.P.

When the moraine dam was eventually breached, river downcutting and lateral erosion removed most of the Late Pleistocene landforms and post-glacial lake sediments from the north and centre of the Hope valley. Remnants of these landforms and deposits on the south side of the valley were overwhelmed by large alluvial and debris-flow fans issuing from the steep valley sides. The over-steepened slopes in Dismal Advance outwash gravel, above the Hope River, also failed repeatedly in large landslides during frequent earthquakes on the Hope Fault.

The Hope and Boyle rivers continued to incise, despite minor pulses of aggradation due to landsliding and increased sediment from tributaries. At Manuka Creek, 3 500 yr BP, the Hope river was flowing 15 m above its present day level, and by 750-800 yr BP it had incised to within 3.0 metres of its present level.

Throughout the Late Quaternary the effects of active tectonism associated with the Hope and Kakapo faults, were superimposed on the landscape. Slope processes were accelerated and drainage patterns were modified in response to repeated ground shaking, landsliding and fault displacement. Lateral displacement on the Hope Fault occurred repeatedly during successive earthquakes and a cumulative offset of almost 300 m is now preserved on the Glynn Wye terminal moraine.

Detailed discussion of the Hope and Kakapo fault offsets and evidence for high rates of fault displacement is presented in Chapter 5.

## 3.8 Summary

At Glynn Wye Station in the Lower Hope Valley, Late Quaternary glacial, fluvio-glacial, and fluvial deposits and associated landforms are traversed and offset by the active Hope and Kakapo faults. A number of workers have previously described the glacial sequence in the Lower Hope Valley, but of these only Clayton (1968) undertook comprehensive field mapping. He recognised five glacial advances in the Hope Valley (three within the last glaciation) and developed a local glacial chronology and stratigraphic nomenclature. Clayton's chronology provides an adequate basis for classifying most of the glacial deposits described in this chapter. The deposits and associated landforms of the last (Otiran) glaciation have been emphasised because of their relevance to the study of Late Quaternary faulting.

Field mapping during this study provided new evidence of the latest last-glacial maximum down-valley ice-limit in the Hope Valley. Previous studies had inferred that the down-valley ice-limits for this advance were 1) upstream from the Hope-Boyle river junction (Suggate 1965), 2) at Lewis Pass with an outwash surface in the Hope Valley 30-45 m above the Hope River (Clayton 1968), and 3) downstream from the Hope-Boyle river junction at Glynn Wye Station (Knuepfer 1984).

In this study the terminal ice-limit is recognised at Dismal Flats, downstream from the Hope-Boyle river junction, but 3.5 km upstream from Knuepfer's inferred position. The broad terrace of Dismal Flats 145 m above the Hope River is the outwash surface of this advance; terraces at lower levels were formed by river degradation during post-glacial time.

An estimate of the rate of post-glacial down-cutting by the Hope River has been made using available radiocarbon dates from former

flood-plain levels. These dates, and a comparison with similar studies of other rivers in the region indicate a probable exponential decrease in the average rate of post-glacial down-cutting by the Hope River since the Late Pleistocene. The Hope River has now re-adjusted from a Late Pleistocene base-level controlled by aggradation to a base-level controlled by relative uplift at the Hope Fault and subsidence within Hanmer Basin.

# CHAPTER 4 THE 1888 AMURI EARTHQUAKE.

## 4.1 Introduction

Shortly after 4.00 a.m. (local time) on September 1 1888 a large earthquake struck the Amuri district of North Canterbury, severely damaging homesteads and farm buildings in the Hope River-Hanmer Plains area.

The destructive surface waves rolled out across North Canterbury and Westland and in many settlements chimneys were cracked or thrown down and crockery smashed. In Christchurch the top eight metres of the cathedral spire broke off.

Sharp earthquakes had been experienced previously in Canterbury, but the Amuri earthquake of 1888 was unquestionably the largest to have occurred in the region since European settlement in the mid-nineteenth century and was felt from Invercargill in the south to New Plymouth and Masterton in the north. News of the severity of the earthquake in the Amuri district soon reached other centres, and newspaper correspondents were immediately despatched from Christchurch to report on the extent of damage.

There were no deaths or serious injury, although several families were made homeless, and during the weeks following the earthquake after-shocks (many of appreciable strength) occurred continuously in the Hanmer area.

Mr Alexander McKay, Assistant Geologist with the N.Z. Geological Survey was subsequently sent to the area by the Government to document the effects of the earthquake and to allay fears among local people, some of whom believed that a volcanic eruption was imminent. His report (McKay 1890) and the numerous detailed observations by newspaper

journalists and eye-witnesses constitute a valuable source of information on the earthquake and its effects. Hutton (1888) also produced a very useful summary of the earthquake and its felt effects, combining much of this material with his own observations.

However, many of the initial post-earthquake accounts of damage were greatly exaggerated, and created a false impression of the severity of the event which has persisted to the present day. For example, Eiby (1968) records felt intensities of MM8 or more in Christchurch and much of North Canterbury and Fellows (1986) assigns MM10 to the Glynn Wye-Hope River area.

Furthermore, there has been little consensus on the true extent of surface rupture estimated at 13-43 km (McKay 1890, 1902); 50 km (Berryman 1984); and approximately 150 km (Knuepfer 1984).

The overall aim of this chapter is to develop an understanding of the 1888 earthquake which may then be applied to the interpretation of Late Quaternary fault movement and the analysis of paleoseismic history (discussed in Chapter 5). In this context the following objectives are addressed.

i) To evaluate the magnitude, rupture length, and intensity variations of the 1888 earthquake.

ii) To argue that ground motions experienced during this earthquake were not as severe as previous estimates would suggest.

iii) To show that serious damage was very localised, and may be attributed generally to complex local site effects and weak construction, and;

iv) to describe geomorphic features of the earthquake and assess the preservation of the 1888 surface rupture in the Lower Hope Valley today.

This chapter is based on an exhaustive review of published scientific articles about the earthquake, contemporary press reports and biographical sources, supplemented by field observations of the 1888 surface rupture made as part of this study. My reassessment of felt intensities strictly follows the guidelines set for the application of the Modified Mercalli Scale in New Zealand proposed by Eiby (1965) (Appendix 3).

## 4.2 Intensity Variations and Damage Reports

The earthquake of September 1, 1888 was felt from Invercargill in the south to New Plymouth and Masterton in the north, but was most severe in the Hope River-Glynn Wye area (Figure 4.1). At the properties of Glynn Wye, Hopefield and Waiau (Figure 4.2), every cob (rammed earth) or stone building was badly damaged or destroyed; but wooden structures although distorted and shifted from foundations, were not badly damaged and many were subsequently repositioned with the aid of jacks and levers (McKay 1890; Jones 1933).

Liquefaction of river terrace sediments near Glynn Wye homestead was accompanied by the formation of large pits and sandblows, some of which were several metres wide, and greater than 1m deep (Cant. Times Sept. 7 1888). Landsliding was particularly intense between Manuka Creek (cf. Shingle Creek, Figure 4.3) and Horseshoe Lake, but primary ground rupture was restricted to a zone a few tens of metres wide on either side of the fault (McKay 1890).

On the basis of these observations and the generally moderate to light structural damage to well built wooden buildings I conclude that in this region, ground shaking although pronounced did not exceed MM9

Figure 4·1

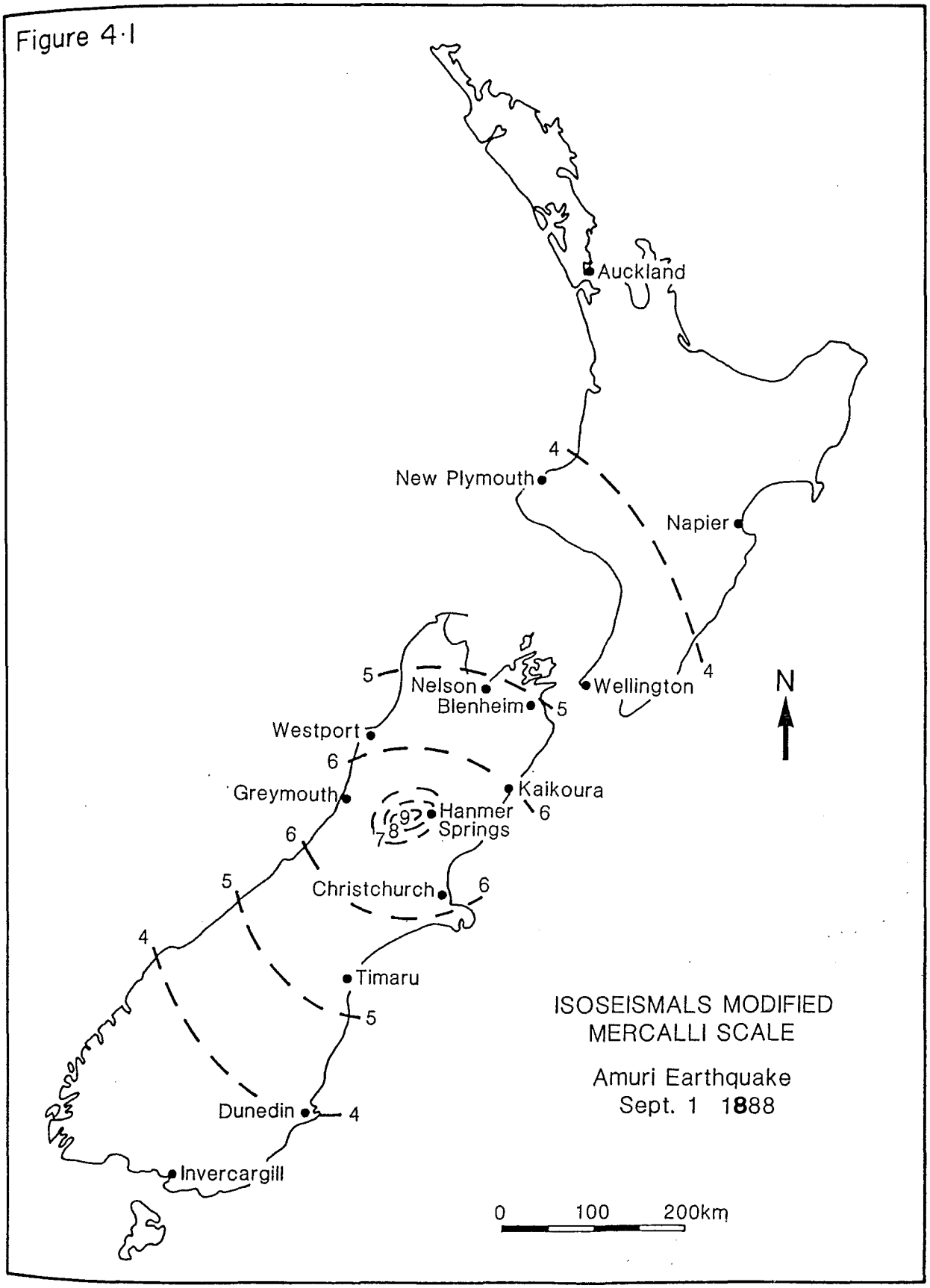
Auckland
New Plymouth
Napier
Wellington
Nelson
Blenheim
Westport
Greymouth
Kaikoura
Hanmer Springs
Christchurch
Timaru
Dunedin
Invercargill
4
5
6
7
8
9
N
ISOSEISMALS MODIFIED MERCALLI SCALE
Amuri Earthquake
Sept. 1 1888
0 100 200km

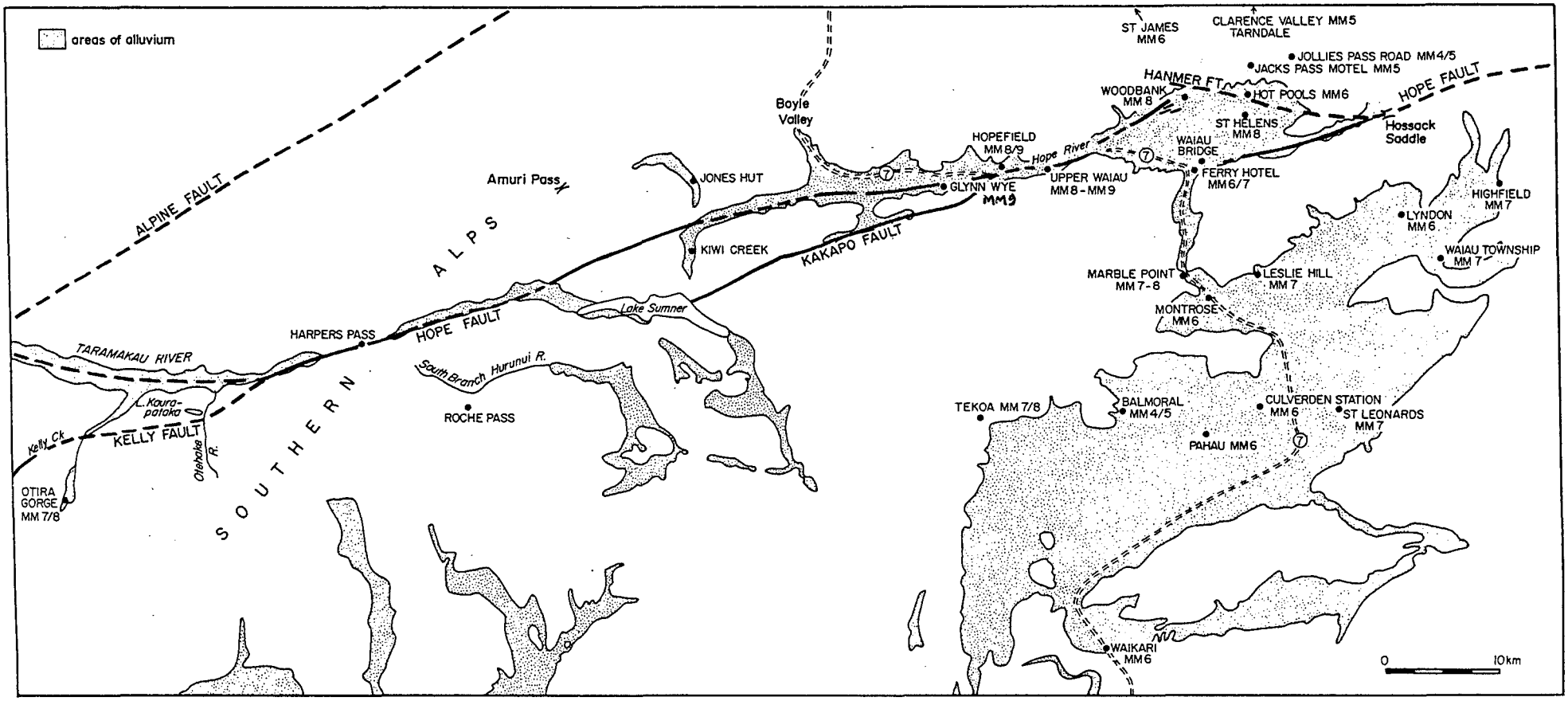


Fig 4·2: Amuri Earthquake: Distribution of Felt Intensities

(Appendix 4).

To the east of Glynn Wye in the Hanmer Basin, ground shaking locally reached MM7 or MM8 (chimney damage, foundation collapse and damage to masonry and brick verneers) but there was little damage to the majority of buildings including those built of cob or stone.

Buildings at Hanmer Springs were undamaged and there was only minor spillage of water and mud at the hot pools (The Press: Sept 4, 1888; McKay 1890). On the south side of the plain, the Waiau Bridge at Hanmer Junction was unscathed, and the old cob-walled Ferry Hotel (Figure 4.2) was only slightly damaged. Notable exceptions in the Hanmer area were the properties of Woodbank and St Helens (Figure 4.2) which suffered considerable chimney damage and cracking of brick and stone work (Appendix 4). Leslie Hills at the north-west margin of the Culverden Plain also suffered serious chimney damage.

However, extreme variations in ground shaking over short distances was one of the most noteworthy characteristics of the 1888 earthquake, summarised in the following eye-witness accounts:

> *"Mr Low's place (St Helens) is a wreck. Fry's Hotel, barely a couple of miles away has hardly a serious crack. Lahmert's (Hotel) at Jack's Pass, had no damage done, nor had the little cottages in the valleys close at hand. Woodbank on the other side of them would have been levelled with the ground, but that the stout new wooden part and a strong verandah propped up the shattered brickwork and broken chimneys of the older portion. The bathhouse stood securely. Leslie Hills on one side of the Waiau is uninhabitable. Montrose on the other escapes scot free...". (Canterbury Times: Sept 14, 1888: p.28).*

And of specific effects at Leslie Hills:

> *"The old detached cob building as sound at the time the shake took place as when erected, had two chimneys sent flying through the roof, and the walls cracked in every direction. The mens huts, not ten chains off, in a far*

> *worse state of repair with the chimney on the balance, received no injury whatever. At the owners house five heavy double chimneys were sent in all directions, and a new addition in wood was wrecked...". (Canterbury Times: Sept 21, 1888: p.26).*

Further:

> *"Over the ranges at the back of Jollies Pass, at the Clarence, St James and Tarndale the earthquake was hardly felt enough to waken people.". (Canterbury Times: Sept 7, 1888 p.18).*

and of the effects at Jollies Pass Hotel:

> *"..the chimney piece ornaments and other articles easily upset were not even displaced. This is supposed to be due to the fact that the hotel (Jollies Pass) as well as that at Jack's Pass, is built almost on the rock; whereas the houses at St Helen's and Woodbank which suffered so severely, are built on loose, open soil with swampy ground in the vicinity. Both St Helen's and Woodbank were old and, it is considered, somewhat badly built houses". (Canterbury Times: Oct 19, 1888 p.17).*

In Westland the strongest ground motions were experienced in inland areas, especially at Otira Gorge where intensities are estimated to have reached MM7 or MM8. In the coastal towns of Hokitika, Greymouth and Westport and in North Canterbury there were numerous reports of chimney damage and breakage of goods, glass and crockery, but overall the strength of ground motions attenuated rapidly. At epicentral distances of 40-60 km, average intensities were no greater than MM6, and there were several localities at shorter distances which experienced ground shaking of MM5 or less (Appendix 4).

In Christchurch, there was very little property damage: parts of eastern Christchurch experienced amplified intensities of up to MM7 and a

few low rise residential buildings suffered minor cracking and chimney damage (Hutton 1888).

Elsewhere in Christchurch even crockery and glass was largely unscathed and intensities may have been lower than MM6. Destruction of the upper 8m of the cathedral spire was widely publicised, but was subsequently attributed to unfavourable construction (Canterbury Times: Sept 7, 1888 p.21; Hutton 1888). The spire was topped by a heavy iron cross and the upper six metres consisted of solid masonry, below which the spire was hollow.

It may be inferred from these combined observations that the severity of site response was strongly affected even at short epicentral distances by local ground conditions, topographic focusing and the considerable thicknesses of alluvial and lacustrine valley and basin fill in the Hope River-Hanmer Plains area.

The 1888 earthquake therefore did not constitute a serious general hazard to well-built low-rise development in North Canterbury, North Westland or Christchurch. The most serious damage was restricted to masonry structures, particularly those constructed of cob, at short epicentral distances. Beyond the immediate vicinity of the fault (approximately <200 metres) the extent of damage to any structure was dependent more on specific site conditions than on the size of the earthquake or the quality or lateral strength of the structure.

## 4.3 1888 Fault Displacements and Structural Controls on Rupture Propagation and Arrest.

In what may constitute the first description of strike-slip faulting in the world, McKay (1890) documented three lateral offsets on wire fences

which crossed the Hope Fault west of Glynn Wye homestead (Figure 4.3).

McKay recorded a 1.5m lateral offset on a fence which extended up the face of the high terrace behind Glynn Wye homestead. The second lateral offset of 2.6m was observed on a fence 1.35 km west of Lake Glynn Wye. This offset was later photographed by Cotton (1947: Figure 7), but he confused it with the westernmost offset of 2.4m at the Glynn Wye Moraine terminus (Figure 4.4). Vertical displacements were locally significant and McKay observed that on the fault, just to the east of Lake Glynn Wye:

> *"over nearly a quarter of a mile (400m) the whole surface is a network of fractures, fissures, slips and dislocations. At one place, an area of about 4 chains (80m) in width and 10 chains or more (>200m) in length has subsided 2ft., as indicated at the fractures, and the middle part of this may have subsided even more than that.". (McKay 1890: p.9).*

The sudden decrease in lateral slip and severe ground deformation at Lake Glynn Wye Graben, and the severe felt intensities at Glynn Wye homestead are consistent with a brief deceleration of the rupture and the radiation of high frequency ground motion as it encountered and was momentarily slowed near the surface by the Lake Glynn Wye Graben.

These observations are consistent with the belief that bends and jogs along strike-slip faults may represent significant barriers to the rapid transfer of slip during earthquakes (Sibson 1985, 1986). Compressional jogs and constraining bends inhibit the rapid transfer of slip due to increased frictional resistance at the jog or bend, which causes deformation to spread out over a broad area. At extensional jogs and releasing bends incipient opening within fluid-saturated crust during earthquakes produces large negative pore pressures (suctional forces) which also strengthen the fault and inhibit the rapid transfer of slip

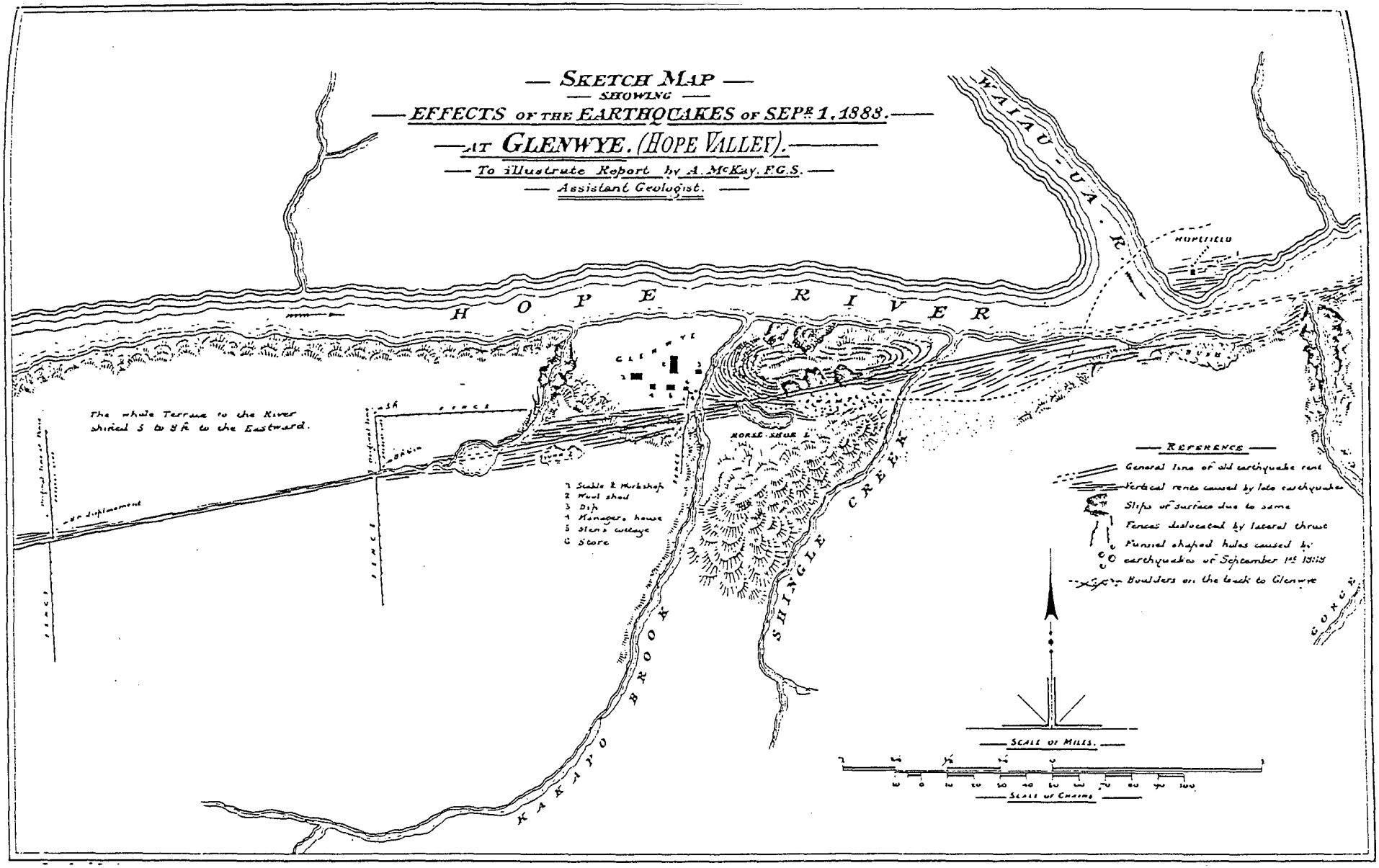


Figure 4.3 From McKay (1890)

(Sibson 1985).

After-shock distributions in the vicinity of larger (>1km wide) extensional fault jogs (cf. Hanmer Basin = 6-7 km wide) indicate that these discontinuities often extend to the base of the brittle crust (10-15 km for typical geothermal gradient) (Sibson 1986). The energy required to to achieve rapid slip transfer against the induced suctions at a jog or bend of these dimensions is comparable to the wave-energy radiated by moderate-large earthquakes. Where rupture is arrested at a large extensional fault jog or releasing bend, a later transfer of fault-slip may occur as fluid pressures re-equilibrate by diffusion allowing strain-energy concentrated at the rupture tip to transfer across the jog or bend (Sibson 1985).

Lake Glynn Wye Graben is only 550-600 m wide and the faults bounding the graben probably converge to form a single plane or narrow zone at a depth no greater than about 500 m (see discussion in Chapter 5). However, the pronounced variation in lateral slip across Lake Glynn Wye Graben indicates that this relatively small extensional fault jog exerted a strong structural control on coseismic rupture propagation during the 1888 earthquake. The implications of these observations for the arrest of the 1888 earthquake and the long term (Late Quaternary) distribution of fault displacement are discussed in Chapter 5.

An hitherto uncited reference to 1888 surface rupture is contained in Jones (1933), and verifies primary fault displacement at McIntosh's Flat (Upper Waiau on Figure 4.2) to the east of Hopefield Station.

Jones writes:

> *"After the earthquake we all learned that the earth fissure which commences at the Hanmer Plains, runs through my old place, and several miles of Glynn Wye, was an old earthquake crack. One side of this crack*

> *seemed to remain firm, while the other side shifted about five feet (1.5 m). I knew this because I had a wire fence running from the hills in a straight line to the river Waiau". (Jones 1933: p.123).*

McKay missed this displacement because

> *"At Jones's station the old earthquake rent passed onto a terrace of lower level, and we had less opportunity for observing it closely". (McKay 1890: p.6).*

## 4.4 Rupture Length

### 4.4.1 Western Limit of Surface Rupture

McKay appreciated that the earthquake had occurred along a pre-existing earthquake fracture, and of the extent of fault displacement he concluded:

> *"as at the furthest west fence on the high terrace flat the amount of shifting was 8ft., (2.4m) and at Glynn Wye Station 5ft., (1.5m) the movement cannot have begun and ended at these places. The displacement of the country to the north of the line of old fracture therefore probably extends from Hopefield Station, at the junction of the Hope and the Clarence (Waiau), to the junction of the Boyle with the Hope, a distance of eight miles.." (13km). (McKay 1890: p.10).*

McKay subsequently changed his mind and increased his estimate of surface rupture to approximately 43 km, for in a later report (McKay 1902) he referred to the 1888 earthquake, stating:

> *"This series of shocks reopened a line of fracture running nearly east and west from the main water divide, between the east and west coasts of the South Island, along the Hope and Waiau-ua valleys, and along the Hanmer Plain to the Hoosack Saddle at the northern*

> *end of the Leslie Hills...beyond this to the eastward the effects of the earthquake were not traceable on the surface". (McKay 1902: p.5 & p.21).*

Recent authors have estimated rupture lengths of 50 km (Suggate et.al. (1978); Berryman (1984)), and 150 km (Knuepfer 1984). The 50 km estimate of surface rupture is presumably the distance from the Hossack Saddle east of Hanmer Plains, westward to the junction of the Hope River and Kiwi Creek, the furthest point examined by McKay west of Glynn Wye. McKay noted:

> *"We might have followed the earth-fractures, old and new, about a mile farther (beyond the river junction), to the edge of the bush on the east side of the low saddle already mentioned; but the day was passing...". (McKay 1890: p.12).*

Surface rupture in the main shock may have extended beyond Kiwi Creek into the Hurunui or Taramakau valleys, though this is more difficult to authenticate. This route to North Westland was frequently used by gold miners and cattle drovers during the 1860's, but by the late 1880's Arthur's Pass formed the principal route from Canterbury to Westland and the upper Taramakau and Hurunui valleys were rarely frequented (Burrows, 1974). Hence, there are no eye-witness reports from this area which might have confirmed the existence of surface rupture.

Yet the strongest ground shaking in Westland was experienced in the Otira Gorge and a vivid eye-witness account of the earthquake from Dyer's Accommodation House at the entrance to the gorge (frontispiece) describes ground motions perhaps of a similar intensity to those experienced at Hanmer Plains, the formation of new springs in the gorge, 3 hot and 1 cold, and a large rift in Kelly's Creek (Canterbury Times: Sept 14,

1888). Hutton (1888) also commented on the rift in Kelly's Creek, but added that he could not obtain further details about it.

Kelly's Creek lies on the trace of the Kelly Fault, which is either the Hope Fault proper or a major splay of the Hope Fault trending WSW from the junction of the Otehake and Taramakau rivers through the valley occupied by Lake Karaupataka (Figure 4.2 ). The "rent in Kelly's Creek" may have been a landslide or simply ground cracking during heavy shaking, but if this or the hot spring activity was the product of primary fault displacement, then the 1888 surface rupture length could be increased to a maximum of approximately 100 km.

The evidence remains equivocal, however, and a surface rupture of >40-50km does not seem consistent with overall felt intensity attenuation data which indicate a magnitude unlikely to generate such a large primary fault displacement (discussion in section 4.5 )

### 4.4.2 Eastern Limit of Surface Rupture

It is not clear from McKay's comment whether the "effects of the earthquake" as far east as the Hossack Saddle were the product of primary fault displacement or simply ground shaking. The decrease in observed surface displacement and ground renting, from west of Glynn Wye Sation to Hanmer Basin indicates that the rupture was decelerating as it travelled eastward along the Lower Hope and Waiau valleys. The concentration of aftershocks in the Hanmer area during the weeks following the earthquake (Section 3.6) provides corroborative evidence of rupture arrest at the Hanmer Basin extensional jog.

There is no direct connection between western and eastern strands of the Hope Fault (Figure 4.2). The Hope Fault bounds the NW and SE sides

of Hanmer Basin which forms a complex junction between western and eastern large-scale segments of the Hope Fault. Formation of the Hanmer Basin has involved the development of active secondary structures such as the Hanmer and Jollies Pass faults (Figure 4.2). The Hope Fault may be linked across the Hanmer Basin via these secondary faults and through a network of interconnecting strike-slip and dip-slip fractures within the basement rocks. If this is correct it is unlikely that surface rupture was transferred rapidly to the eastern strand of the fault during the 1888 earthquake. Recent field mapping of Late Quaternary structures at the western end of Hanmer Basin has identified numerous normal and oblique-normal faults disrupting the Quaternary cover deposits, but there is no evidence of 1888 displacements on the principal strike-slip fault trace, which traverses the NW margin of Hanmer Basin as far as Woodbank (Figure 4.2) where it terminates as a series of complex splays (J. Pettinga pers.comm.).

In view of the probable nature of the Hanmer Basin as a major fault segment boundary, and the apparent absence of lateral displacement on the Hope Fault bounding the NW margin of Hanmer Basin, estimates of rupture taken from an eastern extent at Hossack Saddle seem unlikely.

The main shock of Sept 1, 1888 almost certainly did not generate surface rupture on the eastern strand of the Hope Fault beyond Hanmer Basin. When McKay left the Amuri District he followed the eastern strand of the fault out to Kaikoura, commenting that the damaging effects of the earthquake were

> *"not very noteworthy, only one or two chimney tops having been injured on the Kowhai Flat, and there were a few fallen rocks in the bed of the Charwell River, near Green Hills". (McKay 1890: p.14).*

Knuepfer (1984) believed he could recognise displacements of very young geomorphic features at several sites along the Hope Fault east of Hanmer Plains, which he tentatively attributed to surface rupture along this strand of the fault in strong aftershocks or a second main shock, on Oct 23 and Oct 26 1888. These shocks were felt more strongly in Kaikoura than at Hanmer Plains, and McKay (1890) had speculated that they indicated the extension of surface rupture toward Kaikoura (Appendix 5). However, timing of initial strong motion observations indicate that the shock of Oct 23 originated well to the north of Hanmer Plains (Hutton 1888), and newspaper reports describe the heaviest ground shaking attributed to this shock as having occurred in Taranaki and Northern Wairarapa (Canterbury Times: Oct 25, 1888). These observations are further supported by Hogben (1891) who documented mainly North Island felt reports for the shock of Oct 23, and Wellington as the dominant felt area for the shock of Oct 26.

It therefore seems unlikely that surface rupture extended beyond the Hanmer Basin, either during the main shock, or in subsequent aftershocks. The earthquakes of 23 Oct and 26 Oct are more likely to have originated in the North Island or northern South Island than to have occurred on the Hope Fault, and the description of the ground motions experienced at Hanmer Plains during these shocks (Appendix 5) is more suggestive of the effects of long-period waves at a large epicentral distance.

## 4.3 Foreshocks and Aftershocks

The first pronounced foreshock to the main event occurred at 10:03 p.m. on Aug 30 and was felt strongly in Christchurch, Kaikoura and Westport, but only slightly on the Hanmer Plains. The timing of initial

felt-motion observations at a number of localities indicate a source beneath the Upper Hurunui valley (Hutton 1888).

In Hokitika and Kumara (on the West Coast), frequent tremors were experienced from 10:00 p.m. Aug 31 until the main shock 6 hours later (Canterbury Times: Sept. 7, 1888).

For three days following the main shock, Hanmer Plains experienced frequent tremors, with heavier shocks felt at intervals elsewhere in North Canterbury and Westland. By the evening of Sept. 3, most centres in the region had reported at least 30 felt aftershocks, of which at least one achieved MM5 intensity in Christchurch (Ibid: Sept. 7, 1888).

Minor tremors occurred daily in Westport for a fortnight, and at Reefton for nine days, while Hanmer Plains was the focus of intense aftershock activity for at least a month (Hutton 1888). Heavier shocks were experienced in Westland and at Christchurch on Sept. 9, Sept. 28 and Oct. 12, the latter two events generating ground motions of MM6 in the Amuri District (Ibid: Oct. 25, 1888).

## 4.4 Directivity and Epicenter

Eye-witness accounts of the propagation direction of the earthquake indicate that the fault ruptured from west to east. An observer at Glynn Wye reported:

> *"the shock passed down the valley eastward from Glynn Wye at a measurable rate, and was accompanied by a terrific roaring noise, which died away in the distance, while things were quiet at the place where he stood". (McKay 1890: p.14).*

McKay thus inferred the epicentral region of the Sept. 1 earthquake to have been:

> *"at some point to the west of Glynn Wye, perhaps further west than the junction of the Kiwi with the Hope, and that it travelled eastward with increasing force to Glynn Wye and Hopefield, beyond which places, by what appears at the surface, its destructive character began to be less". (Mckay 1890: p.13).*

The timing of initial strong-motion was recorded in a number of North Canterbury and Westland settlements and used by Hutton (1888), to describe an epicentre to the east of Amuri Pass and about 26km WNW from Glynn Wye. A recent reassessment (basis unknown) locates the epicenter near the junction of the Hope and Boyle rivers (W.D. Smith pers.comm. quoted in Wood 1984) (Figure 4.2).

All three estimates place the epicenter to the west of Glynn Wye. How far to the west remains uncertain, but even in the absence of unequivocal reports of ground rupture beyond Kiwi Creek it may be possible to evaluate potential nucleation points, where large earthquakes may be initiated, by examining the large scale geometry of the Hope Fault between Glynn Wye and the Otira Gorge. This possibility will be discussed in detail in Chapter 5.

## 4.5 Magnitude Estimates

### 4.5.1 Estimates from Felt Intensity

The magnitude* of the Sept. 1 earthquake has previously been estimated at M=7.0 (Hayes 1953), M=6.5-6.75 (Dibble et.al. 1980), and M=7.3 (Smith &

Berryman 1983, 1986). The extent of the region of high felt intensities was less than that for the the 1968 Inangahua earthquake (M=7.1) (Appendix 6). If the 1888 earthquake was a shallow (h<40km) Type B event (Smith 1978), then a magnitude of 6.4 to 6.8 for this event is likely (Appendix 7).

### 4.5.2 Estimates from Rupture Length and Displacement

Relationships between earthquake magnitude and various fault parameters have been recognised from compilations of world-wide historical earthquakes and regressions of magnitude on, rupture length, fault displacement per event, ruptured fault area, and seismic moment. A number of empirical methods for estimating earthquake magnitude have been proposed using these fault parameters (summary in Schwartz et.al. 1984).

i) Slemmons (1982) proposed the following relationship between rupture length and surface wave magnitude (Ms) for strike-slip faults:

$$Ms = 1.404 + 1.169 \text{ Log } L \qquad (3.1)$$

where L = rupture length in metres (m).

*Previous magnitude estimates for the 1888 Amuri earthquake have been given without reference to the magnitude scale used (an exception is Dibble et.al. 1980). However, in the magnitude range 6.0-7.0 $m_b$(body wave magnitude), $M_S$(surface wave magnitude), and $M_L$(local magnitude) are approximately equal (e.g Bath 1981). In this study $M_S$ will be used to describe earthquake magnitude.

For maximum surface displacement versus magnitude, he gives:

$$Ms = 6.974 + 0.804 \text{ Log } D \qquad (3.2)$$

where D = surface displacement in metres (m).

ii) Wyss (1979) proposed a relationship for all fault types, between surface wave magnitude and the total down-dip area of the ruptured fault plane. Down-dip rupture area or fault width is estimated from the spatial pattern of earthquake aftershocks, or from the instrumental seismicity and geological information on local crustal structure. The relationship is:

$$Ms = 4.15 + \text{Log } A \qquad (3.3)$$

where A = down-dip width x rupture length ($km^2$)

iii) Hanks & Kanamori (1979) developed a general moment magnitude scale, where moment magnitude is equivalent to surface wave magnitude in the magnitude range $5< Ms <7.5$. The expression is as follows:

$$Mw = 2/3 \text{ Log } Mo - 10.7 \qquad (3.4)$$

Here, knowledge of the seismic moment ($M_0$ dyne.cm) released in the earthquake is required. This may be measured either directly from a seismogram or calculated from the parameters of surface displacement and

rupture length, according to the expression;

$$M_0 = \mu UA \qquad (3.5)$$

where, $\mu$ = shear modulus of the faulted rock (usually taken as 3 x $10^{11}$ dyne/cm»)

U = average slip across the fault (in centimetres)

A = fault rupture area, (normally defined by the depth and extent of the aftershock distribution, which may extend beyond the observed surface rupture).

Derivation of the moment-magnitude relationship assumes constant stress drop in large earthquakes, thus regional variations in stress drop (due to spatial variations in fault slip) may contribute to errors in calculation (Schwartz et.al. 1984). Spatial variations in fault slip were observed following the 1888 earthquake, but the distances over which these variations were observed are small (4 km ) compared with the estimated rupture length (approximately 40 km), so an estimate of seismic moment based on the static fault parameters (rupture length and average displacement) seems reasonable.

Using rupture lengths of 40 km and 100 km as preferred and upper bound 1888 earthquake rupture lengths respectively, an average displacement of 2.0 metres, and a down-dip fault width of 12 km (the conventional depth model for N.Z. upper crustal earthquakes (N.Z Seismological Observatory 1988)), I have calculated the magnitude of the 1888 earthquake using each of the equations outlined above (Table 4.1).

Magnitude estimates derived using rupture length-versus-magnitude and rupture area-versus-magnitude are identical and at $M_S$=6.8 and $M_S$=7.2

respectively these values are slightly greater than estimates based on felt intensities. The moment magnitude calculation of seismic moment with a rupture length of 100 km, also yields a magnitude estimate of $M_S$=7.2.

The lowest estimate ($M_S$=6.5) is obtained using the inferred seismic moment for a rupture length of 40 km. The largest estimate ($M_S$=7.3) is obtained using the maximum observed fault displacement at Glynn Wye (2.6m).

The exact extent of surface rupture and the size of maximum displacement are poorly constrained and do not permit an unequivocal estimate of magnitude. But assuming that the combination of empirical relationships are applicable to this earthquake and that historical eye-witness reports provide an accurate record of the event, the following conclusions may be drawn.

i) A minimum of 40 km surface rupture occurred west of Hanmer Basin during the 1888 earthquake, therefore the magnitude estimates based on this rupture length represent a lower bound of between $M_S$=6.5 and $M_S$=6.8.

ii) Estimates based on a 100 km surface rupture from Hanmer Basin to Otira Gorge, constrain the magnitude to an upper bound of $M_S$=7.2.

iii) The highest estimate of $M_S$=7.3 derived by using the maximum observed (2.6m) surface displacement is probably an over estimation. The three alternative relationships based on rupture length, rupture area and seismic moment yield similar results and magnitude increases only 0.3 despite doubling the rupture length or area. These arguements indicate that a magnitude range of $M_S$=6.5 to $M_S$=7.2 is likely to encompass the

| | Slemmons (1982) Rupture length vs Magnitude (Ms). | Slemmons (1982) Rupture length vs Magnitude (Ms). | Slemmons (1982) Max. Displacement vs Magnitude (Ms). | Wyss (1979) Rupture Area vs Magnitude (Ms) | Wyss (1979) Rupture Area vs Magnitude (Ms) | Hanks & Kanamori (1979). Moment Magnitude Scale**. | Hanks & Kanamori (1979). Moment Magnitude Scale**. |
|---|---|---|---|---|---|---|---|
| Equation | Ms=1.404 + 1.169LogL | Ms=1.404 + 1.169LogL | 6.974 + 0.804LogD | Ms=4.15 + Log A | Ms=4.15 + Log A | Mw**=2/3logMo - 10.7 | Mw**=2/3logMo - 10.7 |
| Rupture Length L | 40,000 (m) | 100,000 (m) | n.a. | 40.00 (km) | 100.00 (km) | $4.0 \times 10^6$ (cm) | $10.0 \times 10^6$ (cm) |
| Fault Width W | n.a. | n.a. | n.a. | 12.00 (km) | 12.00 (km) | $1.2 \times 10^6$ (cm) | $1.2 \times 10^6$ (cm) |
| Rupture Area Ar = LxW | n.a. | n.a. | n.a. | 480.00 ($km^2$) | 1200.00 ($km^2$) | $4.8 \times 10^6$ ($cm^2$) | $50.0 \times 10^6$ ($cm^2$) |
| Maximum Surface Displacement ($D_{max}$) | n.a. | n.a. | 2.6 (m) | n.a. | n.a. | n.a. | n.a. |
| Average Displacement ($D_{av}$) | n.a. | n.a. | n.a. | n.a. | n.a. | 200.00 (cm) | 200.00 (cm) |
| Shear Modulus (u) (dyne/cm ) | n.a. | n.a. | n.a. | n.a. | n.a. | $3 \times 10^{11}$ | $3 \times 10^{11}$ |
| Seismic Moment Mo =(Ar)x(u)x($D_a$) (dyne.cm) | n.a. | n.a. | n.a. | n.a. | n.a. | $2.9 \times 10^{20}$ | $3.00 \times 10^{21}$ |
| Estimated Magnitude (Ms*). | (6.8) | (7.2) | (7.3) | (6.8) | (7.2) | (6.5) | (7.2) |

Comments

* Surface wave magnitude, body wave magnitude, and local magnitude are approximately equal in the range 6<M<7 (Bath 1979).

** Mw=Ms for earthquakes in the range 6<Ms<7.5 Kanamori (1977).

TABLE 4.1. Estimations of 1888 Amuri Earthquake Magnitude Using Empirical Relationships Between Magnitude and Fault Parameters.

true value.

iv) By combining the empirical estimates of magnitude with those based on felt intensity data in Section 3.3.1, I propose a preferred magnitude range of $M_S$=6.5-6.8 for the 1888 earthquake.

## 4.6 Preservation of the 1888 Surface Rupture

The 1888 earthquake surface rupture occurred along the composite surface trace of the Hope Fault in the Lower Hope Valley. In many places between Horseshoe Lake (State Highway 7) and the junction of the Hope and Boyle rivers, the effects of the 1888 earthquake can be readily distinguished from older features on composite Hope Fault scarps (Figure 4.5 and Map 4). The upthrown (north) side of the fault at the western margin of Horseshoe Lake is deeply pitted with collapse structures which formed during the 1888 earthquake, presumably in response to liquefaction of the underlying sediments (Figure 4.6).

On purely strike-slip sections of the Hope Fault the 1888 surface rupture comprises a 15-20m wide zone of rumpled or disturbed ground forming multiple scarps at angles of typically <20°. In the vicinity of bends or side-steps along the Hope Fault trace the zone of deformation is much wider, developed as a response to extension or compression (>800-900 m in Poplars Graben, >500m at Lake Glynn Wye Graben. Recognition of the 1888 rupture at these localities is restricted to the principal fault trace, or subsidiary splays within 20-30m of this trace.

Where the Hope Fault traverses less intensively grazed parts of Glynn Wye Station, these 1888 scarps are up to 1m in height, thickly vegetated,

Figure 4.4 A 2.4 m lateral offset on a fence constructed across the Hope Fault to the east of Glynn Wye moraine, produced during the 1888 earthquake. (See also Map 1). Photograph by A. McKay.

Figure 4.5 View looking north-east toward the 1888 surface rupture (arrow) superimposed on the composite Late Quaternary Hope Fault scarp formed in Glynn Wye Advance terminal moraine. The fence photographed by Alexander McKay was formerly located in the shelter-belt 400 m to the east (upper right). Note that the height of the scrub covered scarp at this locality relates to the strike-slip juxtaposition of topography: moraine crest on north side versus moraine flanks on south side. However, the grass covered slope (upper right) is underlain by outwash which has been upwarped 15 m at a slight constraining bend in the fault (see discussion in Chapter 5).

and commonly preserve scarp angles of 65-80° (Figure 4.7, Map 4 and discussion in Chapter 5).

The moderately high rainfall (c.1500-1800mm/yr) and limited agricultural activity in the Lower Hope Valley during the late 19th century presumably allowed very rapid re-colonisation of the free-face scarps following the earthquake. Scarps were initially colonised by mosses and ferns, succeeded by tussock and matagouri which even today provides protection to the scarps by discouraging stock trampling and browsing.

## 4.7 Summary

The Amuri earthquake of Sept. 1 1888 was preceded on the evening of August 30 by a widely felt foreshock with a probable origin in the Upper Hurunui or Taramakau valleys. Frequent tremors were felt in parts of Westland during the following night, for six hours before the main shock.

The exact location of the main shock epicenter is unclear, but was to the west of Glynn Wye Station. The main shock of magnitude Ms=6.5-6.8 occurred soon after 4:00 a.m. Sept. 1 1888, on the Hope Fault west of Glynn Wye Station. The shock propagated eastward achieving maximum ground shaking intensities of MM9, with observed fault displacements of up to 2.6 metres.

Fault displacement reduced sharply across the Lake Glynn Wye extensional fault jog, but continued to the Hanmer Basin where the rupture was effectively arrested. This area was the focus of intense aftershock activity for at least a month following the main shock; a number of aftershocks generated local felt effects of at least MM6.

A minimum surface rupture of approximately 40km extended from the

Figure 4.6 Detail of the Hope Fault at the western margin of Horseshoe Lake. Large (6-7 m wide and 2-3 m deep) collapse pits were formed in the terrace surface on the north (upthrown) side of the fault during the 1888 earthquake.

Figure 4.7 An example of 1888 fault scarps preserved along the Hope Fault at Glynn Wye. The grubber is 0.40 m long and the field book is placed at the top of the scarp which is 1.1 m high and dips 74°S. This scarp is located at the constraining bend at the west face of Glynn Wye moraine and represents the largest vertical displacement (1.1 m) observed on 1888 scarps during this study (see further discussion in Section 5.8, Chapter 5).

western margin of the Hanmer Basin, westward at least to Kiwi Stream. The rupture may have extended eastward to Hossack Saddle at the eastern margin of Hanmer Basin, and westward to Otira Gorge, a total distance of approximately 100km, but the evidence for such a large rupture length is equivocal and not consistent with the recognition in this study of Hanmer Basin as a probable major fault segment boundary.

The main shock was felt strongly over a wide area of North Canterbury and Westland and was recorded as far away as Southland, Taranaki and Wairarapa. At epicentral distances greater than 40-50 km, average felt intensities were alarming but did not exceed MM6. Damage to the cathedral spire in Christchurch was widely publicised, but was probably due to poor construction (Canterbury Times, Sept.7 p.21). A few low rise residential buildings mostly in eastern Christchurch, suffered minor cracking and chimney damage, but elsewhere even crockery and glass was largely unscathed.

Damage reports and the spatial distribution of felt effects emphasise extreme variations in seismic effects over short distances. Although ground motions were locally severe, the most damaging earthquake effects were restricted to the immediate vicinity of the fault and isolated serious damage at greater distances can be attributed primarily to weak construction, and pronounced local site effects. Felt intensities of MM9 at Glynn Wye and MM8 in the Hanmer Basin were probably enhanced by topographic focusing, possibly fault jog rupture, and almost certainly by moderate-large (>200m) thicknesses of alluvial and lacustrine valley fill.

The earthquake was a destructive but not disastrous earthquake, and previous estimates of magnitude and felt intensity have been somewhat high. The earthquake occurred at a time in local history when media

communications were sufficiently developed to afford a wide and inquiring coverage of the event, but before the advent of modern (post 1930's) building materials and design codes, which would doubtless have prevented much of the damage. These factors must be given careful consideration when evaluating the record of early historic events, to avoid an excessively conservative assessment of the contemporary seismic hazard associated with faulting in North Canterbury.

The 1888 Amuri earthquake also represents a classic example of strike-slip rupture along a segmented fault zone, which may be used to calibrate a study of the longer term (Late Quaternary) distribution of fault slip at suitable localities along the historic rupture length. These Late Quaternary fault displacements on the Hope Fault at Glynn Wye are discussed in detail in Chapter 5.

# CHAPTER 5 LATE QUATERNARY DISPLACEMENTS ALONG THE HOPE AND KAKAPO FAULTS

## 5.1 Introduction

A number of workers have measured and reported Late Quaternary lateral fault displacements on the Hope and Kakapo faults. The respective studies span 35 years and a revolution in the earth sciences: the international development of plate tectonic theory, and the recognition in this country that large lateral fault displacements have accommodated relative plate motion across central New Zealand during the Late Quaternary (e.g Wellman 1949; Lensen 1964, 1968).

Early workers on the Hope Fault at Glynn Wye such as Wellman (1953), Clayton (1966) and Freund (1971) found that their observations did not find wide acceptance becausethe suggestion of very high rates of Late Quaternary displacement on the Hope Fault was contrary to the weight of contemporary opinion (e.g. Suggate et.al. 1978).

The Glynn Wye locality on the Hope Fault has been one of the most frequently studied because of the clear exposure of displaced landforms in the absence of forest cover and, especially, because of the size of the displacements (and the rates of displacement which they imply). International attention has also focused on the extensional and compressional structures developed at side-steps and bends in the main fault trace (e.g. Aydin & Nur 1982; Mann et.al. 1983; Woodcock & Fisher 1986). With the exception of Clayton's work (1966; 1968), however, all previous studies of the faulting or fault structure have been conducted as a part (often a small part) of studies which have involved a number of localities and a number of faults.

The emphasis given to the Late Quaternary displacements in most previous studies conveys more about the various points which respective authors sought to illustrate, than of the specific size, style and implications of the displacements. Until now there has been no detailed study of the Late Quaternary fault displacements at Glynn Wye.

The following objectives are considered in this Chapter.

i) To describe the Late Quaternary displacements on the Hope and Kakapo faults at Glynn Wye, and discuss the field relationships between the measured displacements and associated landforms which were mapped in detail and surveyed during this study.

ii) To provide a detailed review of the previous faulting studies at the respective offset localities and compare these results with this study.

iii) To describe the results of trenching at two sites on the Hope Fault, and present evidence for the recognition and dating of five earthquakes of characteristic magnitude and recurrence interval on the Hope River Segment of the Hope Fault prior to the 1888 event.

iv) To describe the relationship between fault geometry and the development of extensional and compressional fault jogs (side-steps) and releasing and constraining bends (changes of trend) in the fault trace, and discuss the effect that these structures have on rupture propagation during earthquakes, and the long-term spatial distribution of displacement.

This chapter is divided into five main sections, the first three of which (Sections 5.2 to 5.7 ) provide a description and analysis of Late Quaternary fault displacements at three principal study sites. The

study sites are: (i) Kakapo Fault, Dismal Valley, (ii) Hope Fault, Glynn Wye Moraine Complex, (iii) Hope Fault, Raupo Swamp-Manuka Creek (refer to Map 1). Sections 5.8 and 5.9 discuss the role and significance of fault jogs and fault bends at Glynn Wye; in forming secondary fault segment boundaries (the Hope Fault west of Hanmer Basin is defined as a primary fault segment in this study) and in affecting the short and long-term transfer of slip from one secondary fault segment to another.

Three secondary fault segment boundaries are identified on the primary Hope River Segment of the Hope Fault. These are: (i) an 8 to 13° SW constraining bend south of the Hope-Boyle River junction (visible on satellite photographs, see Figure 1.2), (ii) the 700-900 m wide compound releasing-constraining fault bend bounding Poplars Graben and (iii) the 500-600 m wide extensional fault jog forming Lake Glynn Wye Graben. These features are annotated on Map 1.

## 5.2 The Kakapo Fault: Dismal Valley Locality (Map 2 & 3 in map pocket)

### 5.2.1 Site Description

On the south side of Dismal Valley three kilometres SW of the Glynn Wye advance terminal moraine the Glenhope Advance terminal moraine forms a thin loop of till deposited on a basement ridge. Outwash from the later Glynn Wye Advance has flooded around this moraine, and forms the main aggradation surface in Dismal Valley (Figure 5.1).

The Kakapo Fault strikes 072° along Kakapo Brook on the south side of Dismal Valley and is upthrown to the north. Lateral displacements are recorded on the Glynn Wye Advance outwash surface and a flight of degradational river terraces formed by the Kakapo Brook (Figure 5.2 & Stereopair #1).

Along this reach Kakapo Brook flows on the downthrown side of the fault where bed-load sediment has been trapped forming a floodplain which is braided and up to 200 m wide. Four hundred metres to the east of the offset terraces, Kakapo Brook crosses the projected strike of the fault and enters a gorge produced by down-cutting in response to relative uplift on the fault (Stereopair #1).

### 5.2.2 Late Quaternary Fault Displacements

A lateral offset of 105 ±15 m on the Glynn Wye Advance outwash surface is measured from the break in slope between the Glenhope Advance moraine and the outwash on the north side of the fault, and moraine and the western margin of the small lake which has ponded on Glynn Wye outwash on the south side of the fault (Figure 5.3 & Map 3).

Five hundred metres to the east the fault traverses and laterally

Figure 5.1 View looking south-west toward the south side of Dismal Valley, from ridge top between Hope and Kakapo Faults. Kakapo Fault (arrows) traverses the Glenhope Advance terminal moraine (ghm) Glynn Wye outwash (gwo) and a flight of river degradation terraces (left centre). Kakapo Brook forms a braided floodplain on the south (downthrown) side of the fault. Note also the prominent (c.3 m high) upward slope-facing ridge rent scarps in the foreground.

Figure 5.2 Aspect similar to Figure 5.1, but with emphasis on the offset degradational terraces. Note the trimming of terrace risers on the downthrown side of the fault.


ghm
gwo

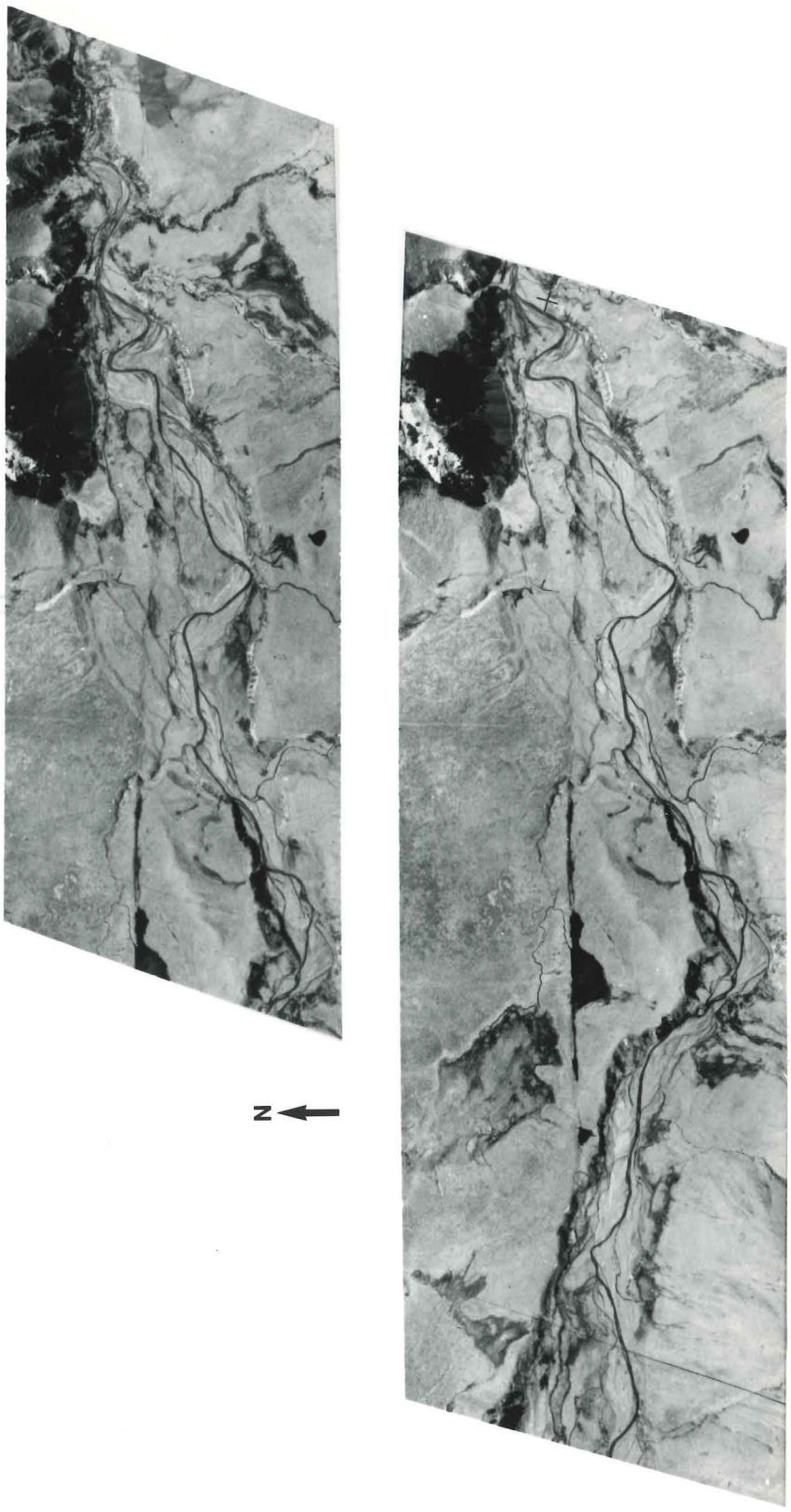


Stereopair #1 : Scale 1:20 000. Kakapo Fault offsetting a flight of degradational river terraces in Dismal Valley. Till of the Glenhope Advance moraine mantles a basement ridge south of the fault and the small lake. The highest offset degradational terrace riser is cut into Glynn Wye Advance outwash. Kakapo Brook forms a braided floodplain on the south (downthrown) side of the fault but meanders sharply where it crosses the axis of relative uplift to the east.

offsets five degradational terrace risers (R1-R5) by 75 ±5 m, 47 ±5 m, 30 ±12 m, an indeterminate offset (R4), and 23 ±2 m respectively (Table 5.1) (Stereopair #2 & Map 3). The oldest of these is cut into the Glynn Wye Advance outwash surface which records a vertical displacement of 6.8 ±0.1 m (Table 5.1). The slope on the outwash surface is negligible at this locality so the measured vertical displacement should not be seriously affected by the 105 ±15 m lateral movement. On the south (downthrown) side of the fault the Glynn Wye surface is 15 m above the modern floodplain of Kakapo Brook; the lowest terrace T5 is only 2 metres above this level.

Measurement of the lateral and vertical displacements at this site is difficult because the terrace risers trend sub-parallel to the fault, and the fault trace across the terraces is diffuse and has been modified by mass movement.

Detailed geomorphic mapping of abandoned channels on the river terraces has shown that the channel patterns cannot be matched on each side of the fault; channels on the south side of the fault trend parallel to the fault where they intersect the fault scarp (Map 3). I infer this to indicate that Kakapo Brook remained active on the downthrown terraces for some time after the equivalent surfaces on the north side of the fault were abandoned. Trimming of the downthrown terrace risers has occurred (as judged from equivalent terrace tread widths on the north side of the fault), but the extent to which fault displacements are exaggerated is difficult to assess, because the terrace risers are sinuous and terrace tread width varies over short distances.

The interaction between fluvial processes and faulting at this locality is clearly complex, and there is some evidence to suggest that


Stereopair #2 : Scale 1:7000. Kakapo Fault offsetting degradational river terraces at Kakapo Brook, Dismal Valley. The highest terrace riser (R1) is cut into the Glynn Wye outwash surface which is 22 m above the active floodplain of Kakapo Brook. Note the diffuse fault trace across the faulted terraces and the channel patterns parallel to the fault on downthrown terrace surfaces, which indicate trimming of the downthrown terrace risers.

| | Features Displaced | Lateral Displacement on Feature (m) | Vertical Displacement on Feature (m) | | Age | Comments |
|---|---|---|---|---|---|---|
| HOPE FAULT: MANUKA CREEK | Terrace Riser R0/Terrace T1 | 36 ± 3 | Terrace T1 | 2.4 0.3 | 3482 ± 77 yr | Terrace T1 is backed by the riser R1. Riser R2 forms the down-dropping riser from T1 to T2 (see Fig. 5.17). |
| | Terrace Riser R1/Terrace T2 | 36 ± 0.5 | Terrace T2 | 2.1 0.3 | <3482 ± 77 yr | Wood was obtained in a trench 1.1 m beneath T1 at 3482 ± 77 yr BP. Displacements were measured |
| | Terrace Riser R2/Terrace T3 | 18 ± 3 | n.d. | | n.d. | from the crest, mid-point, and toe of each riser. |
| HOPE FAULT: GLYNN WYE MORAINE | Eastern depositional face of Glynn Wye advance terminal moraine | 286 ± 6 | n.d. | | 17 000 ± 1000 yr | The displacement was measured at the break in slope between the Glynn Wye Advance outwash surface and the gently undulating terminal moraine |
| Airphoto Run No. GS 544/25-32 | | | | | | |
| Altitude: 2 134 m | Meltwater terrace riser forming west face of moraine | 265 ± 9 | n.d. | | 17 000 ± 1000 yr | This feature is inferred to be of near-equal age to the moraine. The difference in displacement is inferred to be due to shortening and subsidiary faulting at the compressional fault bend along the length of this offset. |
| Focal Length: 100 mm | | | | | | The displacement was measured from 1:3000 scale vertical air photo enlargements. |
| Scale: 1:15 000 | Meltwater Terrace Riser 300 m west of Glynn Wye Moraine. | 148 ± 6 | n.d. | | 17 000 ± 1000 yr | This feature is also inferred to be of near-equal age to the moraine. The greater deficit in offset is attributed to a partitioning of fault slip during successive earthquakes among numerous listric-normal faults within the >600 m wide Poplars Graben. |
| KAKAPO FAULT: DISMAL VALLEY | Morphological contact between the Glenhope Advance terminal moraine and the Glynn Wye Advance outwash surface. | 105 ± 15 | n.d. | | 17 000 ± 1000 yr | It is the age of the Glynn Wye outwash which constrains the age of this displacement. The absolute age of the Glenhope moraine is not critical. |
| Airphoto Run No. GS 450/1-15 | Degradational River Terraces of the Kakapo Brook | | | | | The riser R1 is cut into the Glynn Wye outwash forming the main surface in Dismal Valley. I infer that flood-plain level remained high until deglaciation at about 14 000 yr BP. |
| Altitude: 1 676 m | Terrace Riser R1/Terrace T1 | 75 ± 5 | Glynn Wye Outwash | 6.8 ± 0.1 | 17 000 yr | No age estimates were obtained for these terraces in this study, but Knuepfer (1984) records an age of 4890 ± 680 yr for what was either T3 or T4 of this study. Wellman (1985) records an age of 5900 yr BP for apparently the same surface. Both estimates were derived from weathering rinds. |
| Focal Length: 100 mm | Terrace Riser R2/Terrace T2 | 47 ± 5 | Terrace T1 | 3.2 ± 0.1 | n.d. | |
| Scale: 1:10 500 | Terrace Riser R3/Terrace T3 | 37 ± 5 | Terrace T2 | 0.9 ± 0.1 | n.d. | |
| | Terrace Riser R4/Terrace T4 | n.d. | Terrace T3 | 2.1 ± 0.1 | n.d. | |
| | Terrace Riser R5/Terrace T5 | 23 ± 2 | Terrace T4 | 1.2 ± 0.1 | n.d. | |
| | | | Terrace T5 | 1.1 ± 0.1 | n.d. | n.d. n.d. |

Notes: n.a.= not applicable
n.d.= not determined

TABLE 5.1. Late Quaternary Displacements on the Hope and Kakapo Faults.

in the last 1000 years Kakapo Brook has alternated between phases of aggradation and degradation in this part of its catchment. Augering on the down-thrown terrace T5 at the base of the Kakapo Fault scarp revealed a 1.1 m thickness of overbank sands and silts. Terrace T5 north of the fault is underlain by 0.4 m of loessic soil.

Evidence of a recent phase of aggradation comes further east where the projected strike of the fault crosses the modern floodplain of Kakapo Brook. At this site a 2.3 m thick sequence of overbank silts and peats is exposed in the bank of the lowest, apparently unfaulted terrace (Figure 5.4). This surface is 1.5 m above the modern floodplain but is not correlated with terrace T5 upstream. The base of this exposure is about 0.5 m below the average height of the modern floodplain.

Peat from the interval -1.00 to -1.05 m, and burnt wood from -0.40 m was sampled for $^{14}C$ dating, to estimate the (maximum) age of the overlying surface. The peat was dated at 605 ±55 yr BP and the burnt wood was young (i.e. <250 yr B.P.) (NZ 7584 and NZ 7589 respectively, Appendix 1). The age from the peat indicates that the recent aggradation period began at least 600 years ago, from a level which was probably 2.0 ±0.5 m below the present.

This evidence of repeated renewal of activity on the lowest surfaces above Kakapo Brook, frustrates an assessment of recent faulting on the basis of geomorphic evidence alone. Trenching will be required, before any definitive statement of activity may be made, but this was considered beyond the scope of this project.

A comparison between the geomorphic expression of the Kakapo and Hope fault scarps in deposits of inferred equal age, indicates that the Kakapo Fault is far less active. Scarp angles on the Kakapo Fault typically range from 10-25° across fluvial gravel terraces, and 20-45°

Figure 5.3 View looking north-west toward an offset of 105 ±15 m across the Kakapo Fault, measured at the break in slope between Glenhope Advance moraine and Glynn Wye outwash on the north side of the fault, and the north-west margin of the small lake ponded on the south (downthrown ) side of the fault (match the dots).

Figure 5.4 Exposure beneath the youngest, apparently unfaulted terrace in the west bank of Kakapo Brook 400 m east of the offset terraces in Figure 5.2. The section consists of up to 2.2 m (1.5 m exposed) of overbank silts and sands incorporating several thin (<150 mm thick) fibrous peat horizons. Radiocarbon dates of <250 yr BP (i.e. young), and 605 ±55 yr BP were obtained from burnt wood at -0.50 m (1) and fibrous peat at -1.1 m (2), respectively.


2

in till.

In contrast, scarps in fluvial gravels and till along the Hope Fault commonly preserve angles of 65-80°. The variation in scarp profiles between fluvial and glacial deposits simply reflects textural differences; the higher proportion of fines in the glacial tills results in greater cohesiveness and steeper angles on scarps of equivalent age.

### 5.2.3 Previous Work

Gregg (1964) is credited with recognition of the Kakapo Fault, but Clayton (1965, 1968) and Freund (1971) were among the first to document Late Quaternary offsets. Little detailed work has been carried out, but Knuepfer (1984) measured displacements of 105 ±15 m, 75 ±10 m, 32 ±6 m, and 15 ±5 m, across what he referred to as an 'aggradation riser' (p.352) and three of four offset degradational terraces T1-T4 respectively, but he did not provide a map or sketch of this locality, so his data are difficult to evaluate.

Wellman (1985) measured displacements of 70 m, 50 m and 30 m respectively on terraces T1, T2-T3, and T5 of this study.

### 5.2.4 Review of Age Estimates of Landforms and Deposits

Clayton (1968) attributed the terminal moraine in Dismal Valley to the Glenhope Advance of the Hope Glaciation, on the basis of moraine size, relative position, and the height of an associated outwash surface downstream. He correlated the Glenhope Advance with the Blackwater 1 advance in the Waimakariri Valley and the West Coast Kumara $2_1$ glacial advance of the Otiran Glaciation (see Table 3.1 in Chapter 3), but there

is poor dating control. In this study an age of >25,000 years is assumed for features associated with the Glenhope Advance (Chapter 2).

In contrast, Knuepfer (1984) described the Glenhope Moraine as a late-glacial moraine and he inferred that the outwash surface and first degradation terrace are similar in age to those at Glynn Wye Moraine from which he obtained weathering rind age estimates (Table 3.2 Chapter 3.2). In this study, I assume an age of 17 000 ±1000 yr BP for the Glynn Wye moraine and associated outwash surface. This is a compromise between the weathering rind age estimates of Knuepfer (1984) and Suggate's (1988) review of the North Westland late Otiran chronology. It should encompass the likely range in age for the final retreat from the Glynn Wye glacier terminus. The actual age of the Glenhope moraine is not critical to the offset rate determination, because the datum is the break in slope against Glynn Wye outwash so it is the age of the latter which is significant.

The ages of the offset degradational river terraces have not been determined in this study, but Knuepfer (1984) and Wellman (1985) independently dated one of the terraces (inferred to be T2 and T3 of this study) at 4890 ±680 years, and 5900 years (no error given) respectively. Their respective estimates of offset on this terrace were 32 ±6 m (probably T3 here) and 50 m (probably T2 here), implying a Mid-Late Holocene lateral slip-rate of ~4.8 mm/yr or ~8.5 mm/yr.

### 5.2.5 Comparison of Displacements and Slip-Rates with Previous Results

In this study a tentative Late Quaternary lateral and vertical slip-rate is estimated from the Glenhope Moraine-Glynn Wye outwash surface offset and the throw on the Glynn Wye outwash surface respectively. The

slip-rate estimates calculated in this study are compared with those of Knuepfer (1984) and Wellman (1985) in Table 5.2. Knuepfer (1984) calculated a lateral slip-rate of 7.5 ±1.8 mm/yr for an offset of the same size, but it is not clear which features he measured to derive this slip-rate. Knuepfer records no vertical displacement for this feature. In this study no dating of the degradational terraces has been achieved, but the Knuepfer (1984) and Wellman (1985) age estimates for terrace T3 (37 ±5 m offset) are used to calculate a slip-rate based on my displacement data (Table 5.2).

| Author | Feature | Displacement Lateral | Displacement Vertical | Slip-Rate (mm/yr) Lateral | Slip-Rate (mm/yr) Vertical |
|---|---|---|---|---|---|
| KNUEPFER (1984) | Aggradation Riser (GHGW) | 105 ±15 | | 7.5 +1.7 -1.9 | n.d. |
| | Terrace 1 (T1) | 75 ±10 | 2.5 ±0.1 | n.d. | n.d. |
| | Terrace 2 (T2 + T3) | 32 ±6 | 3.1 ±0.1 | 4.8 +2.8 -1.7 | 0.5 ±0.1 |
| | Terrace 3 (T4) | n.d. | 0.8 ±0.1 | n.d. | n.d. |
| | Terrace 4 (T5) | 15 ±5 | 0.9 ±0.1 | n.d. | n.d. |
| WELLMAN (1985) | Terrace 1 (T1) | 70 ± n.d. | 4.0 ± n.d. | 5.5 ± n.d. | n.d. |
| | Terrace 2 (T2 + T3) | 50 ± n.d. | 2.0 ± n.d. | 8.5 ± n.d. | n.d. |
| | Terrace 3 (T5) | 30 ± n.d. | 1.0 ± n.d. | n.d. | n.d. |
| COWAN (THIS STUDY) | GH moraine GW outwash | 105 ±15 | 6.8 ±0.1 | 6.2 +1.3 -1.2 | 0.4 ±0.02 |
| | Terrace 1 | 75 ±5 | 3.2 ±0.1 | n.d. | n.d. |
| | Terrace 2 | 47 ±5 | 0.9 ±0.1 | n.d. | n.d. |
| | Terrace 3 | 37 ±5 | 2.1 ±0.1 | 7.6 +2.3 -1.9 Knuepfer's age<br>6.3 +0.9 -0.9 Wellman's age | |
| | Terrace 4 | n.d. | 1.2 ±0.1 | n.d. | n.d. |
| | Terrace 5 | 23 ±2 | 1.1 ±0.1 | n.d. | n.d. |

Notes: 1. All displacements are in metres.
2. Parentheses (e.g. (T3) denotes equivalence in this study.
3. Knuepfer (1984) measurements from riser crests.
4. This Study measurements from riser crest, mid-point and toe.
5. n.d. not determined.

TABLE 5.2 Comparison of Displacement Data: Kakapo Fault, Dismal Valley.

## 5.3 The Hope Fault: Glynn Wye Moraine Complex (Map 2 & 4 in map pocket)

### 5.3.1 Site Description

South of The Poplars and 160 m above the Hope River the Glynn Wye Advance terminal moraine forms a broad low ridge of undulating topography trending NNE from the valley margin south of the Glynn Wye Station road (Map 2). The eastern (downstream) face of the moraine is depositional and slopes gently over hummocky ground, toward the associated outwash surface. Much of the moraine surface is now under high quality pasture and few boulders or cobbles remain.

The west face of the moraine is a 20 m high meltwater terrace riser which was formed when ice retreated from its terminal position. The terrace riser drops at 15° to 20° to a meltwater terrace which forms a broad surface extending approximately 300 m west from the moraine (Figure 5.5 ). The second terrace riser drops from this surface to the floor of a channel formed by meltwater flowing around the snout of a receding late-Glynn Wye Advance glacier, which deposited three recessional moraines within 1 km of the main terminus (Map 2).

The Hope Fault traverses and laterally offsets the Glynn Wye Advance terminal moraine and the two recessional meltwater terrace risers (Stereopair #3). Only a small remnant of the second terrace riser is preserved on the north side of the fault.

The geometry of the Hope Fault at this locality is complex. It is characterised by a compound bend in the surface trace which has resulted in the development of extensional and compressional structures, disrupting the broad meltwater terrace surface upstream from the moraine (Map 1). The zone of extensional faulting is known as Poplars Graben and

Figure 5.5 View looking NNE toward Glynn Wye Advance terminal moraine (gm) and the Hope Fault which forms a scrub covered scarp up to 25 m high trending from west to east across the moraine. A meltwater terrace riser forms the west face of the moraine and drops to the terrace tread which extends 300 m westward to a second terrace riser. Only the remnant of this on the north side of the is visible at the edge of the 160 m high riser, down-dropping to the active Hope River floodplain. The west face of the moraine (also scrub covered) records a 265 ±9 m lateral offset on the Hope Fault (arrows). Numerous fault scarplets disrupt the meltwater terrace north and south of the main Hope Fault, forming Poplars Graben. Note also a 15-20° constraining bend in the fault (b).

Figure 5.6 Same aspect as Figure 5.5: detail of a pressure ridge formed in the meltwater terrace tread on the north-west side of the 15-20° constraining fault bend. The pressure ridge is 20 m high and 300 m long


gm
b
gm

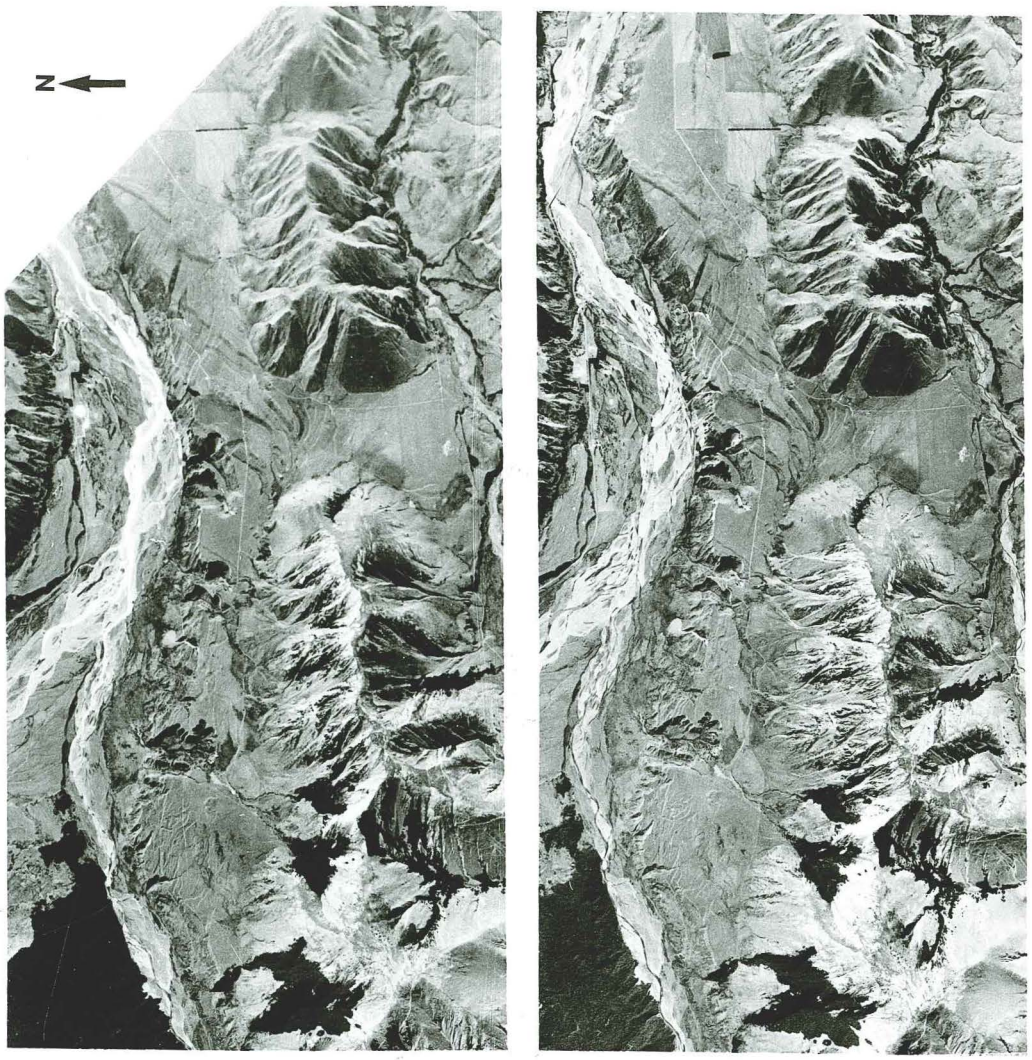


Stereopair #3 : Scale 1:80 000. Lower Hope Valley from the west end of Dismal Flats eastward to the Glynn Wye Advance moraine, and south to Kakapo Brook in Dismal Valley. The Hope Fault offsets the meltwater terrace riser forming the west face of Glynn Wye moraine and a meltwater terrace riser in Poplars Graben. The meltwater terraces are related to three closely spaced recessional moraines formed across the north entrance to Dismal Valley. Note the broad (700 to 900 m wide) zone of extensional faulting in Poplars Graben; the west end of the graben is obscured beneath the active floodplain of the Hope River. The Hope Fault emerges from the Hope River floodplain south of the Hope-Boyle River junction and trends 085° across the western end of Dismal Flats. The Kakapo Fault is visible on the Glynn Wye outwash surface at Kakapo Brook in Dismal Valley. Note the mega-boudinage within the block between the Hope and Kakapo Faults, marked by cross-cutting valleys and saddles.

extends up to 600 m to the south of the principal slip surface and 200 to 300 m to the north (Frontispiece). Poplars Graben is expressed at the surface by numerous fault scarplets inferred to be listric-normal and normal (some pivotal) faults trending parallel or sub-parallel to the Hope Fault and forming complex ramp structures in the Late Quaternary cover (Map 1 & Map 4).

On the north side of the fault at the NE corner of Poplars Graben a 20 m high and 300 m long doubly-plunging anticlinal ridge in the meltwater terrace surface has formed at a 15° to 20° constraining bend in the Hope Fault (Figure 5.6). A Riedel shear pattern of small oblique-normal subsidiary faults radiates WNW and ESE from this constraining bend, across the meltwater terrace and moraine surface respectively (Map 4).

### 5.3.2 Late Quaternary Displacements

To the east of the Glynn Wye Advance moraine terminus the Hope Fault strikes 080° and forms a narrow (<30 m wide) furrow in the outwash surface (Figure 5.7). The gently undulating eastern face of the Glynn Wye moraine contrasts morphologically with the associated outwash channels and the moraine terminus records a right-lateral displacement of 286 ±6 m measured from the break in slope between outwash and moraine on both sides of the fault (Figure 5.8 and 5.9 & Stereopair #4). Between these two displaced points, a change in the trend of the fault has resulted in compression (a left bend under dextral shear) and the outwash surface and moraine juxtaposed on either side of the bend have been up-warped 15 m metres (Map 4 & Figure 4.5 in Chapter 4). Further west the fault cuts through the meltwater terrace riser forming the west face

Figure 5.7 View looking east along the Hope Fault from the eastern face of Glynn Wye moraine. A shelterbelt is established along the fence-line, offset by 2.4 m during the 1888 earthquake (Fig. 4.4). Note that there is negligible vertical displacement across the fault at this locality.

of the moraine, and further trends toward the south with a strike of 067°, around the 20 m high anticlinal ridge on the north side of the fault (Map 4). Along this 300 m fault segment the terrace riser records a lateral displacement of 265 ±9 metres, measured from the inferred crest, mid-point and base of the terrace riser, but this is poorly defined on the south side of the fault (Stereopair #5).

At the western end of the bulge, the fault swings abruptly toward the north with a strike of 107°, and extends 500 to 600 m to the west across the recessional meltwater terrace, before disappearing beneath the active floodplain of the Hope River 160 m below. The 107° trend of this fault segment facilitates extension relative to the general 080° dextral shear and the 700-900 m wide, complexely faulted, Poplars Graben has developed in the terrace surface to the south of the main fault strand. The fault scarp at this point is 20 m high, and at its extreme western edge a displacement of 148 ±6 m is recorded on the second terrace riser (Stereopair #6 & Map 4).

### 5.3.3 Review of Previous Studies

The Glynn Wye Moraine Complex is undoubtedly the best known and most studied of any site on the Hope Fault. No fewer than six different authors have already measured and interpreted one or more of the three important displacements; all have produced differing results, with little consensus on their interpretation (Table 5.3). At first glance, the range of values in Table 5.3 might be thought to illustrate simply the amount of scope for the interpretation of such features.

However, a detailed analysis of these results indicates that some of the differences can be attributed to measurement error and others to

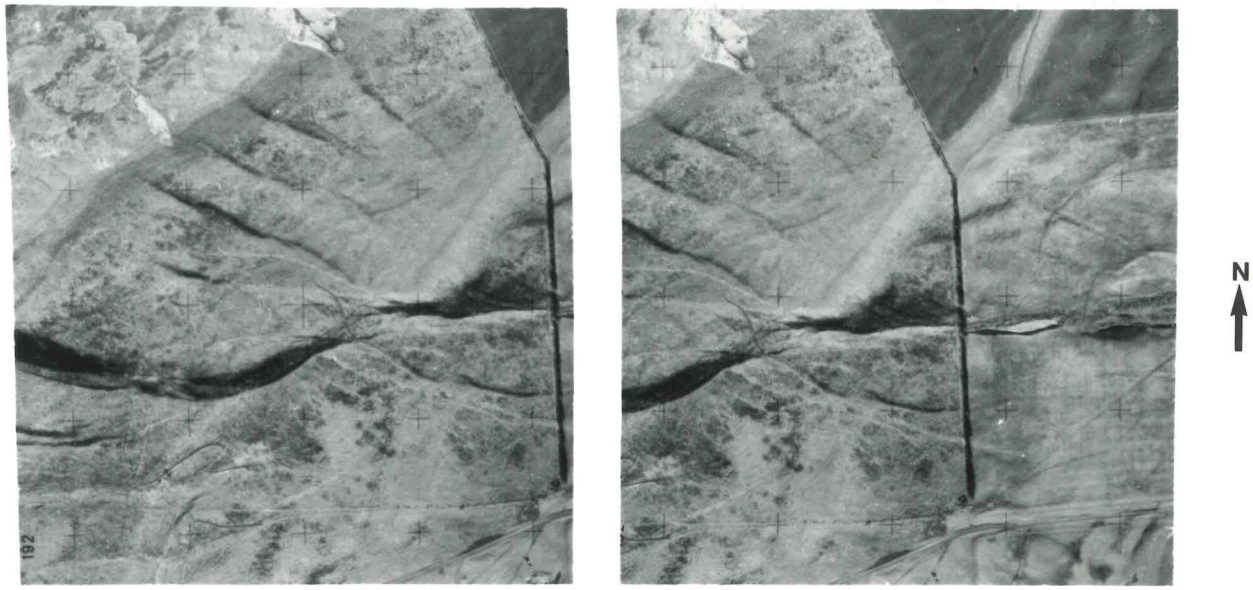


Stereopair #5 : Scale 1:10 000. The Hope Fault offsetting the west face of Glynn Wye Advance moraine by 265 ±9 m. The measurement is recorded from the crest, mid-point and toe of the terrace riser, but this is poorly defined on the south side of the fault. Note the location of the offset relative to a 15° constraining bend in the fault and the development of a doubly-plunging, 20 m high anticlinal ridge in the meltwater terrace surface on the north side of the fault. Oblique-normal Riedel shears radiate WNW and ESE from the bend, across the meltwater terrace and moraine respectively.

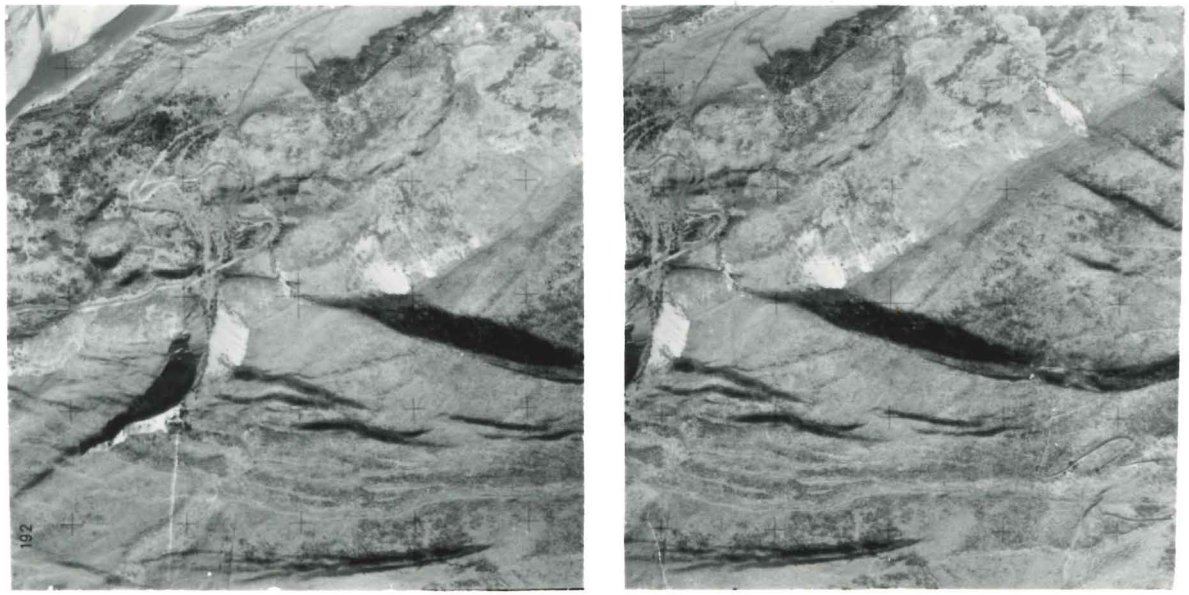


Stereopair #6 : Scale 1:10 000. The Hope Fault offsetting a second meltwater terrace riser in Poplars Graben, 300 m west of Glynn Wye moraine. The offset is 148 ±6 m measured from the crest, mid-point and toe of the riser. Note the large landslides at the base of the high terrace scarp toward the Hope River, and the numerous fault scarplets forming complex ramp structures in Poplars Graben, sub-parallel to the 20 m high principal fault scarp.

Figure 5.8 Looking NNE across Glynn Wye moraine and Poplars Graben. The eastern face of the moraine records a lateral offset of 286 ±6 m (see detail in Fig. 5.9). The west face of the moraine is offset 265 ±9 m and 300 m further west, the second terrace riser is offset by 148 ±6 m (arrows).

Figure 5.9 Detail of the eastern Glynn Wye moraine terminus showing a 286 ±6 m lateral offset measured from the morphological transition between moraine and outwash. Compare with Figures 4.4 and 5.7 for a contrasting perspective of this locality.

differences in conceptual approach and interpretation. The critical factors to be determined are 2) the size of the displacements, and 1) the age of the feature(s) displaced.

The age of the Glynn Wye moraine has been variously estimated at between 16,000 and 20,000 years (discussion in Section 5.3.3), but the measurement technique, and the size and interpretation of displacements at this locality, have been the subject of disagreement since Clayton (1965, 1966) first described a 305 m dextral displacement of the west face of Glynn Wye moraine, which he assumed to be 20 000 yr (summarized in Hardy & Wellman 1984). Clayton's displacement and age equals an average slip-rate of 15 mm/year for the Late Quaternary, a rate nearly four times that of the Wairau section of the Alpine Fault which until recently was widely believed to have accommodated the highest rate of Late Quaternary transcurrent displacement across central New Zealand (e.g. Suggate et.al. 1978).

Freund (1971) described the west face of the moraine as a terrace riser and measured a 149 m displacement on this feature. He also recognised a 149 m displacement on a terrace riser 300 m to the west of Glynn Wye moraine in the Poplars Graben. Freund was evidently concerned by the structural complexities, conceding that displacements were difficult to measure, but he argued that "the distances between the two risers on each side of the fault are equal", concluding, "there is little doubt that they were displaced by the same amount", and he reduced Clayton's displacements by half (Freund 1971: p.11, & Fig 4).

Hardy & Wellman (1984) summarised previous estimates of displacement, and provided their own, measured from 1:120 000 scale, high altitude vertical air photographs. At this small scale their data are too crude to be of any practical value, but they noted for the first time that

displacements across the west face of the moraine and across the western terrace riser are different. Adopting an age of 20 000 yr for the moraine and assuming a uniform slip-rate, they concluded that from the ratio of the two displacements, the western terrace riser is only about 14 000 yr old, and that flood-plain level must have therefore remained high until the end of the last glaciation.

Wellman (1985) subsequently changed his mind, and presented an argument for equal age and displacement for both terrace risers based upon the likelihood that the moraine and meltwater terrace represent no more than a few hundred years during the same episode of glacial history. He "proved" that the best way to determine the displacements is to measure first, the shortest right-angle distance between the displaced reference lines on the north side of the fault, and the respective parallel extensions from the south side of the fault (Figure 5.10). The pure strike-slip fault displacements may then be calculated from the oblique angle, parallel to the regional 080° strike-slip fault trend.

The result is an apparently equal displacement of 221 metres (200 m in the text) for the two terrace risers, which Wellman suggests should be intermediate between the 300 m offset for his dextral-reverse fault segment and the 169 m offset for his dextral-normal fault segment and accord better with the inferred near-equal age (Figure 5.10).

An interpretation of very different results was offered by Knuepfer (1984), who observed large variations in displacement across the east and west faces of the moraine, and the terrace riser to the west. Knuepfer was the first to document separately the eastern moraine face displacement and he observed that previous workers had mistaken the terrace riser forming the west face of the moraine, for a morainic depositional form, thereby underestimating the displacement of the

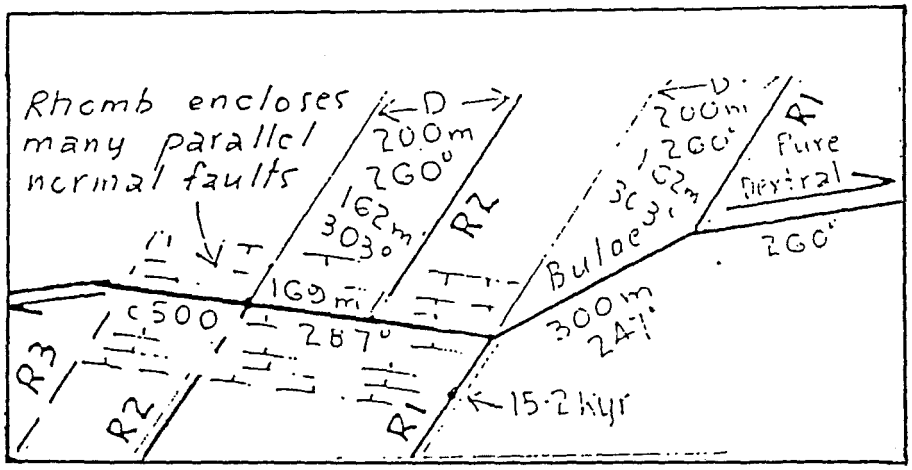


Figure 5.10 Map of the most critical feature of the figure - the dextral displacement of moraines R1 and R2. There are three fault segments. From east to west: a pure dextral segment with a 260° strike, a dextral-reverse segment with a 247° strike, and a dextral-normal segment with a 287° strike. The inset also shows how the 200 m of dextral displacement for both ridges is calculated from the 162 m right angle displacement for both ridges and the oblique angle of 43° (303° - 260°).
From Wellman (1985)

moraine itself. He suggested that the terrace risers were likely to be much younger than the moraine, and used weathering rind data obtained from the moraine and along the former river channel below the western terrace riser, to argue for significant age differences between these features, thereby accounting for the pronounced variations in offset (Knuepfer 1984) (Table 5.3).

Evidently Knuepfer was unaware that the offset terrace risers were derived from meltwater channels associated with three closely spaced recessional moraines behind the Glynn Wye moraine (Suggate 1965, Fig 9; Clayton 1966 p. 101; Clayton 1968, Figs 2 & 3; and Map 2 this study). Furthermore, prior to the development of Poplars Graben, the meltwater channels were at least 12 metres higher than the Dismal Flats outwash surface one kilometer to the west. This surface may be traced westward to a moraine ridge preserved along the northern edge of Dismal Flats (Figure 3.9 in Chapter 3). This moraine was mapped as recessional from the Glynn Wye Advance (Suggate 1965, p.23; Clayton 1968, Fig 3), but is inferred in this study to represent the latest-Otiran glacial maximum in the Hope Valley (Chapter 2). In either case, whether recessional or latest-Otiran it means the meltwater channels are close in age to the Glynn Wye moraine.

Clearly, there has been little consensus. Several authors have recognised and accepted true variations in offset, which they have attributed to significant age differences between the respective features (Hardy & Wellman 1984; Knuepfer 1984). Others, on the basis of field relations infer parity in age for the displaced features, and have rejected any notion of true variations in offset on the grounds that structural complexities have obscured or modified true and equal displacements (Freund 1971; Suggate et.al. 1978; Wellman 1985)

| | Depositional Eastern Face of Glynn Wye Moraine Displacement (m) | Meltwater Terrace Riser forming West Face of Moraine Displacement (m) | Meltwater Terrace Riser 300 m west of Glynn Wye Moraine Displacement (m) | Ages M=moraine R1=riser 1 R2=riser 2 | Slip-Rate mm/year | Comments |
|---|---|---|---|---|---|---|
| Clayton (1965,1968) | n.r. | 305 m | 213 m | M = 20 000 yr | M= 15.25 n.s. | Clayton describes a 305 m lateral offset on the west face of the moraine and a 213 m offset on a terrace riser to the west. |
| Freund (1971) | n.r. | 149 m | 149 m | R1=M= 20 000 yr<br>R2 n.s. | R1=M= 7.45 n.s. | Freund reduces Clayton's estimate of moraine displacement by half and measures a 149 m lateral displacement on the second terrace riser to the west, which he considers to be offset by the same amount as the moraine. |
| Suggate et.al.(1978) | n.r. | <147 m | <147 m | M = 18 000 yr<br>R1= 18 000 yr n.s.<br>R2= 18 000 yr n.s. | R1=M= <8.2 n.s. | They consider previous estimates of displacement to be too high and probably unreliable due to structural complexity and slumping of the offset terrace surface toward the Hope River. |
| Hardy & Wellman (1984) | n.r. | 336 m | 216 m | R1=M= 20 000 yr<br>R2= 14 000 yr | R1=M= 17.00.<br>R2= 17.00. | Hardy & Wellman recognise that displacements on R1 and R2 are different and infer different ages based on uniform slip-rate. Measurements were taken from small scale air photographs. Hardy & Wellman did not recognise the eastern moraine face offset, and they equated R1 with M |
| Knuepfer (1984) | 348 ± 7 m | 260 ± 20 m | 135 ±6 m | M= 16 630 ±3230 yr<br>R2= 8 910 ±2530 yr | M= 20.90.<br>R2= 15.20. | Knuepfer recognises eastern face moraine offset and different displacements on risers R1 and R2. He infers that the features are of different age, and dates the moraine and R2 using orthodox weathering rind technique, obtaining a late Pleistocene age for the moraine and an early Holocene age for R2. |
| Wellman (1985) | n.r. | 200 m | 200 m | R1=M= 15 000 yr<br>R2= 15 000 yr | M= 13.30.<br>R2= 13.30. | Wellman now believes that R1 and R2 are near-equal age and describes a technique for measuring equal displacements on these features (see Figure 5.10 and discussion in text) Wellman dates Glynn Wye Moraine using an unorthodox sampling approach which includes measurement of rinds on argillaceous rocks as well as greywacke. |
| Cowan (this study) | 286 ± 6 m | 265 ± 9 m | 148 ±6 m | M= 17 000 ± 1 000 yr<br>R2=R1=M ± 500 yr | M= 16.80.<br>R1.. n.d.<br>R2.. n.d. | I recognise the eastern moraine face as the only reliable displacement for estimating the Late Quaternary slip-rate. R1 and R2 are of near-equal age, but have been displaced by different amounts due to the partitioning of vertical and lateral displacement within Poplars Graben and around a bend in the Hope Fault at the west face of Glynn Wye Moraine. |

Notes: n.s.= not stated, but a numerical value is provided where implied.

n.r.= not recognised by the respective author.

TABLE 5.3. Comparison of Age Estimates and Measured Lateral Displacements from All Studies at Glynn Wye Moraine.

A consistent theme is the consideration of only two, seemingly exclusive options: equal age or equal displacement. The possibility that these features of near equal age could be recording systematic spatial variations in fault slip has not been addressed by previous workers.

### 5.3.4 Review of Age Estimates for the Glynn Wye Moraine Complex.

The Glynn Wye Advance has traditionally been correlated with the Blackwater 2 advance in the Waimakariri Valley, and the West Coast Kumara $2_2$ advance of the Otira Glaciation (see Table 3.1 Chapter 3).

Suggate et.al. (1978) consider the Kumara $2_2$ advance to have begun prior to 23 300 yr BP, and to have reached a maximum by 18 000 yr BP. Suggate (1988) revises this chronology slightly, and suggests that the Kumara $2_2$ advance culminated between 17 000 and 18 000 yr BP.

Several authors describing this locality in previous studies have assumed an age of about 20 000 yr BP for the Glynn Wye moraine (Clayton 1966, 1968; Freund 1971; Hardy & Wellman 1984).

Knuepfer (1984) calculated a weathering rind modal age of 16 630 ±3230 yr BP for the moraine, whereas Wellman (1985) using a sampling program which included argillaceous as well as greywacke sandstone cobbles, derived an age of 15 200 yr BP (no error given). Knuepfer realistically adopted the wide margin for his date, which he believed would cover the likely range in age for the Glynn Wye Advance. He also noted that the retreat of the Glynn Wye glacier from its terminal moraine is the most relevant event in the study of Late Quaternary fault displacements at this site, because fault displacements would probably not be preserved while the moraine was actively accumulating.

The somewhat younger estimates of age for the Glynn Wye Advance

obtained by weathering rind dating may reflect a later culmination of the Kumara $2_2$ equivalent advance at Glynn Wye, or they may reflect a wide margin of error in the dating itself, possibly due to unobserved environmental factors such as the removal of original cobbles and boulders on the moraine surface for pasture development, and the exhumation of formerly buried cobbles during heavy ground shaking in earthquakes and by discing.

Knuepfer (1984) considered the terraces and channels west of the moraine terminus to be early post-glacial features, and for the offset terrace riser in Poplars Graben he calculated a modal rind age of 7770 ±1240 yr BP and a mean age of 8910 ±2530 yr BP. Morphologically, these features are clearly meltwater channels which form part of a set of three recessional moraines, closely spaced behind the main Glynn Wye moraine (Suggate 1965; Clayton 1966, 1968; Wellman 1985; see Stereopair #3 this study). They are unlikely to be more than a few centuries apart in age, and probably closely post-date the retreat from the maximum moraine terminus; the rind date thus seems to be anomalously young (see discussion in Chapter 2).

In this study, I assume an age of 17 000 ±1000 yr BP for the Glynn Wye moraine, the associated outwash surface, and the offset meltwater terrace risers. This is a compromise between the age estimates of Knuepfer (1984) and Suggate's (1988) review of the North Westland late Otiran chronology: it should encompass the likely range in age for the final retreat from the Glynn Wye glacier terminus.

### 5.3.5 Comparison of Displacements and Slip-Rates with Previous Results

At the Glynn Wye Advance moraine there are some important differences in

measured displacements and the interpretation of field relationships between this study and those adopted in previous studies.

Firstly, the 286 ±6 m displacement of the depositional eastern face of the moraine is 18% less than the 348 ±7 m recorded by Knuepfer (1984). Combining this with the age estimate of the Glynn Wye moraine, I obtain a Late Quaternary slip-rate of between 15.5-18.25 mm/yr (Table 5.3). These values represent an average 20% drop in the estimation of Late Quaternary slip-rate from Knuepfer's 17.1-26.5 mm/yr, but an increase of 27% from Wellman's 13.2 mm/yr. Clayton did not present his faulting data in terms of average slip-rates, but they represent a value of 15.25 mm/yr (based on his moraine age of 20 000 yr) and provide the closest match to the result obtained in this study.

The 265 ±9 m offset measured on the west face of the moraine is smaller than Clayton's 305 m displacement, but is close to Knuepfer's measurement of 260 ±20 m. The 148 ±6 m offset across the western terrace riser in Poplars Graben accords well with Freund's 149 m displacement of this feature.

The interpretation of these displacements is the crucial aspect in which this study differs significantly from previous studies because: (i) the eastern terminus displacement is the only Late Pleistocene offset that I consider to be relatively free from the effects of secondary structural complications along the fault, and reliable enough to use for the derivation of an average Late Quaternary slip-rate, and (ii) the displacements recorded in this study were obtained with the aid of high resolution, low altitude air photographs not available to previous workers and which greatly aided the definition of the features for EDM surveying measurement. Use was also made of air photographs at other scales, each of which provided better resolution of certain features than

others. It became evident from precisely measured ground control utilizing EDM surveying equipment that the published general scale of the photographs was inadequate to measure displacements accurately, and it is not clear whether previous workers allowed for the effect of topography in their studies as only the general scale is quoted.

I support previous interpretations of the offset terrace risers as being near-equal in age to the moraine and derived from Late Pleistocene meltwater during the recession from the Glynn Wye terminus. I disagree with those authors who suggest that the displacements are equal. Field and air-photo measurements carried out as part of this study, indicate that lateral displacement across the strike-slip segment (080°), is greater than the lateral offset across the oblique-reverse or oblique-normal segments of the fault.

The two terrace risers record proportionally lesser lateral displacements than the moraine, due to their location with respect to the compound releasing-constraining fault bend which causes a greater proportion of fault displacement in successive earthquakes to be partitioned into a vertical component of subsidence or uplift. It follows that slip-rates derived from such offsets will be unreliable, because the lateral offset will not record the total fault displacement. These factors will be further discussed in Section 5.8.

## 5.4 The Hope Fault: Dismal Flats Locality (Map 1)

Five kilometers west of the Glynn Wye moraine, the Hope Fault reappears from the active floodplain of the Hope River, and strikes at 085° across landslides which have occurred in outwash of the late-Otiran Dismal Advance, south of the Hope River (Figure 5.11). Where the Hope Fault

Figure 5.11 In the foreground (lower left and right) fault scarps up to 3 m high mark the surface trace of the Hope Fault superimposed on large landslides north of Dismal Flats. The active and overbank Hope River floodplain extends eastward and obscures the Hope Fault. Five kilometres downstream the Hope Fault again emerges from the floodplain and forms the large, dark-coloured scarp at Poplars Graben (upper right).

Figure 5.12 A Late Holocene gully wall recording a 40 ±2 m lateral offset on the Hope Fault at the western end of Dismal Flats (location on Map 1).

crosses a large gully incised into the Dismal Flats (Map 1) a lateral displacement of 40 m ±2 m, and a throw of 2.0 m, north side up, is recorded in the west side of the gully (Figure 5.12). The age of the displaced gully may be described only as Late Holocene, but the chief significance of this displacement is that it confirms the position and trend of the main Hope Fault, just to the east of the 8 to 13° WSW fault bend (Map 1). Previously, only scarps associated with landsliding had been mapped at this locality (Freund 1971, Map 3), and the geometry of the principal fault trace remained uncertain.

## 5.5 The Hope Fault: Manuka Creek-Raupo Swamp Locality (Figure 5.13)

### 5.5.1 Site Description

Three hundred metres west of the Manuka Creek bridge on State Highway 7, the Hope Fault surface trace is clearly visible 50 m north of the highway, striking 080°across three offset degradational terraces of the Hope River (Figure 5.13 & Stereopair #7). The Hope River has since migrated to a relatively narrow braided floodplain on the north side of the main valley and is incised 17 m below the highest degradational terrace.

The offset terraces formed across the eastern entrance of a small valley developed along the fault trace, formerly occupied by Kakapo Brook and a braid of the Hope River. These rivers abandoned the valley progressively, in response to dextral faulting and relative uplift of the former stream channel 1200 m to the west; a large, presumably earthquake generated landslide finally blocked the valley 700 m to the west, creating Horseshoe Lake (Figure 5.14).

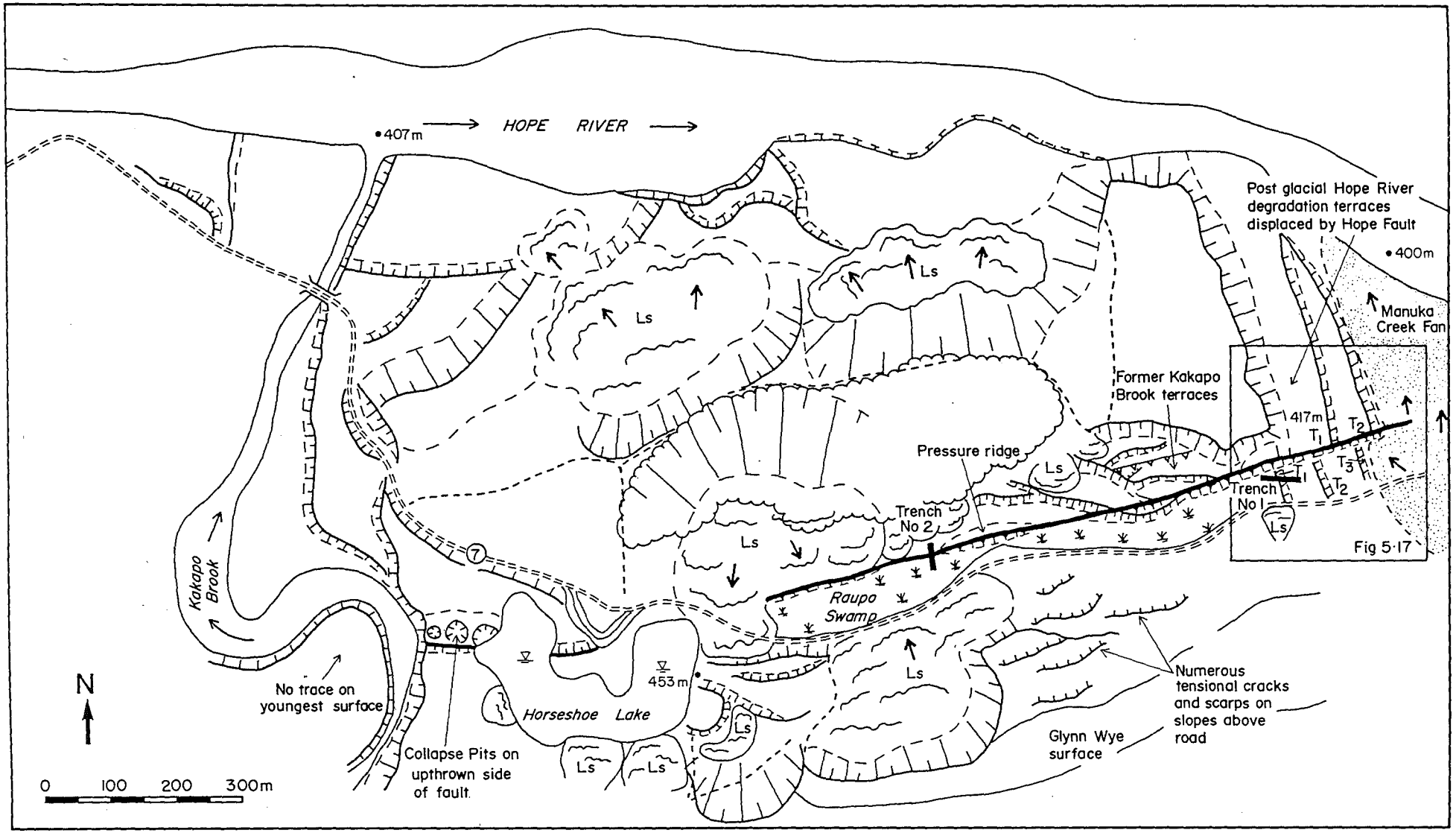


Fig 5·13: Geomorphology of the Horseshoe Lake Area - State Highway 7

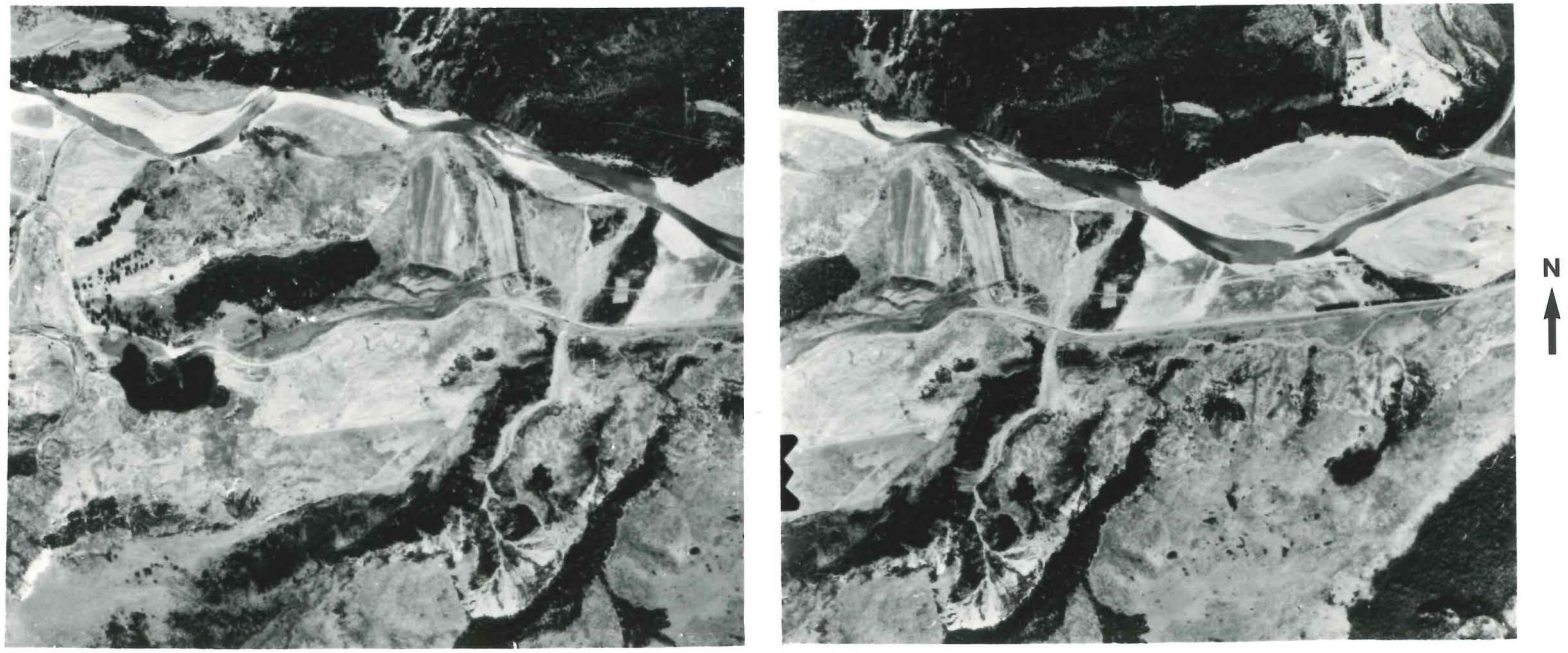


Stereopair #7 : Scale 1:25 000. The Hope Fault offsetting Late Holocene degradational terraces of the Hope River, 300 west of Manuka Creek on State Highway 7. Three terrace risers are displaced, but only one of these (R2) is clearly visible on the photograph.

The Kakapo Brook and a braid of the Hope River occupy a floodplain more than 40 m above the present day and flow through the valley along the Hope Fault, forming an island in the centre of the valley.

River downcutting has lowered the floodplain level to approximately 17 m above the present and repeated faulting has moved the valley entrance away from the mouth of Kakapo Brook which is incised within a gorge south of the fault. Only a small stream is now active in the valley along the Hope Fault, but the valley may be subject to inundation by the Hope River during flood events.

During an earthquake on the Hope Fault a large landslide is triggered in outwash gravels mantling the ridge slopes to the north of the fault. The landslide blocks the valley and initiates the formation of Horseshoe Lake.

Kakapo Brook and Hope River have incised a further 17 m and a swamp now occupies the old stream channel to the east of Horseshoe Lake. The lake is impounded on its western margin by river gravels and lake sediments which have been upthrown to the north and tilted to the east during repeated faulting events.

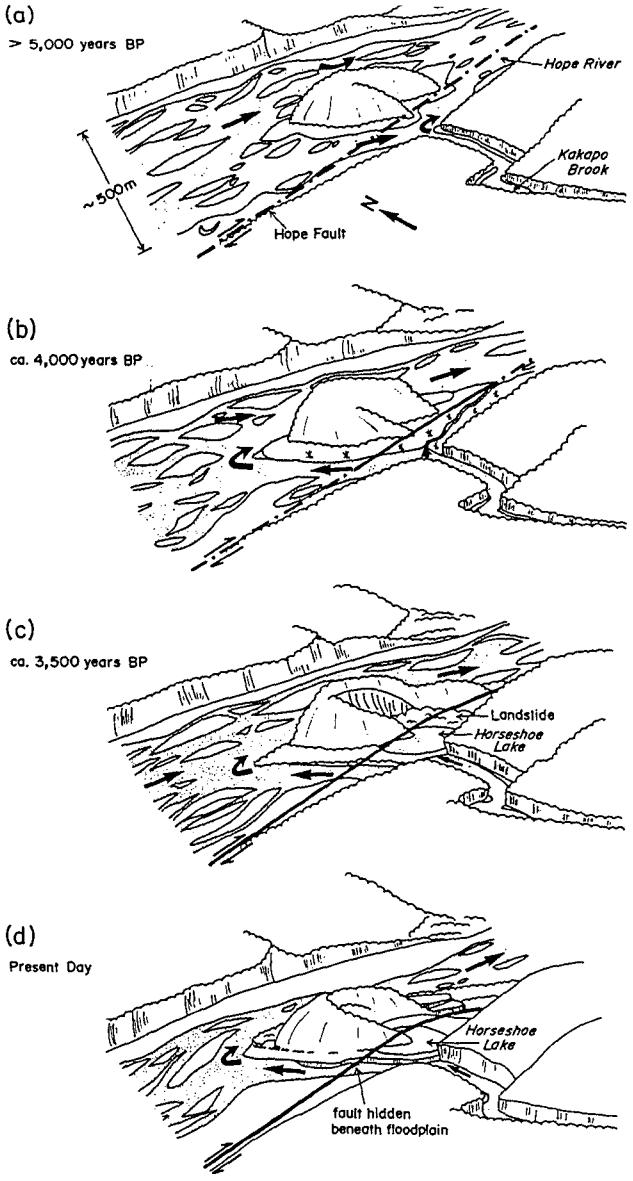


Fig 5·14: Geomorphic history of Hope Fault: Horseshoe Lake - Manuka Creek

A swamp now occupies the old river channel east of Horseshoe Lake forming two levels separated by a 60 m long and 5 m high anticlinal pressure ridge developed on the fault trace (Figures 5.15 & 5.16). The lower swamp mantles the offset terrace riser R1, and tread T1, on the south side of the fault at the eastern end of the valley.

To the east of the offset terraces a large fan forms the lower reach of Manuka Creek. The fan has encroached onto Terrace T3 and completely buried lower and younger terraces of the Hope River.

### 5.5.2 Late Quaternary Fault Displacements at Manuka Creek

Three offset terrace risers, R1 to R3, record perpendicular right-lateral displacements of: 36 m ±3 m, 36 m ±0.5 m, and 18.0 m ±3.0 m respectively (Figure 5.17). Only R2 is clearly visible from the highway or on air photos (Figure 5.18 & Stereopair #7). Throw across the terraces T1 and T2 is north side up, 2.4 ±0.3 m, and 2.1 ±0.3 m respectively (cartoon). The throw across T3 is unclear due to stream erosion and encroachment onto this surface by the Manuka Creek fan.

To the east of the offset terraces, younger and correspondingly lower terraces have been eroded or buried by the rapidly aggrading Manuka Creek fan. No lateral or vertical displacements are preserved on the fan surface, or apparent from available exposures in Manuka Creek.

### 5.5.3 Trenching at the Manuka Creek Site

At the eastern valley entrance, a backhoe trench was excavated subparallel to and 15 m from the Hope Fault, through the face of offset terrace riser R1 and into the tread gravels beneath T1, at the eastern

Figure 5.15 View looking ENE from ridge south of Horseshoe Lake, State Highway 7. The Glynn Wye outwash forms the broad bush covered terrace on the far side of Hope River. The grass covered surfaces (centre) are post-glacial river degradation terraces formed when Kakapo Brook and a braid of the Hope River were active in the valley, prior to the formation of Horseshoe Lake. Raupo Swamp now occupies the abandoned channel bottom to the east of the lake and is traversed by the Hope Fault. Note the large landslides (ls) centre right.

Figure 5.16 View looking west toward a pressure ridge (60 m long and up to 3 m high) developed along the Hope Fault surface trace in Raupo Swamp (cf. Fig.5.15). Trench No. 2 was excavated across the fault at the west end of this feature (arrow).


ls

end of the swamp (Figure 5.17 & Trench Log #1 in map pocket). The purpose of the trench was to evaluate the stratigraphic relationship between the former Kakapo Brook-Hope River channel and the offset degradational river terraces, and to obtain organic material from the base of the overlying peat to date the onset of swamp formation.

Behind the offset terrace riser R1 and beneath the former Kakapo Brook-Hope River channel (in the valley now occupied by the swamp), the trench exposed a 16 m length of coarse to fine sandy gravels and coarse sands, overlain by 0.2-0.4 m of grey peaty clay, and 0.4 m of brown fibrous peat (Trench Log #1). Also exposed was the crest and face of R1, which has evidently been eroded by the stream formerly active in the channel now occupied by the swamp, prior to the damming of Horseshoe Lake. A wedge of sandy silt occurs at the base of R1, and interfingers to the east with well-rounded, fine to medium gravels and coarse sands forming the degradational terrace T1 deposited by the Hope River (Trench Log #1).

Wood was obtained from within the sandy silt wedge at the base of riser R1, and was dated at 3482 ±77 yr BP (NZ 7591, Appendix 1). Small branches of Nothofagus sp., from the base of the overlying fibrous peat were dated at 575 ±60 yr BP (Trench Log #1 and NZ 7588, Appendix 1).

I assume that the wood with an age of 3482 ±77 yr BP was incorporated within sediments beneath terrace T1 (possibly during a flood) while the Hope River was active at this level. The tree did not appear to be in growth position. The $^{14}C$ date relates to the death of the tree which may or may not be significantly older than the time of burial, but the location of the sample is especially fortuitous as it represents a point in time before the formation of R2, and probably between formation of R1 and R2, both of which are displaced by near-equal amounts. The $^{14}C$ date

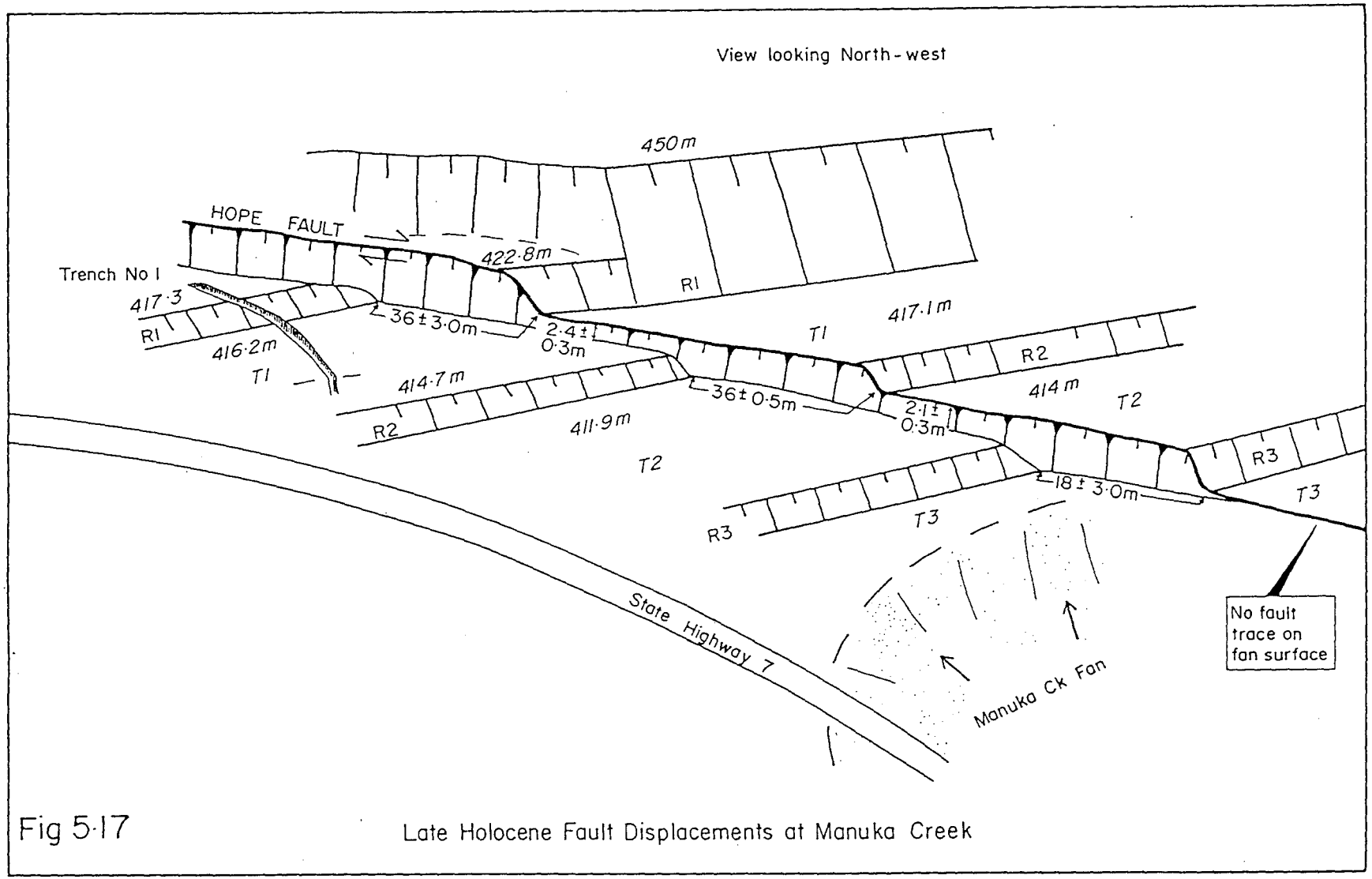


Fig 5·17 Late Holocene Fault Displacements at Manuka Creek

Figure 5.18 Late Holocene river degradation terraces 300 m west of Manuka Creek Bridge, State Highway 7. Terrace riser R2 records a lateral offset of 36 ±0.5 m (match the dots).

thus provides a maximum age for R2 and its 36 ±0.5 m displacement.

The latest Holocene minimum lateral slip-rate at this locality for the period prior to 1889, is therefore 10.6 ±0.3 mm/yr. The minimum vertical slip-rate for the same period is 0.71 ±0.1 mm/yr*.

A second trench was excavated across the Hope Fault in the upper level of Raupo Swamp west of Manuka Creek, with the aim of exposing fault disrupted stratigraphy and to obtain organic material from crucial stratigraphic horizons in order to evaluate the recent fault displacement history. The results of the second trenching study are discussed in Section 5.6.

### 5.5.4 Previous Work

Wellman (1953) was the first to document an offset at this locality from air-photos, but Freund (1971) records the earliest field measurement of a 36.6 m displacement of a terrace riser (≐ R2 this study). Knuepfer (1984) gave a revised measurement of 32.7 ±3 m for this offset, and described additional displacements of 18.1 ±3.5 m, across a younger terrace riser, and 25.4 ±2.0 m across a stream channel on the next terrace tread below (T3 of this study). All of Knuepfer's measurements were made from riser

(*Note: This estimate of slip-rate is based on an age of 3482 ±77 minus the 100 years elapsed since the last event. The compensation for elapsed time assumes that the fault-slip is entirely coseismic. The estimate derived on this basis would represent a maximum slip-rate only if the first increment of slip occurred immediately following the abandonment of terrace T2, and the final lateral cutting of R2).

crest to crest. Wellman (1985) recorded two 36 m displacements: one across his original riser offset, and the second across an older and higher terrace riser (= R1 this study) which Knuepfer had recognised but declined to measure because of erosion of the riser crest on the south side of the fault.

### 5.5.5 Age Estimates for the Offset River Terraces

Knuepfer (1984) used weathering rinds to date the terrace treads below his two offset terrace risers T2 & T3 (=T2 & T3 this study) and he derived rind mode ages of 4 010 ±520 yr BP, and 1 220 ±100 yr BP, respectively (Table 5.4).

Wellman (1985) also calculated rind ages for the treads below each of his offset risers (T2 of Knuepfer and this study, and T1 of this study), but he used a different approach to weathering rind sampling and his rind ages of 1 800 yr BP for both surfaces are significantly younger than Knuepfer's (Table 5.4).

Wood obtained from beneath T1 during this study has been dated at 3482 ±77 yr B.P. (Appendix 1). This date represents a maximum age for the overlying terrace tread T1 if the age of the wood is close to the time of the burial event, and if the surface were formed immediately following deposition of the wood. It is also a maximum age for the younger tread, T2 and the riser R2 separating T1 and T2.

### 5.5.8 Comparison of Displacements and Slip-Rates with Previous Results

At Manuka Creek, there is general agreement on the measurement of the fault displacements, but differences between the various age estimates

| | Terrace T1 | Terrace T2 | Terrace T3 | Ages | Slip-rates (mm/yr) | Comments |
|---|---|---|---|---|---|---|
| Freund (1971) | n.d. | 36.60. | n.d. | n.d. | n.d. | Revised Wellman's (1953) measurement of 46 m measured from air photographs. |
| Knuepfer (1984) | n.d. | 32.7 ± 3 | 18.1 3.5 | T2 = 4010 ± 520 | 8.2 +2.0. -1.6. mm/yr | Recognised terrace T1 but did not measure displacement on backing riser (R1 of this study, due to erosion of riser crest south of fault. Displacements were measured from the crests of risers backing each terrace. Ages are derived from greywacke cobble weathering rinds. |
| | | | | T3 = 1220 ±100 | 14.8 +4.5. -3.7. mm/yr | |
| Wellman (1985) | 36.00. | 36.00. | n.d. | T1 = 1800 | 20.0 mm/yr | Displacements measured in the field (points unknown) Age estimates are from weathering rinds using unorthodox sampling technique which involved applying a correction for the use of argillaceous rocks which develop thinner rinds than greywacke on rocks of equivalent age. |
| | | | | T2 = 1800 | 20.0 mm/yr | |
| Cowan (this study) | 36 ± 3 | 36 ± 0.5 | 18 3 | T1max = 3482 ±77 | n.d. | Displacements measured from crest, mid-point and toe of risers backing each terrace. Riser R1 (behind T1) was measured from within a trench excavated through R1, 15 m south of the Hope Fault. Age estimate for the terraces T1 & T2 is a radiocarbon date from wood recovered from a silt lens 1.1 m beneath the surface of T1. |
| | | | | T2max = 3482 ±77 | 10.6 ±0.3 mm/yr | |
| | | | | T3 .. n.d. | n.d. | |

Notes: 1. Errors are quoted only where stated.
n.d. = not determined.

TABLE 5.4. A Comparison of Age Estimates and Measured Lateral Displacements from All Studies at Manuka Creek.

for the terraces results in a wide range of calculated slip-rates (Table 5.4).

The offset of 36.0 ±0.5 m on R2 measured in this study, is slightly larger than Knuepfer's 32.7 ±3.0 m, but almost identical to that of Freund (1971) and Wellman (1985). This displacement combined with the $^{14}C$ date of 3482 ±77 yr as a maximum age estimate for R2, results in a minimum lateral slip-rate of 10.6 ±0.3 mm/yr, and a vertical slip-rate of 0.71 ±0.1 mm/yr for this locality. This represents an average 2.4 mm/yr increase in lateral slip-rate, from Knuepfer's weathering rind derived estimate of 8.2 ±1.8 mm/yr, but the estimate of vertical displacement in this study is identical to Knuepfer's estimate 0.7 ±0.1 mm/yr. The latter result may be explained by errors cancelling; Knuepfer's higher estimate of throw was proportionally the same as his higher estimate of terrace age, resulting in an identical rate of vertical slip on the fault. The radiocarbon date provides a useful calibration for the weathering rind derived ages at this locality. Wellman's rind ages of 1 800 years are in error by 48%, and may reflect the fact that by using argillaceous rocks as well as greywacke in his sampling program, he sampled a significantly greater proportion of thinner rinds, and therefore derived much younger ages. Knuepfer's age of 4 010 ±520 yr BP for the terrace T2, is in error by an average of only 13%, but ranges from 0-25%. This weathering rind estimate of age is much closer to the radiocarbon age, and although the radiocarbon date represents a maximum age for a feature which is older than those estimated by the rinds, the difference in the offset of risers R1 and R2 is negligible, indicating that the associated terrace surfaces are unlikely to differ in age by more ±150 years (on the basis of seismic recurrence intervals derived later in this discussion).

## 5.6 Evidence for the Last Five Pre-Historic Earthquakes on the Hope River Segment of the Hope Fault

### 5.6.1 Trenching Across the Hope Fault in Raupo Swamp

In Raupo Swamp north of State Highway 7 (Figure 5.13) and three hundred metres east of Horseshoe Lake a second trench was excavated perpendicular to the Hope Fault, across the western end of a small anticlinal ridge developed along the fault trace. The trench was excavated so as to expose the fault and faulted stratigraphy within the swamp and to obtain organic material associated with faulted or un-faulted horizons, with the aim of reconstructing a paleoseismic history for the Hope Fault at this locality.

This 27 m long trench extended from 8 m south of the fault to 19 m north of the fault, at an average depth of 1.5 to 2.0 metres. The trench exposed a major contrast in lithology between laminated fine gravels, sands, and silts, overlain by fibrous peat on the north side of the fault, and brown fibrous peat containing three silt horizons and overlying a fourth silt horizon south of the fault (Trench Log #2 in map pocket).

Two samples of wood were obtained from the highest and lowest exposed horizons (vertical separation 0.8 m) within the laminated inorganic sediments on the north side of the fault. These samples were dated at 3547 ±73 yr BP and 3536 ±60 yr BP respectively (NZ 7587 and NZ 7585 respectively, Appendix 1), but the ages overlap and the sediments are inferred to have been deposited rapidly. The Hope Fault itself is marked by clay gouge and pronounced shearing within coarse, sub-rounded to sub-angular gravels including boulders up to 1.3 m diameter, underlying

the peat and which have been upwarped to form the asymmetric anticlinal ridge that extends eastward 60 m from the trench (Trench Log #2). The bouldery gravels are inferred to represent a landslide cover on the original channel surface.

Two monoliths of the peat column (ML1 & ML2) from the trench wall south of the fault were obtained for $^{14}C$ dating and palynological analysis by Dr M.McGlone (Botany Division, DSIR). Monoliths ML1 & ML2 were taken 4 metres apart, and comprise 70 mm x 35 mm continuous vertical sections, for the intervals 0.00 m (ground level ±0.12 m) to -0.86 metres, and -0.37 to -1.44 metres respectively (Trench Log #2).

The swamp stratigraphy south of the fault is characterised by brown fibrous peat incorporating three visually distinct 70-100 mm thick, fine silt horizons. These horizons are located at -0.44 to -0.51 m; -0.74 to -0.84 m and -1.02 to -1.09 m, and are fully penetrated by the peat. The uppermost horizon is present only in ML1, and could not be traced north along the trench wall for more than 1 m. The latter two horizons may be traced discontinuously over a distance of four metres, from ML1 to ML2.

A peat sample from the interval -1.225 to -1.25 m was dated at 569 ±55 yr BP (NZ 7586, Appendix 1), and indicates that the base of the swamp at -1.35 m is probably less than 700 yr BP.

### 5.6.2 Paleoseismic Interpretation of Buried Silt Horizons in Raupo Swamp

At the eastern margin of Raupo Swamp, terrace riser R2 has been laterally offset 36 m in a maximum of 3382 ±77 years (Radiocarbon age less the time since the last earthquake). The observed distribution of lateral slip following the 1888 earthquake (Chapter 3) indicates that at this locality it was approximately 1.5 metres. On the assumption that this represents

a characteristic displacement per event at this point on the fault, then about 24 events occurred from the time terrace T2 was abandoned by the Hope River until just after the 1888 earthquake, with an average recurrence interval of 141 ±3 years. The error estimate incorporates the standard error of the $^{14}C$ date (i.e. Recurrence interval = 3382 ±77 years divided by 24 events).

By considering this estimate of average recurrence interval in relation to an estimate of the rate of peat accumulation in Raupo Swamp, it is possible to evaluate whether or not the silt horizons within the peat could coincide with predicted prehistoric rupture events. If prehistoric ruptures were of the same intensity as the 1888 earthquake, they could be expected to produce fresh fault and landslide scars which would contribute inorganic sediment to the swamp.

A peat accumulation rate of 2.2 ±0.2 mm/yr is calculated using the 1.24 m depth of peat above the mid-point of the interval dated by radiocarbon at 569 ±55 yr BP. The stated uncertainty in the peat accumulation rate incorporates the standard error of the radiocarbon age. The assumption of uniform peat accumulation is difficult to test without further $^{14}C$ dating, and may be invalid due to changes in catchment conditions, seasonal climate, or land-use over time (P. Tonkin pers.comm.)*. However, loss-on-ignition tests showed that although the background level of inorganic sediment in the peat is moderately high, only the visually apparent silt layers account for significantly higher concentrations (Trench Log #2). These results suggest a relatively uniform influx of inorganic sediment into the swamp at most times. The peat is not compacted and at the monolith sampling sites it was not significantly disturbed by trench excavation. Implicit in the entire approach is the assumption that, because the silt horizons are thin and

mixed with peat they do not represent a significant hiatus in peat accumulation.

If the average recurrence interval of 141 ±3 years is valid, there should be evidence in Trench No.2, for four earthquakes since 569 ±55 yr B.P. Using an average peat accumulation rate of 2.2 ±0.2 mm/yr, evidence for the 1888 earthquake should occur at -0.2 ±0.02 m. Evidence of earlier events at 241 ±3 yr BP, 382 ±3 yr BP, and 523 ±3 yr BP should occur at -0.53 ±0.06 m, -0.84 ±0.08 m, and -1.15 ±0.13 m respectively. Extrapolating beyond 569 ±55 yr BP to the base of the swamp, a fifth event at 664 ±3 yr BP is predicted at -1.46 m.

South of the fault there is no evidence of a silt layer at -0.2 ±0.02 m which could be attributed to the 1888 earthquake. But the predicted locations of the next two earlier events coincide with the base of two silt layers (Trench Log #2). The oldest predicted event shows a fair match with the base of the lowest silt layer, but is less well constrained because of the increase in the margin of error with increasing age and thickness of peat.

At -0.2 m on the north side of the fault, a 0.1-0.2 m thick peaty silt layer intervenes between upper and lower units of brown peat. Peat accumulation at a rate of 2.2 ±0.2 mm/yr would constrain the age of the base of the overlying peat to between 83 and 100.5 years B.P.. This would be consistent with an influx of sediment from landslides on the

*An additional sample of peat from the interval, -0.84 to -0.86 m has been submitted to Institute of Nuclear Sciences (INS) for dating and results will be reported shortly. An age within the range 386 ±42 yr B.P. for this interval would support the hypothesis of uniform peat accumulation.

north side of the fault following the 1888 earthquake (see Figure 4.3 in Chapter 4). The absence of a similar layer south of the fault may be apparent only, as there is no reason to expect that sediment would necessarily be distributed uniformly within the swamp. It is also possible that the 1888 earthquake caused the small pressure ridge east of the trench to propagate further to the west, blocking the transfer of sediment from north to south across the scarp and resulting in a greater accumulation north of the fault. This is consistent with field relationships which show the peaty silt layer pinching out behind on the upthrown side of the fault (Trench Log #2).

An estimate of specific recurrence interval between the last five earthquakes (this includes the 1888 event) may be calculated using the peat accumulation rate and thickness of peat between the mid-points of respective silt horizons. The data indicate an average recurrence interval of 134 ±27 years (Trench Log #2). Further $^{14}C$ dating will be required to evaluate the assumption of uniform peat accumulation, but the recurrence interval calculated on this basis is consistent with the Late Holocene average recurrence interval of 141 ±3 years.

### 5.6.3 Alternative Interpretations of the Silt Horizons

Alternative origins for the silt horizons within the peat section must be considered seriously before a paleoseismic source can be invoked. Of these the most likely are: i) slope failure and sediment run-off following severe storm events, and ii) slope failure and sediment run-off following fire.

i) Raupo Swamp may receive a small portion of its water budget as base-flow beneath the landslide blocking Horseshoe Lake, but probably derives most of its water from direct precipitation and surface run-off from surrounding slopes. Erosion of surrounding hillslopes during storm events could, therefore, result in an increased sediment input to Raupo Swamp. But the regular spacing of a small number of sediment horizons does not seem consistent with what could be more frequently occurring random events. If the three sediment horizons were deposited during rare storm events, it should be possible to recognise thinner bands of sediment, deposited during more frequent and smaller events. This is not supported by loss-on-ignition tests which indicate a moderately high, but relatively uniform inorganic sediment content between the visually distinct silt horizons (Trench Log #2).

ii) A second alternative source of the silt horizons is sediment run-off from surrounding slopes following fire. Pollen spectra from the base of the swamp at -1.35 m up to -1.2 m (measured by M.McGlone, Botany Division, DSIR) indicate the local predominance of beech (Nothofagus fusca type) forest during this period of peat accumulation (Trench Log #2 ). At -1.1 m, beech and podocarp trees drop to below 10% of the pollen sum, and there is a corresponding increase in the percentage of bracken (Pteridium esculentum). This is coincident with the base of the third silt layer and is consistent with major forest clearance that occurred in many parts of the eastern South Island at about this time, and which has been attributed to early Polynesian burning (M.McGlone pers.comm.). Increases in bracken at other points in the peat column probably reflect repeated firing of vegetation in the Lower Hope Valley, but are not coincident with other silt horizons.

### 5.6.4 Evidence Supporting a Paleoseismic Interpretation

There is palynological evidence which indicates major ground-baring events coincident with the silt layers at -0.53 and -0.84 m respectively. Above each of these silt layers there is a large increase in the amount of matagouri (Discaria sp.) pollen present (Trench Log #2). Matagouri is a coloniser of bared and stony ground but it has a prostrate habit which inhibits widespread dispersal of pollen, and it is not normally represented in such high proportions in pollen spectra (M.McGlone pers.comm.). In the study area today, matagouri occurs on the margins of active fans but is especially common on scarps of the Hope Fault, many of which reactivated during the 1888 earthquake (e.g. refer Figure 5.12). The valley surrounding Raupo Swamp was heavily shaken during the 1888 earthquake and the numerous landslides mapped in this area by McKay (1890) are now covered by matagouri. Based on the known ecology of matagouri and its prevalence on sites which were bared during the 1888 earthquake, I infer that the matagouri peaks in the pollen record indicate the occurrence of surface rupture and landsliding during two earthquakes on the Hope Fault, at 241 ±3 yr BP and 382 ±3 yr BP.

The initial deforestation event at -1.1 to -1.2 m is almost coincident with the base of the third silt layer (-1.09 m) and could explain its presence, but does not preclude a paleoseismic interpretation. Pollen was sampled only at 50 mm intervals and closer sampling is required to establish whether the inferred forest clearance occurred at -1.1 m or between -1.1 m and -1.2 m.

The most significant fire to occur during the 600-700 year swamp history is represented by the largest charcoal peak, between -0.2 and

-0.25 m. This is accompanied by a significant increase in bracken and a further reduction in beech forest (Trench Log #2). The first appearance datum of exotic plant species such as Sorrel (Rumex sp.) occurs at or just below this horizon, and I infer these changes to indicate a major firing of remaining forest in the Lower Hope Valley by European pastoralists (about 115 ±11 yr BP). The important point to note is that this significant firing event is not accompanied by any increase in the amount of silt introduced to the swamp (Trench Log #2).

Interpretation of the third silt horizon at -1.02 to -1.09 m is equivocal and its origin may be due to slope failure and sediment-run-off following deforestation, but the absence of a silt layer corresponding to late-nineteenth century burning indicates that earlier forest clearance and deposition of the third silt layer may be coincidental.

Two smaller charcoal peaks at -0.5 m and -0.9 m are not matched by a vegetation or major sediment response to firing.

The oldest event which may be recognised at this site is the event which probably initiated swamp development via landsliding at the eastern end of the valley. Using the calculated peat accumulation rate and extrapolating for a fifth predicted event requires evidence for this event to occur at -1.46 m which is within the silt layer beneath the base of the peat (Trench Log #2). This event has a predicted date of 664 ±3 yr BP based on the Late Holocene average recurrence interval of 141 ±3 yr. This recurrence interval may be extended to a predicted sixth event at approximately 805 ±3 yr BP for which there is evidence from a large landslide SW of Hope Bridge, State Highway 7. Vegetation growing on a terrace 3.0 m above the Hope River and buried by the landslide has been dated at 778 ±60 yr BP (Knuepfer 1984).

### 5.6.5 Conclusions from the Trenching Studies at Manuka Creek and Raupo Swamp

1. A Late Holocene average recurrence interval for earthquakes on the Hope Fault at Manuka Creek is calculated from a terrace offset of 36.0 ±0.5 m at the eastern end of Raupo Swamp. The terrace offset has a maximum age of 3482 ±77 yr BP but 100 years are deducted for the calculation of recurrence interval to allow for the elapsed time since the last event. Calculation of the recurrence interval assumes that slip is generated exclusively during earthquakes on this segment of the Hope Fault, and in increments of approximately 1.5 m, the amount of displacement known to have occurred at this locality during the 1888 earthquake.

2. Four silt horizons were exposed in a trench excavated across the Hope Fault in Raupo Swamp east of Horseshoe Lake. The silt horizons are interpreted as the product of sediment run-off from fresh fault and landslide scarps following four prehistoric earthquakes at this locality.

3. Palynological analysis of the peat column has provided evidence of an ecological response by matagouri (Discaria sp.) to major ground-baring events which are coincident with the -0.53 m and -0.84 m silt layers. Matagouri pollen increases significantly above these silt layers and is inferred to reflect a vigorous colonisation of exposed fault and landslide scarps following surface rupture and heavy ground shaking during large earthquakes on the Hope Fault.

4. Major deforestation of the area occurred between 500 and 550 yr BP and again during the late-nineteenth century. The -1.02 m silt layer is coincident with the pollen response to early forest clearance and a paleoseismic interpretation of the silt is equivocal. This silt layer and the deforestation may be unrelated, however, because the late-nineteenth century burning is not accompanied by any significant increase in silt.

5. The -1.35 m silt layer occurs beneath the base of the peat swamp and probably relates to the seismic event which initiated swamp formation by closing the eastern valley entrance at Manuka Creek with a landslide.

6. An estimate of specific recurrence interval between the last five earthquakes (this includes the 1888 event) may be calculated using the peat accumulation rate and thickness of peat between the mid-points of respective silt horizons. The data indicate an average recurrence interval of 134 ±27 years. Further $^{14}C$ dating will be required to evaluate the assumption of uniform peat accumulation, but the recurrence interval calculated on this basis is consistent with the inferred Late Holocene average recurrence interval of 141 ±3 years.

7. A fifth pre-historic event may be inferred from vegetation buried by a large landslide SW of Hope Bridge and dated in a previous study at 778 ±60 yr BP. The predicted timing of this event based on the Late Holocene recurrence interval is approximately 800 yr BP.

## 5.7 The Origin of Horseshoe Lake

At the eastern valley entrance wood was obtained from beneath the Hope River degradational terrace T1 at the toe of riser R1, and was dated at 3482 ±77 yr BP. The crest of terrace riser R1 at the eastern valley entrance has been eroded (Trench Log #1) by a stream flowing down the fault controlled valley. From this and the similarity between $^{14}C$ dates from the toe of R1 and those obtained within the laminated sediments exposed in Trench #2, I infer that a stream was still active in the valley when R1 was cut by the Hope River, 3482 ±77 years B.P. This conclusion is also supported by a reconstruction of paleo-stream gradients for the Kakapo Brook and Hope River.

Kakapo Brook today flows across the Hope Fault at an altitude of 420 m and enters the Hope River at 407 m (Figure 5.13). Downstream below the offset terraces, the Hope River floodplain is at 400 m, 17 m below terrace (T1). Assuming that for the last 3300 years river gradient along this reach has remained essentially constant (i.e. no significant variation in particle size) then Kakapo Brook at the Hope Fault must have been flowing at approximately 435 m while the Hope River was forming terrace (T1) at the eastern valley entrance. This is approximately the level of the former river channel in the valley, prior to the damming of Horseshoe Lake. It therefore seems possible that at least a small branch of Kakapo Brook was active in the valley at this time (Figure 5.14).

The final damming of the valley must have occurred very soon after the abandonment of T1 because the crest of the younger degradational terrace riser R2, shows no sign of stream erosion, and yet records essentially the same fault offset as riser R1 (cf. R1 = 36 ±3 m and R2 = 36 ±0.5 m ).

## 5.8 Short and Long-Term Structural Controls on Rupture Propagation and Fault Displacement

### 5.8.1 The Significance of Fault Discontinuities: Fault Jogs and Bends

Increasingly in recent years attention has been focused on the importance of fault segmentation in governing the nucleation and arrest of moderate to large magnitude earthquakes (e.g Schwartz & Coppersmith 1986). In many cases where it has been possible to compare the surface rupture during a historical event with that from previous events, the individual displacements are observed to be almost identical. Further, there is often good agreement between the amount and rate of short-term (Holocene) deformation, and the amount of long-term (Late Pleistocene) deformation ( Sieh & Jahns 1984; Schwartz & Coppersmith 1984; 1986). These observations have contributed to the growing belief that slip distribution along a fault segment may be essentially constant, that individual segments can persist for long periods of time and that fault segments rupture separately (Schwartz & Coppersmith, 1986; Sibson, 1986; Barka & Kadinsky-Cade, 1988).

Strike-slip fault segments are typically bounded by bends or discrete side-steps in the principal fault trace, although criteria for the recognition of segments are by no means clear-cut. Based on their morphological expression, these features have been variously referred to as: (i) tectonic depressions and bulges (Clayton 1966), (ii) rhomb graben and rhomb horst (Aydin & Nur 1982), (iii) pull-apart basins and pressure ridges (Mann et.al. 1983; Rodgers, 1984), (iv) dilatational and antidilatational fault jogs (Sibson 1986).

In this discussion I will refer to the style of step-over regions as extensional and compressional fault jogs or releasing and constraining bends.

Fault jogs and bends represent both short and long-term obstacles to the transfer of slip and are believed to provide the physical basis for the concept of 'fault barriers' which may control the stick-slip behaviour of faults (e.g. Aki 1984). Transfer of slip across compressional fault jogs is accommodated by widespread subsidiary faulting, and shortening within the step-over region (Sibson 1986). The transfer of slip across extensional fault jogs is likely to involve opening of a linking fracture system (Segall & Pollard 1980; Sibson 1986). Rapid transfer of slip across extensional fault jogs during earthquakes may be inhibited by the development of transient, but very large, negative pore pressures as a result of volume increases, which soak up strain energy at the propagating rupture tip, resulting in rupture deceleration and even rupture arrest (Sibson 1986).

Fault jogs and bends may occur at a range of scales, from a few tens of metres to several kilometres. Hanmer Basin and Lake Glynn Wye on the Hope Fault are internationally celebrated examples of extensional fault jogs (e.g. Mann et.al. 1983; Woodcock & Fisher 1986), although the fault separation across the latter is only 200 m (Table 5.5).

In a study of historical earthquakes in Turkey, Barka & Kadinsky-Cade (1988) classify fault jogs and bends according to scale, and from their observations they suggest that only moderate to large jogs >5 km width, and bends >30° are likely to influence or impede earthquake rupture. From geometrical considerations the master faults bounding small (i.e. <1km wide) jogs, should converge to form a single plane at shallow depths (e.g. Naylor et.al. 1986; Grapes & Wellman 1988) and intuitively should

not significantly influence the propagation of earthquake rupture in the crust.

Paradoxically, during the 1888 Amuri earthquake lateral fault slip decreased from 2.6 m to 1.5 m across Lake Glynn Wye and a minimum of 0.61 m subsidence was recorded in this area with surface deformation distributed within a zone of up to 80 m wide and 400 m long (McKay (1890): Chapter 4). The Lake Glynn Wye Graben clearly exerted a strong structural control on rupture propagation during this event, despite its relatively small size and shallow depth (Table 5.5).

The implications of primary and secondary fault segmentation for the evaluation of seismic hazard and the estimation of true average Late Quaternary slip-rates at individual localities is now discussed.

### 5.8.2 Primary and Secondary Segmentation of the Hope Fault

The Hope Fault between Hanmer Basin and the Hope Boyle River junction is referred to in this study as the Hope River Segment, in recognition of the fact that the Hanmer Basin represents a large scale (primary) discontinuity separating the western and eastern strands of the fault.

There are two large scale (>5°) constraining bends in the surface trace of the Hope Fault west of Hanmer Basin, which may also represent primary segment boundaries and locking points focusing strain accumulation between earthquakes. One of these occurs south of the junction of the Hope and Boyle rivers west of Dismal Flats where the Hope Fault bends through 8 to 13° from a strike of 085° to 072° (Map 1, Figure 1.2, and Figure 4.2 ). This locality may have been the epicentre for the 1888 earthquake if the strength of ground-shaking at Glynn Wye is an indication of epicentral intensities (Chapter 4). The other recognisable

| | Lake Glynn Wye Graben (Freund 1971) | Lake Glynn Wye Graben (This Study) | Lake Glynn Wye 1888 Subsidence (Freund 1971) | Lake Glynn Wye 1888 Subsidence (This Study) | Constraining Fault Bend Glynn Wye Moraine Freund ( 1971 ) | Compressional Fault Bend Glynn Wye Moraine (This Study) | Poplars Graben (Freund 1971) | Poplars Graben (This Study) |
|---|---|---|---|---|---|---|---|---|
| Amount of Strike-Slip Displacement | 152 m | 286 m | 2.6 m | 2.0 m | 152 m | 286 m | 152 m | 286 m |
| Distance Between Bounding Faults | 182 m | 200 m | 182 m | 200 m | n.s. | 130 m | 305 m | 300 m |
| Width of Depression or Constraining Bend | 548 m | 600 m | 548 m | 600 m | 152 m | 130 m | 884 m | 900 m |
| Length of Depression or Constraining Bend | 1800 m | 1800 m | 1800 m | 1800 m | 305 m | 290 m | 2286 m | 2300 m |
| Maximum Depth or Height | 40 m | 40 m | 0.61 m subsidence | 0.61 m subsidence | 18 m | 20 m | 38 m | 40 m |
| Volume= WxLxDepth/3 | $13.15 \times 10^6$ m3 | $14.4 \times 10^6$ m3 | $2 \times 10^5$ m3 | $2 \times 10^5$ m3 | $3.1 \times 10^5$ m3 | $2.5 \times 10^5$ m3 | $25.59 \times 10^6$ m | $27.6 \times 10^6$ m |
| Depth of Bounding Fault Convergence = Volume x 2 / Movement x Strike-Slip Displacement. | 951 m | 503 m | 848 m | 1000 m | n.s. | n.s. | 1104 m | 643 m |

Notes: The model proposed by Freund (1971) for calculating the tectonic depth of the topographic depressions at Glynn Wye is adopted in this study.
The model assumes 1. That the volume of the topographic depression (area x depth ÷ 3) should be equal to the volume of the tectonic gap.
2. Tectonic depth should be equal to the volume of the topographic depression divided by the area of the tectonic gap and multiplied by two, since the gap must taper downward, and the average width will be at half its total depth.

TABLE 5.5. Volume Calculations for the Lake Glynn Wye and Poplars Graben and the Compressional Fault Bend at Glynn Wye Advance moraine: A Comparison between This Study and Freund (1971).

large bend in the surface trace occurs 50 km further west at the Otehake River (Figure 4.2 Chapter 4). Here, the fault bends or side-steps 20° SW, forming a trace which has previously been mapped as the active "Kelly Fault" (Gregg 1964).

Microseismicity studies in the Arthur's Pass region (Rynn & Scholz 1978) have delineated a zone of high activity in the vicinity of this fault bend, which extends WSW along the trend of the "Kelly Fault" . All events were found to occur within the upper 15 to 20 km of the crust and decreased in frequency towards the south-west. Focal mechanism solutions showed that strike-slip faulting predominates, with the right-lateral nodal plane striking parallel to the Hope Fault.

The concentration of microearthquake activity beneath this fault bend may indicate that the bend extends to seismogenic depths, forming a zone of increased mean stress and a potential nucleation point for strain release in moderate to large earthquakes.

The Hope River Segment is also segmented at a secondary scale length of between three and ten kilometres. Poplars Graben marks the next secondary segment boundary to the east. The active floodplain of the Hope River obscures the trend and geometry of the fault between Dismal Flats and Poplars Graben, but an inferred eastward projection of the strike from Dismal Flats indicates that there is a step over or trend toward the south (Map 1). A third and further step-over toward the south occurs at Lake Glynn Wye Graben, which was the site of observed subsidence and the significant reduction in the amount of lateral slip during the 1888 earthquake. Between Lake Glynn Wye Graben and the Hanmer Basin the fault is not visibly segmented and this is corroborated by the observation of two equal lateral displacements during the 1888 earthquake, nine kilometres apart at Glynn Wye and Hopefield respectively

(Chapter 4).

The effects of a constraining bend on fault slip are clearly shown further west toward the Glynn Wye moraine where the 1888 surface rupture remains very well preserved. It was possible as part of this study to survey an accurate profile of the 1888 rents, from the Glynn Wye moraine terminus to the constraining fault bend west of the moraine. The 20 m high anticlinal ridge associated with this constraining bend at the NE corner of Poplars Graben is volumetrically a surficial structure (Table 5.5), but it influenced the amount of lateral slip recorded in the Late Quaternary cover following the 1888 earthquake. Eight scarp profiles are presented on Map 4, and illustrate an increase in vertical displacement from 0.1 to 0.2 m at the moraine terminus, to 0.9 to 1.0 m at the constraining bend. These observations combined with those of McKay (1890) indicate that the fault bends and jog at Glynn Wye partitioned the total slip in 1888 into vertical and lateral components whose values depended on location along the fault, and may account for the observed reduction in the total lateral slip across Lake Glynn Wye Graben (Chapter 4).

Structural controls have also affected long-term displacements. This is seen most clearly by the different displacements across the Glynn Wye moraine and associated recessional meltwater terraces of inferred near-equal (~17 000 yrs) age. The eastern face of the moraine is offset 286 ±6 m. The meltwater terrace riser forming the western face of the moraine is displaced 265 ±9 m along the 15-20° constraining bend and the second meltwater terrace riser 300 m to the west, is displaced 148 ±6 m along the northern edge of Poplars Graben.

Levelling profiles were surveyed at right-angles across the anticlinal ridge at the constraining bend; these indicate that shortening

across the constraining bend parallel to the regional fault strike (080°) is between 2% and 9 % (Map 4). This corresponds closely to the 2.15-12.33 % range of the difference in displacement between the western and eastern faces of the moraine.

The offset deficit between the moraine terminus and the second terrace riser in Poplars Graben is a much greater 49-55%. But the zone of listric-normal faulting which defines Poplars Graben is between 700 and 900 m wide. If the 148 ±6 m lateral displacement on the terrace riser is added to an estimate of the horizontal component of faulting in Poplars Graben and compared with displacement on the eastern face of the moraine (Figure 5.19) the offset deficit between the moraine terminus and the terrace riser reduces to a range of 18% to 26%.

Furthermore, it should be noted that the estimate of horizontal fault displacement is a minimum due to the possibility of i) extension and listric-normal faulting occurring beyond the obvious margins of the graben, and (ii) distributed strain in weak loose deposits. These factors would further reduce the offset deficit. Further, this estimate of horizontal faulting in Poplars Graben indicates that a significant proportion (up to 26%) of the total fault displacement (286 ±6 m) is distributed as strike-slip displacement on faults within Poplars Graben. Evidence of this comes from the small lateral displacements on the meltwater terrace risers where they are bisected by faults within the graben (Map 4). The estimate of shortening across the constraining bend is also a mimimum value which takes no account of potential telescoping of gravels beneath the folded surface, or of the intense subsidiary faulting around the bend (see Map 1 and attached cross-section).

Given that the estimates of shortening and extension are minimum values and that the standard error of measured displacements will remain

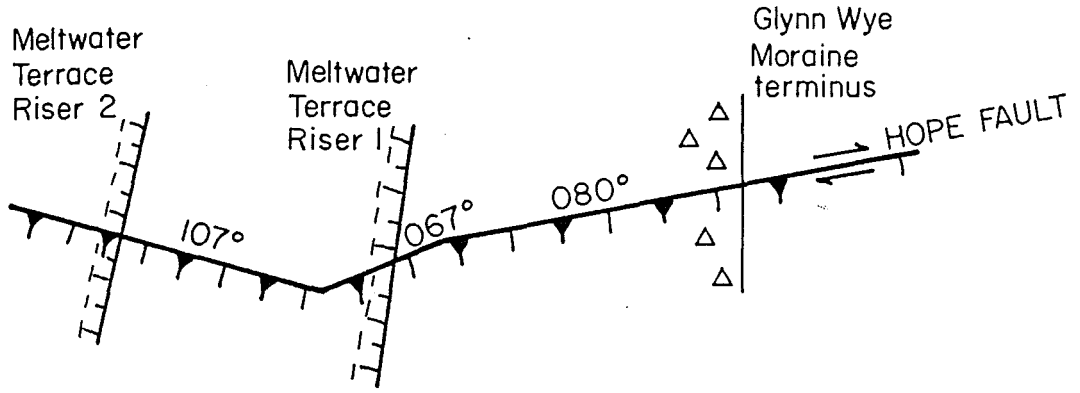


a. Glynn Wye Moraine Complex prior to fault displacement c. 17,000 ± 1,000 yr BP

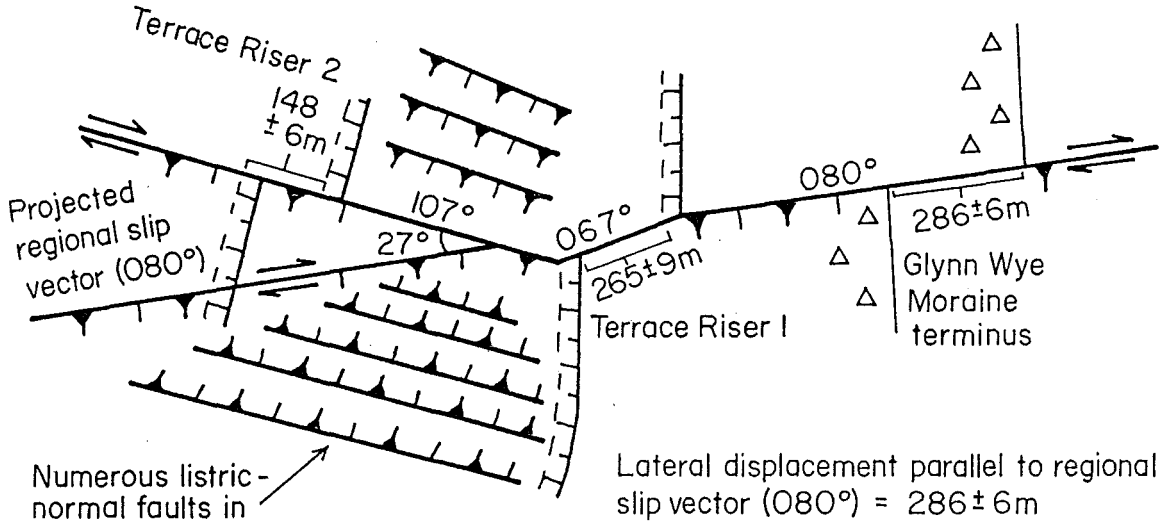


b. Glynn Wye Complex - Present Day

Lateral displacement parallel to regional slip vector (080°) = 286 ± 6m

Observed lateral displacement on Terrace Riser 2 = 148 ± 6m

Estimated horizontal displacement on Terrace Riser 2 tan 27 x 148
= 75 m

286 - (148 + 75) = 63m of **lateral** displacement distributed across Poplars Graben

Fig 5·19: Measurements of Lateral and Horizontal Fault Displacement at Glynn Wye Moraine Complex

at between 2% and 4%, it appears that partitioning of slip into vertical and lateral components at these secondary segment boundaries can fully account for the variations in lateral offset across features of similar age.

These spatial variations in offset are cumulative (and by implication consistent) which implies that the secondary segment boundaries have remained persistent obstacles to the transfer of slip since at least the Late Pleistocene. The close match between the historical (1888) and geomorphic distribution of surface deformation and the longevity of the segment boundaries at Glynn Wye is consistent with observations of fault segmentation on the Wasatch Fault Zone, Utah (Schwartz & Coppersmith, 1986), and the Oued Fodda Fault, Algeria (King & Yielding, 1984). In all these cases the distribution of lateral and vertical slip varies systematically along the fault and is controlled by fault segmentation via changes of fault geometry.

The observed variations in lateral slip during the 1888 earthquake and the spatial variations in offset across the Late Pleistocene Glynn Wye Advance landforms indicates that even segment boundaries of <1 km width and segments at a scale length of only three to five kilometers can and do exert a strong structural control on the spatial variation in slip. As the calculation in Table 5.5 shows, the Glynn Wye moraine constraining bend at which lateral fault displacement is observed to decrease involves only a shallow depth of surficial deposits. Evidently the volume or penetrative depth of this fault bend is not a major factor in deciding its influence on the surface expression of fault displacement.

The large variations in surface displacement across secondary fault segment boundaries means that one must know the geometry of the fault in

order to evaluate slip-rates calculated from individual locations. Maximum lateral surface displacement in each segment will occur only away from the segment boundaries. The implications of this structural control for the interpretation of slip-rates derived for different time-periods at different localities on the Hope Fault are now discussed.

## 5.9 Spatial versus Temporal Variations in Late Quaternary Slip-Rate

Knuepfer (1984) used weathering rinds and soil development indices to date Late Quaternary geomorphic surfaces offset by faulting at a number of sites throughout Marlborough, including Glynn Wye Station.

He argued that average latest Pleistocene lateral slip-rates across the Hope Fault are greater than the sum across the other main Marlborough faults (the Wairau, Awatere and Clarence faults), but that Late Holocene lateral slip-rates, both from individual sites and calculated from transects across Marlborough, are substantially less than incremental early-mid Holocene rates. He concluded that plate boundary motions have varied over intervals of 3 000 to 5 000 years during the last 15 000 to 20 000 years.

Knuepfer's age and displacement data from the Glynn Wye Advance moraine and the degradational terraces at Manuka Creek are reproduced in Table 5.6. The study sites are of Late Pleistocene and Late Holocene age respectively, and the data thus describe an apparent decrease in lateral slip rate during the mid-late Holocene.

Conversely, the results of this study clearly indicate that on the Hope River segment of the Hope Fault there is no evidence for true temporal variations in lateral slip-rate. Firstly, an evaluation of Knuepfer's data (Chapters 2 and 5) ) suggests that Knuepfer erred in

| Author | Features | Period (years BP) | Slip-Rate (mm/yr) |
|---|---|---|---|
| KNUEPFER (1984) | Eastern Face Glynn Wye Moraine and Terrace Riser R2. | 16 600 to 4 400 | +6.1<br>25.0<br>-4.0 |
| | Offset Degradational Terraces at Manuka Creek | 4 400 to 0 | +2.0<br>8.2<br>-1.6 |
| COWAN (THIS STUDY) | Eastern Face Glynn Wye Moraine | 17 000 to 3 500 | +2.0<br>18.5<br>-1.7 |
| | Offset Degradational Terraces at Manuka Creek | 3 500 to 0 | 10.6 ±0.3 |

Notes: 1. All displacements are in metres
2. Displacements and Age Estimates from Tables 5.3 and 5.4

Table 5.6. Comparison of Late Pleistocene and Late Holocene Incremental Slip-Rate Estimates for the Hope Fault at Glynn Wye Moraine and Manuka Creek.

measuring the Glynn Wye Advance moraine terminus displacement and in estimating the age of the second meltwater terrace riser. These errors exaggerate the Late Pleistocene slip-rate recorded by the moraine, and reduce the early to mid Holocene slip-rate based on the age estimate of the terrace riser. This apparent trend is supported by Knuepfer's Late Holocene data from Manuka Creek, which describe a further reduction in lateral slip, (Table 5.6). (continued overleaf.)

However, inferences of changes in slip-rate can only be valid if there are no spatial variations in slip among the study sites. This study has documented variations in lateral slip across Lake Glynn Wye following the 1888 earthquake, and a systematic increase in the height of 1888 rupture scarps between the Glynn Wye Advance moraine terminus and the constraining fault bend 700 m to the west. Furthermore, systematic and cumulative spatial variations in slip across features of near-equal age are also inferred from the three different displacements at the Glynn Wye Advance moraine (Section 5.8).

The important hypothesis to test is whether the displacements at Manuka Creek record a true reduction in slip-rate during the Late Holocene, or whether they reflect simply a spatial variation in slip distribution along the fault, due to their location with respect to the Lake Glynn Wye Graben.

The Late Holocene slip-rate calculated in this study from the dated terrace offset at Manuka Creek is 10.6 ±0.3 mm/yr and represents approximately 57% of the 18.5 mm/yr incremental Late Pleistocene slip, calculated from the Glynn Wye Advance moraine terminus offset (Table 5.6). I believe that this is not a temporal decrease in slip-rate can be explained in terms of fault segmentation and systematic spatial variations in displacement. During the 1888 earthquake two 1.5 m offsets were recorded to the west and east of Manuka Creek respectively, and without apparent structural complications in between, the lateral slip at this locality is inferred to have been the same. This value is 57% of the 2.6 m slip observed west of Lake Glynn Wye, and shows an exceptionally good match with the ratio between the apparent Late Holocene rate and the apparent Late Quaternary rate (Table 5.6).

Furthermore, the Late Holocene slip-rate at Manuka Creek is

consistent with the evidence in Raupo Swamp for characteristic earthquake magnitude and recurrence during the last 600 years.

The internal consistency between the historic, prehistoric and geologic rates of faulting at this locality strongly suggests that the 1888 earthquake was a characteristic event for the Hope River Segment of the Hope Fault. It further implies that the rate of activity has been essentially constant throughout the Late Quaternary but that systematic spatial variations in lateral slip-rate are expressed in surficial materials, due to earthquake rupture interaction with the fault jogs and bends which form secondary fault segment boundaries along the Hope Fault at Glynn Wye.

From volumetric considerations (Table 5.5) it seems unlikely that these fault jogs and bends derive from deep-seated crustal discontinuities. Their development may relate to basement rock topographic relief and in the jog or bend regions at depth the spatial variations in lateral slip are probably accommodated within anastomosing domains of cataclastic shear and widspread micro-fracturing.

## 5.10 Summary

Late Quaternary displacements on the Hope and Kakapo faults were measured directly in the field and from enlarged high-resolution vertical aerial photographs. The displacements were combined with age estimates for the faulted landforms to derive Late Quaternary slip-rates on the Kakapo Fault in Dismal Valley and on the Hope Fault at the Glynn Wye Advance terminal moraine and the Hope River degradational terraces at Manuka Creek.

A comparison of these results with those obtained in previous studies

indicated some large discrepancies in both measured displacements and age estimates of faulted surfaces. The most pronounced example is at the Glynn Wye Advance terminal moraine, where the moraine terminus and two meltwater terrace risers of inferred near-equal age are displaced by different amounts. Previous workers have explained these displacements either by assuming a closely similar age for the offset features and adopting measurement methods which derived more equal displacements, or by accepting the variable offsets and assuming significantly different ages.

Detailed field mapping and measurement of the displacements during this study indicate that the moraine and terrace risers are of near-equal age. The displacements on these features are different because of their location relative to a compound bend in the fault trace. In successive earthquakes a component of slip oblique to the regional slip vector has formed the 700 to 900 m wide Poplars Graben.

I infer that the meltwater terrace risers record only a proportion of the total Late Quaternary lateral slip because they have also slipped oblique to the fault. Only the moraine terminus offset which is almost free of structural complication may be used to calculate a Late Quaternary slip-rate at this locality. In this study an age of 17 000 ±1000 yr BP is assumed for the retreat of ice from the moraine terminus and the displacement which post-dates this was measured at 286 ±6 m. The resultant estimate of true Late Quaternary slip-rate is between 15.5 mm/yr and 18.25 mm/yr. Late Quaternary slip-rates estimated from features near fault segment boundaries will not be accurate.

Wood from a trench excavated in one of three Hope River degradational terrace risers traversed and offset by the Hope Fault at Manuka Creek provided a $^{14}C$ date of 3482 ±77 yr BP from beneath the terrace tread and

a maximum age for the terrace riser down-dropping to the next level. The lateral displacement on the lower terrace riser is 36 ±0.5 m and a Late Holocene slip-rate of 10.6 ±0.3 mm/yr is calculated for this feature, with an allowance made for the elapsed time (100 yr) since the last event.

A comparison of the Manuka Creek slip-rate with the Late Quaternary slip-rate indicates an apparent decrease in lateral slip-rate between the Late Pleistocene and Late Holocene. Knuepfer (1984), also inferred a large reduction in the rate of lateral slip during this period across all of the Marlborough faults, but especially the Hope Fault.

A review of the 1888 earthquake has shown that fault jogs affected the lateral slip during the earthquake. Lateral slip was not distributed uniformly along the fault: significant reductions in lateral slip occurred across Lake Glynn Wye Graben. Detailed field mapping and surveying of scarp profiles at the moraine locality also identified an increase in the amount of vertical displacement (and by implication a reduction in lateral displacement) on 1888 fault scarps in the vicinity of a 15-20° constraining fault bend.

The different displacements across the Glynn Wye moraine features of near-equal age show that such spatial variations in lateral slip distribution are systematic and occur over long ($10^5$ yr) time intervals. These systematic and cumulative spatial variations in lateral slip emphasise the persistence of the causative fault bends or jogs over similar periods of time and highlight the segmented nature of the Hope Fault.

Segmentation is evident at a large scale with the Hanmer Basin forming a complex major junction between western and eastern strands of the Hope Fault. There is also some evidence for a segment boundary south

of the Hope-Boyle River junction and 50 km further to the west, where the "Kelly Fault" diverges from the Hope Fault at the junction of the Otehake and Taramakau rivers.

On a smaller scale length of between three and ten kilometers, the Hope River Segment of the Hope Fault is itself segmented, where segment boundaries are coincident with Poplars Graben, and Lake Glynn Wye Graben respectively (Map 1). The implication of this internal or secondary segmentation of the Hope Fault is that slip-rate estimates derived from measurement of displacement at a single locality are likely to be unique to that locality. Only estimates from locations unaffected by jogs or bends at segment boundaries can be extrapolated beyond the individual locality.

I do not believe, however, that it is possible to infer temporal variations in slip-rate from displacements of different age at localities on either side of segment boundaries and conclude that apparent temporal variations in lateral slip are more likely to be spatial variations in disguise. In this case the 1888 decrease in lateral slip across Lake Glynn Wye Graben is equivalent to the ratio between the Late Quaternary slip-rate estimated at Glynn Wye moraine and the Late Holocene degradational river terraces to the east of Lake Glynn Wye Graben at Manuka Creek.

Corroborative evidence of a relatively constant rate of slip during the Late Holocene was obtained from a trench excavated across the Hope Fault, in Raupo Swamp between Horseshoe Lake and the offset terraces at Manuka Creek. Four silt horizons were identified within the fibrous peat of the swamp and are inferred to represent an influx of sediment following surface rupture in pre-historic earthquakes. The four silt horizons coincide with expected datum stratigraphic features compatible

with evidence of paleo-earthquakes, based on an average Late Holocene recurrence interval of 141 ±3 years calculated from the dated terrace offset at Manuka Creek, divided by the inferred 1.5 m displacement at this locality during the 1888 earthquake. I predicted the location of the silt horizons within the peat based on an average peat accumulation rate of 2.2 ±0.2 mm/yr which was calculated utilizing a $^{14}C$ date near the base of the peat. Further $^{14}C$ dating is required to refine this estimate, but coincidence between the predicted horizons and the silt layers is good. Pollen analysis of the peat column provided evidence of an increase in the abundance of matagouri coincident with two of the silt layers. Matagouri is a coloniser of barren stony surfaces and its presence in significant proportions only at these horizons, is inferred to indicate an ecological response to surface rupture. One of the silt horizons coincides with a major deforestation event 500 to 600 years BP, and although equivocal, the two events are inferred here to be unrelated, because further deforestation during the late-nineteenth century produced a similar pollen response at the site, but no increase in silt content.

The peat thicknesses between the silt horizons and the thickness between the top silt horizon and the estimated datum for the 1888 earthquake indicate an average recurrence interval for faulting during the last 600 years of 134 ±27 years which is consistent with the Late Holocene average (based on lateral slip) of 141 ±3 years.

The fact that the Late Holocene recurrence estimate is based on the assumption of approximately 1.5 m lateral displacement per event implies that the Hope River segment of the Hope Fault ruptures with characteristic magnitude, and with similar point-specific displacement in successive earthquakes. This further supports the arguement in this

study for secondary fault-segmentation and systematic spatial variations in fault displacement.

# CHAPTER 6 SEISMIC HAZARD EVALUATION

## 6.1 Introduction

In this chapter the principles and assumptions of seismic hazard analysis are introduced and placed in a New Zealand context. Previous studies of regional seismic risk in New Zealand are discussed and the results of these studies are considered with a particular view to assessing seismic risk in the Amuri District, North Canterbury.

Information obtained in this study from the review of the 1888 earthquake and the field studies in the Lower Hope Valley are then combined with an attenuation expression (which describes the decay of ground motion as a function of epicentral distance) to infer likely seismic effects in Amuri District accompanying future earthquakes on the Hope and Kakapo faults.

## 6.2 Summary of New Data Applicable to Seismic Hazard in the Amuri District, North Canterbury

The 1888 Amuri earthquake has been reviewed in detail and coseismic surface rupture in that event was evidently restricted to the Hope Fault west of Hanmer Basin.

Two alternative rupture lengths of 40 km and 100 km respectively, have been evaluated on the basis of felt intensities, observed ground rupture and the geometry of the Hope Fault at possible large-scale fault segment boundaries. The 100 km rupture length estimate is based largely on unverified, circumstantial evidence of fault rupture in the Otira Gorge but the 40 km estimate is preferred because it is more consistent

with the size of the region of high felt intensities and observed seismic effects.

The estimated magnitude of the 1888 earthquake is here revised downward, from M = 7.3 to a range of M = 6.5-6.8, on the basis of reinterpreted strong motion attenuation and empirical relationships between magnitude and the fault parameters of rupture length, ruptured area and inferred seismic moment.

Re-evaluation of 1888 earthquake felt intensities and damage reports suggest that although ground-shaking probably reached MM9 in the Hope River area, the damage was of limited extent and beyond the immediate vicinity of the fault can be attributed to poor construction or local site response.

Extreme variations in site response were, in fact, characteristic of the 1888 earthquake effects in Amuri District, and this precludes a detailed local analysis of the spatial distribution of seismic effects in future events, until additional data on the controls governing local site response are available.

In the preceding chapter, the significance of carbon-14 dating of wood from a trenching site at the Hope Fault between Horseshoe Lake and Manuka Creek was described providing a well constrained, locality-specific date for an offset river terrace. The derivation of a Late Holocene slip-rate of 10.6 ±0.3 mm/year was discussed. A second trench excavated across the fault nearby, permitted the tentative recognition of four prehistoric faulting events at this locality, and the inference of a fifth from a radiocarbon-dated dated landslide near the Hope River Bridge.

Evidence for these events consisted of four silt layers within a column of fibrous peat which occupies a swamp traversed by the Hope Fault

to the north of State Highway 7, 300m east of Horseshoe Lake.

The silt layers are inferred to reflect the influx of inorganic sediment into the swamp following ground rupture and landsliding, and imply an average earthquake recurrence interval of 134 ±27 years. The dating of these events is presently based on the assumption of a constant rate of peat accumulation between the silt layers, calibrated by a single $^{14}C$ date. The validity of this assumption was discussed in Chapter 5 and was not considered unreasonable as a first approximation. Additional samples of the peat column have been submitted to the Institute of Nuclear Sciences for radiocarbon dating to refine the dating of the silt layers. The results will be reported shortly.

The average recurrence interval between silt-depositing events derived using the existing data shows an extremely good match with a recurrence interval of 141 ±3 years based on the Late Holocene slip-rate at Manuka Creek calculated in Chapter 5, and the known 1.5 m displacement at this locality during the 1888 earthquake.

Long-term spatial variations in slip-rate are inferred from a good match between the geomorphic distribution of Late Quaternary lateral versus vertical fault slip, and the style and size of displacements associated with surface rupture during the 1888 earthquake.

When adjusted for inferred long-term spatial variations in fault slip, the Late Holocene slip-rate at Manuka Creek corresponds closely to the Late Pleistocene slip-rate derived from the 286 ±6m offset across the 17000 ±1000 year Glynn Wye advance terminal moraine, 6 km west of Manuka Creek.

The internal consistency between the historic, the inferred prehistoric and the geologic rates of slip at Manuka Creek is believed here to provide compelling evidence for characteristic earthquake

recurrence and magnitude on the Hope River Segment of the Hope Fault.

Less is known about the activity of the Kakapo Fault, but on the basis of Late Pleistocene and Holocene terrace offsets, the Kakapo Fault has sustained about half the Hope Fault rate of Late Quaternary displacement. A comparison of Hope and Kakapo Fault scarp morphology in deposits of the same age and textural characteristics indicates that the Kakapo Fault has been much less active in recent times, but as there is no information available regarding the size and timing of the most recent movement at Glynn Wye a more specific discussion of the hazard cannot be made.

## 6.3 Historical Earthquakes in the Region.

The 1888 Amuri earthquake ($M_S$=6.5-6.8) is one of the largest earthquakes to have occurred in North Canterbury since post-European settlement. Following the 1888 earthquake several previous earthquakes felt strongly in Canterbury were reinterpreted, and assigned epicenters in the Lake Sumner area (Hogben 1890; 1891).

One of these (December 5th, 1881) was widely felt in Canterbury and North Westland (apparently intensity MM6 in Christchurch), but there are no felt reports from the Hanmer area, despite settlement by pastoralists at that time.

The 1929 Arthurs Pass earthquake ($M_S$=6.9) generated maximum intensities above MM8 in the mountainous country north-east from Arthurs Pass. Speight (1933) mapped the area of most intense landsliding caused by this earthquake; a narrow elliptical zone elongate ENE-WSW across the head of the Poulter River, and along the south branch of the Hurunui River. Speight tentatively recognised primary surface rupture in the

vicinity of Roche Saddle, and suggested that the earthquake might represent a south-westward extension of activity from Glynn Wye and Hanmer Plains.

In fact, the zone of maximum disturbance does lie directly along a westward projection of the Kakapo Fault which may have ruptured in this area in 1929, possibly in response to a transfer of stress from the Hope Fault, during the 1888 earthquake 41 years earlier (see Figure 4.2 in Chapter 4). Overall, within the last 120 years, a number of earthquakes of between magnitude 5.0 and 7.0 have occurred in the North Canterbury region, some of which have generated local ground shaking intensities of up to MM7. These have been reviewed by Eiby (1968), and Fellows (1986); and are listed with comments in Appendix 8.

## 6.4 Seismic Hazard Analysis

### 6.4.1 Principles

To arrive at estimates of ground motion versus recurrence interval, it is necessary to have either a representative record of moderate-large magnitude earthquakes, or a means of accurately modelling the rate of activity of faults within a seismic region.

In regions where the surface expression of faulting is diffuse, or the history of activity on specific faults is too short, or poorly constrained to determine a fault-specific recurrence relationship, the traditional approach to seismic hazard assessment is to assume a uniform spatial distribution of earthquakes and an exponential distribution of magnitudes, of the Gutenburg-Richter (Richter 1958) form:

$$\log N(m) = a - bm$$

where N(m) is the cumulative number of earthquakes of magnitude greater than m; a defines the rate of occurrence; and b the exponential decay with increasing magnitude.

The parameters a and b are constants of the seismicity model, unique to a tectonic province, and usually calculated from a catalogue of historical seismicity, supplemented where possible by geologic data of recent faulting (e.g. Peek et.al. 1980; Smith & Berryman 1983, 1986).

When combined with an appropriate attenuation expression, the seismicity model may be used to derive return periods, or probabilities of exceedence for specified levels of ground motion. This classical seismic hazard analysis was advanced by Cornell (1968) and has been applied to New Zealand by among others Peek (1980); Mulholland (1982); and Smith & Berryman (1986).

Where geological studies of faults within highly active fault zones have resulted in the recognition of individual paleoseismic events it has been observed that the fault zones typically are segmented, and that individual fault segments often rupture independently with similar locality-specific displacement, and generating earthquakes of similar magnitude (Sieh 1984; Schwartz & Coppersmith 1984; King and Yielding 1984; Wesnousky et.al. 1983; Youngs & Coppersmith 1985). These observations suggest that on at least some individual faults, a characteristic earthquake model provides a more realistic expression of earthquake recurrence than the exponential magnitude distribution. Seismic hazard estimates based on the exponential magnitude distribution are biased toward smaller but more frequent events which dominate the seismicity catalogue (Figure 6.1) (Youngs and Coppersmith 1985; Schwartz

& Coppersmith 1986).

On the Hope Fault in the Lower Hope Valley the recognition of four prehistoric earthquakes and tentative recognition of a fifth creates an opportunity to consider a characteristic earthquake model for the Hope River fault segment of the Hope Fault. This possibility lies beyond the immediate scope of this discussion. For the purposes of this study the potentially high level of seismic activity in North Canterbury and Marlborough, and the presence locally of other active faults about which very little is known (e.g. the Kakapo, Hanmer and Jollies Pass faults), justifies the continued use of regional seismicity parameters (based on all seismic sources) to calculate the local hazard.

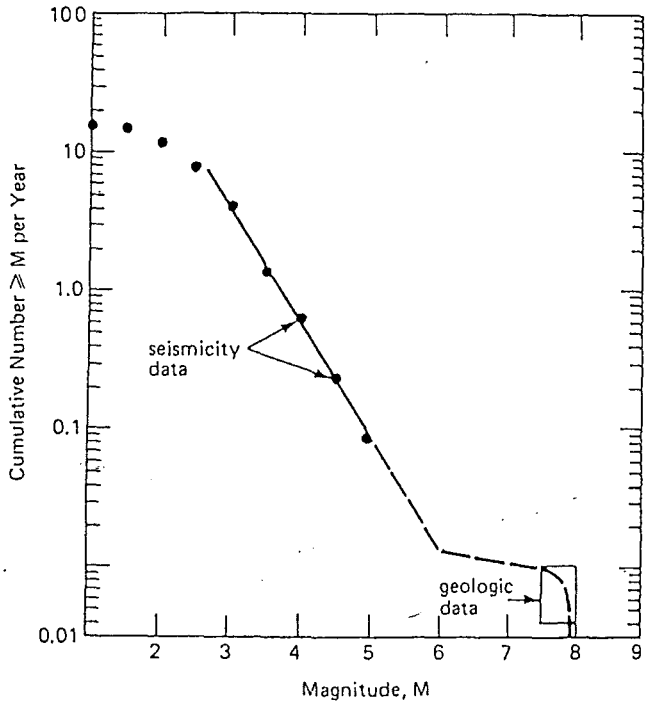


Figure 6.1 Cumulative frequency–magnitude recurrence relationship for an individual fault. A low b value is required to reconcile the small–magnitude recurrence with geologic recurrence, which is represented by the box (from Schwartz and Coppersmith 1984).

Nevertheless I believe this study represents the first essential step toward establishing a recurrence model for large magnitude, shallow foci earthquakes on the Hope Fault which represents the largest and one of the most recently active structures in North Canterbury.

### 6.4.2 Previous Studies

In New Zealand, previous studies have produced regional estimates of seismic hazard for the whole country, based on exponential magnitude distribution in some cases supplemented by geologic data on long-term fault activity.

A number of seismicity models have been proposed to describe the rates of seismic activity in different tectonic provinces (e.g. Matuschka 1980; Peek et.al. 1980; Smith & Berryman 1983, 1986). All assume uniform spatial distribution of earthquakes with an exponential distribution of magnitudes.

Peek (1980) and Mulholland (1982) reviewed available attenuation models derived from strong-motion records and, using the limited NZ strong-motion data base, Mulholland combined the attenuation model of Katayama et.al. (1978) with New Zealand seismicity models, to produce 150 year return period comparative risk maps of acceleration response with 5 percent damping at a natural period of 0.15 seconds (Figures 6.2 & 6.3).

Smith & Berryman (1983, 1986) used a revised seismicity model incorporating more geologic data to produce risk maps contouring mean return periods for Modified Mercalli intensities MM6-MM9, (Figure 6.4).

Fellows (1986) combined Krinitzky & Marcusons' (1983), and Medvedev (1962) empirical estimates of peak ground acceleration for given Modified Mercalli intensities, with Smith & Berryman (1983) estimates of the mean recurrence for a range of Mercalli intensities. On this basis she inferred 150 year average peak ground accelerations of 0.35-0.40 g, for MM8-MM10 in North Canterbury, and an upper bound mean acceleration of 0.95 g for intensity MM10 (Appendix 9).

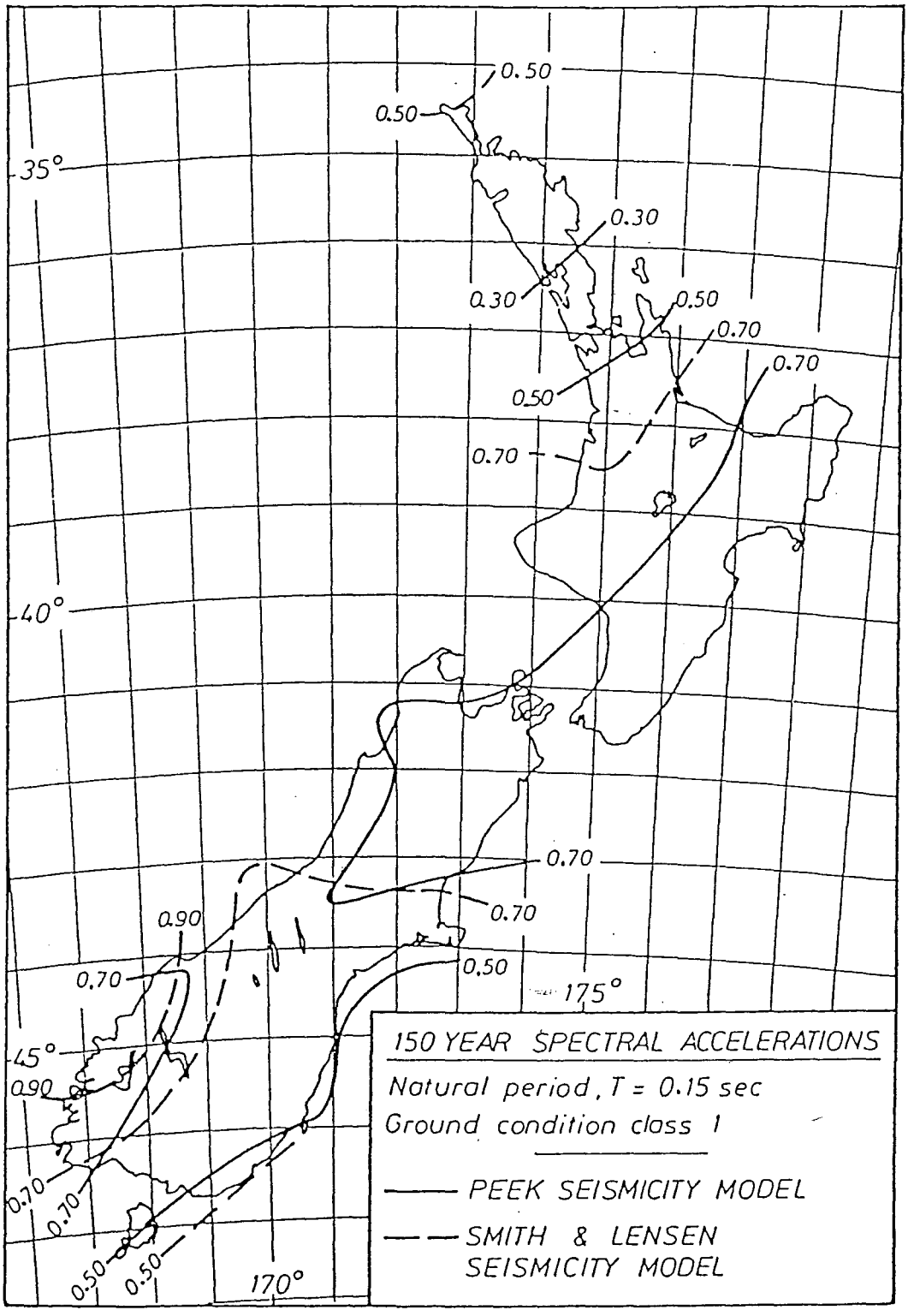


Figure 6.2. From Mulholland (1982).
Ground Class 1 defined in Table 6.1.

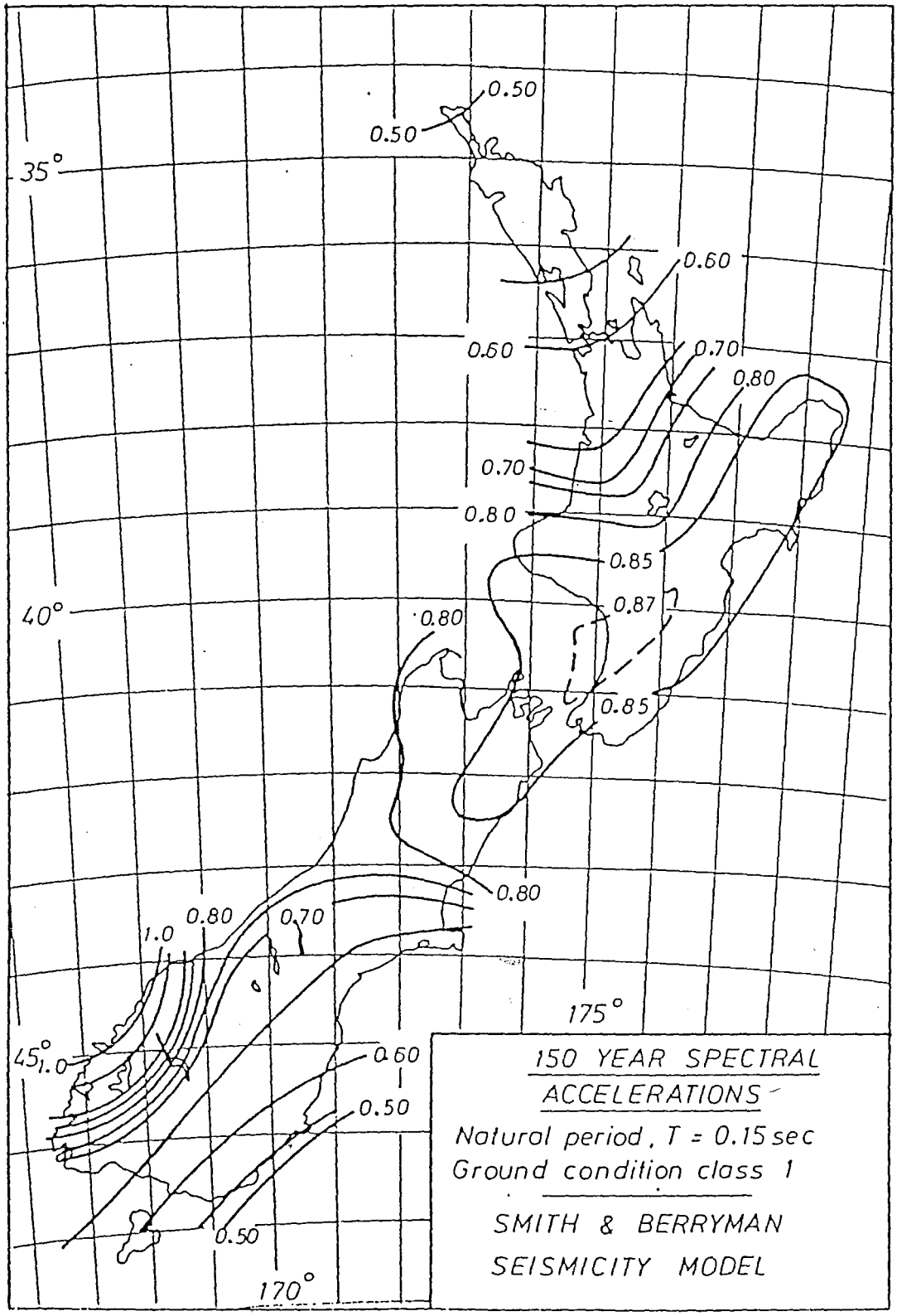


Figure 6.3. From Mulholland (1982).
Ground Class 1 defined in Table 6.1.

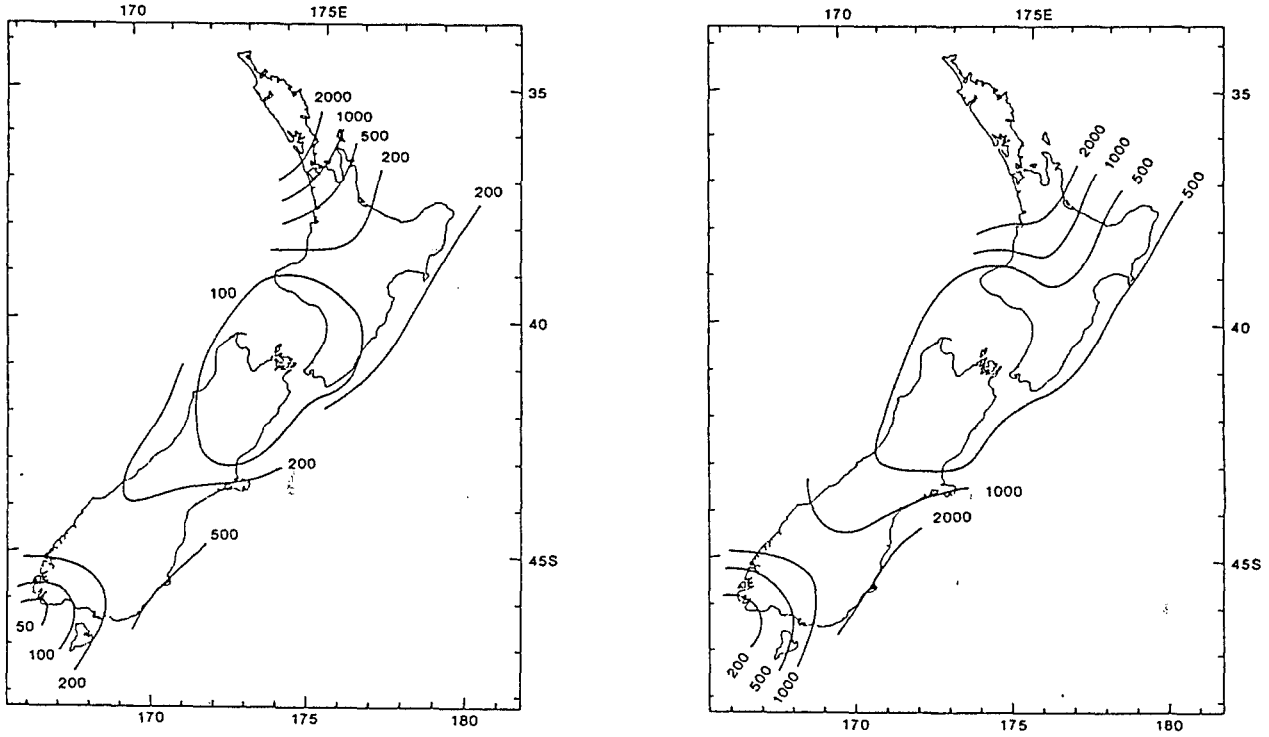


Figure 6.4. a) Mean Return Periods (years) for intensity MM 8

b) Mean Return Periods (years) for intensity MM 9.

From Smith and Berryman (1986).

### 6.4.3 Estimates of Local and Regional Seismic Risk Based on Intensity Attenuation Patterns

When intensity-recurrence functions are determined for a number of sites with assumed uniform local ground conditions the results may be represented by sets of seismic probability maps, each map showing contours of intensities that correspond to a given return period .

However, differences in earthquake source mechanisms, propagation paths, local site conditions, and geological controls on the rupture process can introduce systematic deviations in the correlation of actual to predicted intensities and energy radiation patterns (Esteva 1976; Madariaga 1983). Modification of regional seismic risk maps is therefore required for a local analysis of predicted risk. This practice is known as microzoning and traditionally involves first, the calculation of seismic intensities on solid ground by means of an appropriate attenuation expression, followed by the amplification of these intensities based on a knowledge of the local site conditions.

There are not sufficient data available concerning site conditions to conduct a microzonation of the Lower Hope Valley-Hanmer Springs area. The attenuation model of Katayama et.al.. (1978) is combined here with magnitude estimates of characteristic earthquakes on the Hope Fault and used to predict acceleration response at bedrock and alluvial sites in the Amuri District, during potential future earthquakes on the Hope River Segment of the Hope Fault.

Acceleration response has been calculated for accelerations at a natural period of T = 0.15 seconds (approximately that of 1.5 storey structures) with 5 percent damping, and generated by an earthquake of $6.4 < M < 6.9$ on the Hope Fault at a range of epicentral distances (Table

6.1).

Accelerations predicted at bedrock sites up to 20 km from the epicentral region (probably the Hope-Boyle River junction in 1888) are likely to range from 0.23 g to 0.34 g. At epicentral distances of less than 20 km the response for a site on alluvium is between 0.21 g and 0.31 g respectively. The predicted response 100 km away at Christchurch is between 0.1g and 0.13g respectively.

### 6.4.4 Comparison of Seismic Risk Estimates with Previous Studies

By interpolation from the Mulholland (1982) general risk maps (Figures 6.2 & 6.3), 150 year 0.15s spectral accelerations for the seismic hazard in the Hanmer-Hope River area (bedrock site) range from 0.75g to 0.82g. Mulholland's values exceed the spectra predicted in this study, because they encompass the range of magnitudes, epicentral distance, attenuation and site conditions represented by all faults in the region, and contain more spectral components than most individual natural events.

When converted to peak ground accelerations using the empirical correction of Newmark et.al. (1973), these values reduce to 0.28 g to 0.31 g, which are consistent with the estimates obtained here.

Fellows (1986) estimated average peak ground accelerations of 0.35 g to 0.40 g, for 150 year recurrence of intensity MM8-MM10 in North Canterbury. These values are higher than those predicted in this study because they are based on a prediction of larger magnitudes and intensities, which include those generated in earthquakes on large faults (such as the Clarence and Awatere Faults) beyond the area considered in this study.

| | Ground Condition Type I | Ground Condition Type II | Ground Condition Type III | Ground Condition Type IV |
|---|---|---|---|---|
| MAGNITUDE M = 6.1 to 6.7 | | | | |
| Epicentral Distance: | | | | |
| 6 to 19 km | 0.23 g | 0.19 g | 0.21 g | 0.18 g |
| 20 to 59 km | 0.14 g | 0.12 g | 0.13 g | 0.11 g |
| 60 to 119 km | 0.10 g | 0.08 g | 0.09 g | 0.08 g |
| MAGNITUDE M = 6.8 TO 7.4 | | | | |
| Epicentral Distance: | | | | |
| 6 to 19 km | 0.34 g | 0.29 g | 0.31 g | 0.27 g |
| 20 to 59 km | 0.21 g | 0.18 g | 0.19 g | 0.17 g |
| 60 to 119 km | 0.15 g | 0.13 g | 0.14 g | 0.12 g |

Notes: 1. All terms are from Katayama et.al. (1978), see Appendix 10.

2. The tabulated values are predicted acceleration spectral amplitudes for T = 0.5 s and h = 0.05, where T= natural period and h = 5 percent damping factor.

3. Ground Condition Classes at Recording Site

Type I: Bedrock.

Type II: Alluvium with H <10 m.(where H = Depth to Bedrock)

Type III: Alluvium with H <25 m including soft layer (*) with thickness less than 5 m.

Type IV: Other than the above, usually Soft Alluvium or Reclaimed Land.

* Soft Layer Vulnerable to Liquefaction

TABLE 6.1. Predicted Absolute Acceleration Response For Earthquakes of Magnitude 6.1< M <7.4 at a Natural Period of 0.15 seconds and with 5 Percent Damping.

These estimates of acceleration may not be unduly conservative, because they apply to the regional seismic hazard derived from all faults, the magnitude potential of which is poorly known.

If the Hope Fault can be regarded as representative of the major active faults in this region then some insight into likely parameters may be gained.

On the Hope River Segment of the Hope Fault, however, there is the historical 1888 earthquake which in this study has been assigned a magnitude of M = 6.5 to 6.8; a reduction from most traditional estimates of 7.0 to 7.3.

The Hope Fault is the largest recognised through-going active structure in North Canterbury, and the evidence obtained in this study for repeated earthquakes of characteristic magnitude and recurrence interval during the past 800 years, indicates that the 1888 earthquake and its associated effects may be representative of larger magnitude future events occurring within Amuri District.

The extreme variations in felt intensity over very short distances in the Amuri District, was an important characteristic of the distribution of seismic effects during the 1888 earthquake and emphasizes the importance and complexity of local ground conditions in determining site response to an earthquake of given magnitude. The large intensity variations observed in the Hanmer and Culverden Basins during the earthquake may be due to variability in soil conditions, rupture interaction with fault splay terminations (near Woodbank for example), and to patterns of constructive and destructive interference related to the normal modes of vibration of the basins.

### 6.4.5 Predicted Seismic Effects During Future Earthquakes on the Hope Fault.

Using the revision of the 1888 earthquake effects for calibration and the evidence from the Hope Fault at Manuka Creek for five prehistoric ruptures of similar magnitude, some destructive aspects of a future earthquake on the same segment of the Hope Fault may be anticipated with confidence.

Any further anticipation of the distribution of local felt intensities in future events, however, is unrealistic due to considerable uncertainty in predicting site specific response and the extent of damage beyond the immediate vicinity of the fault.

i) Future earthquakes on this fault segment are likely to range in magnitude from $6.4 < M < 7.0$ and may generate felt intensities of MM8-MM9 in the Hope River area, with average intensities of MM6 experienced at epicentral distances of 50-150 km.

ii) Coseismic rupture will terminate at the Hanmer Basin which will become the focus of intense after-shock activity; some after-shocks may generate felt intensities of MM6-MM7.

iii) Right-lateral strike-slip ground rupture of up to three metres will occur on the Hope Fault west of Glynn Wye, decreasing to between one and two metres between Glynn Wye and Hanmer Basin. Average vertical displacements are not likely to exceed 0.1-0.2 metres, except locally in the vicinity of compressional or extensional fault segment boundaries at Glynn Wye, where

relative uplift or subsidence of up to one metre respectively will occur.

iv) Damage to State Highway 7 will occur between the Hanmer Springs junction and Boyle River, and is likely to be severe between Handysides Stream and Hope River Bridge (Figure 6.5)*. Much of this section of the State Highway 7 is constructed on or very close to the fault. Slope failures should be anticipated wherever steep and unsupported cuts have been made in Quaternary gravels and lake sediments.

v) Large landslides have been identified in this study to the north and south of State Highway 7, between Manuka Creek and Horseshoe Lake. Numerous landslides occurred here during the 1888 earthquake and this locality has experienced large mass movements in prehistoric events (one of which dams Horseshoe Lake). Prehistoric landslides have also occurred in gravels forming steep slopes to the north of the Glynn Wye outwash surface, south-west of Hope River Bridge (Map 2).

vi) Bridges likely to be seriously damaged or destroyed include those at Shale Peak Stream and Boundary Stream which have been constructed on the Hope Fault. Several other small bridges along this section of State Highway 7 are within 200 m of the fault and may suffer varying degrees of damage.

* **Figure 6.5 in map pocket**

## 6.5 Summary

A detailed review of the 1888 Amuri earthquake, field mapping, and site investigations conducted during this study have provided new data for the evaluation of seismic hazard in Amuri District, North Canterbury.

Firstly, the estimated magnitude of the 1888 earthquake is here revised downward, from M = 7.3 to a range of M = 6.5 to 6.8, on the basis of reinterpreted strong motion attenuation and empirical relationships between magnitude and the fault parameters of rupture length, ruptured area, and inferred seismic moment.

Secondly, results from the trenching studies on the Hope Fault at Manuka Creek indicate that the Hope River Segment of the Hope Fault has ruptured repeatedly during the past 800 years, in earthquakes of characteristic recurrence and magnitude. The 1888 earthquake and its associated effects is here interpreted as a characteristic event for this segment of the fault, and may be inferred to represent an average upper magnitude for earthquakes centred in Amuri District because the Hope Fault is the largest fault in the region. On this basis a characteristic earthquake model may provide a more realistic expression of earthquake recurrence than the exponential magnitude distribution, but the presence locally of other potentially active faults such as the Kakapo Fault, and the effect of earthquakes occurring on large faults beyond the study area (e.g. Clarence and Awatere Faults) justifies the continued use of regional seismicity parameters to calculate the overall hazard, at least until similar detailed studies on those faults have been completed.

A microzonation of predicted site response to strong ground motion in Amuri District is beyond the scope of this study and requires data concerning local ground conditions which as yet are unavailable. As a

first step in the process of evaluating site specific response, the 1888 earthquake and its inferred magnitude of M = 6.5 to 6.8 is adopted as representative of likely future large events within the area and combined with a strong motion attenuation expression, to predict the acceleration response at sites on different ground types for a range of epicentral distances.

The results indicate that on bedrock sites at short (<20 km) epicentral distances accelerations of between 0.23 g and 0.34 g may be anticipated. These values are slightly lower than previous estimates of risk in this area which have been based on larger predicted earthquake magnitudes and intensities.

There is a proviso - the parameters suggested by this study are probably reasonable as applied to dominantly strike-slip faulting. It is becoming evident that thrust faulting also occurs in the Marlborough area - possibly inherited but now acting to transfer slip between strike-slip segments. Whether a thrust like the Jordan River Thrust (Van Dissen 1987) is highly active may yet need to be established (J. Campbell pers.comm.). Inherently, thrusts are likely to release a greater accumulated strain energy than strike-slip faults and the potential hazard is therefore correspondingly greater.

Predicted seismic effects in the Amuri District during future earthquakes on the Hope River Segment of the Hope Fault are here inferred from the distribution of intensities in the 1888 earthquake, but generalisations of hazard beyond the immediate vicinity of the fault are unrealistic due to local variations in site response. The extreme variations in felt intensity over very short distances in the Amuri District was an important characteristic of the distribution of seismic effects during the 1888 earthquake. This emphasizes the importance and

complexity of local ground conditions in determining the site response to an earthquake of given magnitude.

# CHAPTER 7 CONCLUSIONS AND RECOMMENDATIONS

1. Field mapping during this study provided evidence for a new interpretation of the latest Otiran (15 000 to 14 000 yr BP) maximum down-valley ice-limit in the Hope Valley. Previous studies had inferred that the down-valley ice-limits for this advance were: (i) upstream from the Hope-Boyle river junction (Suggate 1965), (ii) at Lewis Pass with an outwash surface in the Hope Valley 30-45 m above the Hope River (Clayton 1968), and (iii) downstream from the Hope-Boyle river junction at the Glynn Wye moraines (Knuepfer 1984). In this study the terminal ice-limit for the latest Otiran advance is recognised at Dismal Flats, south of the Hope-Boyle river junction, 3.5 km upstream from Knuepfer's inferred position. The ice-limit is represented by a subdued moraine ridge preserved on the northern edge of Dismal Flats, 145 m above the Hope River. The associated outwash surface merges with the Glynn Wye advance surface a few kilometres downstream from the Glynn Wye moraine. The Dismal Flats moraine and outwash surface have previously been described as recessional from Glynn Wye moraine.

   Terrace deposits at lower levels typically comprise a thin horizontal gravel cap unconformable on lake sediments which accumulated in the lake formed behind the Dismal Flats moraine during glacier retreat. Radiocarbon ages of between 11 000 and 13 500 yr BP from bottomset beds of this lake have been reported in previous studies and indicate a final ice retreat from the Hope Valley prior to 13 000 yr BP.

   The terraces at various levels between the Dismal Flats surface and the active Hope River floodplain were formed by river

degradation during post-glacial time.

2. Radiocarbon dates constraining the ages of former Hope River flood-plain levels in the Lower Hope Valley provide an estimate of the rate of post-glacial down-cutting by the Hope River.

The dates, and a comparison with similar studies of other rivers in the region indicate a probable exponential decrease in the average rate of post-glacial down-cutting by the Hope River since the Late Pleistocene. The Hope River has now re-adjusted from a Late Pleistocene base-level controlled by aggradation to a base-level controlled by relative uplift along the Hope Fault and subsidence within Hanmer Basin. During the past 3500 years the Hope River at Manuka Creek has down-cut at an average rate of 4.8 m/kyr. Uplift on the Hope Fault at Manuka Creek, however, has been only 0.7 m/kyr indicating that subsidence within Hanmer Basin may represent the most important tectonic control on local river base-level.

3. The Amuri earthquake of Sept. 1 1888 was felt strongly over a wide area of North Canterbury and Westland and was recorded as far away as Southland, Taranaki and Wairarapa. The main shock of magnitude Ms=6.5 to 6.8 occurred soon after 4:00 a.m. Sept. 1 1888, on the Hope Fault west of Glynn Wye Station and propagated eastward achieving maximum ground shaking intensities of MM9, with observed fault displacements of up to 2.6 metres at Glynn Wye.

4. The earthquake was a destructive but not disastrous earthquake, and previous estimates of magnitude and felt intensity have been somewhat high. At epicentral distances greater than 40-50 km, average felt intensities were alarming but did not exceed MM6. Damage to the cathedral spire in Christchurch was widely publicised, but was probably due to poor construction. Parts of eastern Christchurch experienced amplified intensities of up to MM7 and a few low rise residential buildings suffered minor cracking and chimney damage. Elsewhere in Christchurch even crockery and glass was largely unscathed and intensities may have been lower than MM6.

5. The estimated magnitude of the 1888 earthquake is revised downward, from M = 7.3 to a range of M = 6.5 to 6.8, on the basis of reinterpreted strong motion attenuation and empirical relationships between magnitude and the fault parameters of rupture length, ruptured area, and inferred seismic moment.

6. Damage reports and the spatial distribution of felt effects emphasise extreme variations in seismic effects over short distances. Although ground motions were locally severe, the most damaging earthquake effects were restricted to the immediate vicinity of the Hope Fault and, isolated serious damage at greater distances can be attributed primarily to weak construction and pronounced local site effects. Felt intensities of up to MM9 at Glynn Wye and MM8 in the Hanmer Basin were possibly enhanced by topographic focusing, secondary fault segment boundary rupture, and by moderate-large (>200m) thicknesses of alluvial and lacustrine

valley fill.

7. The exact location of the main shock epicenter is unclear, but was to the west of Glynn Wye Station, possibly near the junction of the Hope-Boyle River which is identified in this study as a probable fault segment boundary.

8. A minimum surface rupture of approximately 40 km occurred between the western margin of the Hanmer Basin, and the junction of Kiwi Stream and Hope River. The main shock rupture arrested at Hanmer Basin which was the focus of intense aftershock activity. Several aftershocks generated local Modified Mercalli felt intensities of up to MM6 or MM7 and these may have effected a transfer of slip eastward as far as Hossack Saddle at the eastern margin of Hanmer Basin. High felt intensities (MM7-MM8) at Otira Gorge and unauthenticated reports of ground renting in Kelly's Creek indicate a possible westward extent of surface rupture at Otira Gorge and a total rupture length of 100 km. The evidence for such a large rupture length is equivocal and is not consistent with the regional attenuation of strong ground motion.

9. The earthquake occurred prior to the development of modern (post 1930's) building materials and design codes, which would probably have prevented much of the damage. These factors must be given careful consideration when evaluating the records of early historic events, to avoid an excessively conservative assessment of

contemporary seismic hazard associated with faulting in North Canterbury.

10. Late Quaternary displacements on the Hope and Kakapo faults were measured directly in the field and from enlarged high-resolution vertical aerial photographs. A comparison of these results with those obtained in previous studies indicated some large discrepancies in both measured displacements and age estimates of faulted surfaces.

The most pronounced example is at the Glynn Wye Advance terminal moraine, where the moraine terminus and two meltwater terrace risers west of the moraine are displaced by different amounts. Previous workers have explained these displacements either by assuming a closely similar age for the offset features and adopting measurement methods which derived more equal displacements, or by accepting the variable offsets and assuming significantly different ages.

I argue that the meltwater channels are of near-equal age and that the displacements on these features are different because of their location relative to a compound bend in the fault trace. In successive earthquakes a component of slip oblique to the regional slip vector has formed the 700 to 900 m wide Poplars Graben. The meltwater terrace risers record only a proportion of the total Late Quaternary lateral slip because they have also slipped oblique to the fault.

Only the moraine terminus offset which is almost free of structural complication may be used to calculate a Late Quaternary slip-rate at this locality.

11. The resultant estimate of true average Late Quaternary slip-rate (as expressed at the surface) on the Hope Fault is between 15.5 mm/yr and 18.25 mm/yr. The estimate of Late Quaternary slip on the Kakapo Fault is between 5.0 mm/yr and 7.5 mm/yr.

12. Segmentation of the Hope Fault is evident at a number of scales. The Hanmer Basin forms a complex primary junction between western and eastern fault segments. The Hope Fault from Hanmer Basin to the Hope-Boyle River junction is referred to in this study as the Hope River Segment.

There is some evidence for a segment boundary (possibly primary and associated with the epicentral region of the 1888 earthquake) south of the Hope-Boyle River junction, and another 50 km further to the west where the "Kelly Fault" diverges from the Hope Fault at the junction of the Otehake and Taramakau rivers.

On a smaller scale length of between three and ten kilometers, the Hope River Segment of the Hope Fault is itself segmented, where secondary segment boundaries are coincident with zones of oblique-extensional faulting at Poplars Graben, and Lake Glynn Wye Graben.

13. Rupture interaction with secondary fault segment boundaries at Glynn Wye affected the distribution of lateral slip during the 1888 earthquake. A significant reduction in lateral slip (42%) occurred across Lake Glynn Wye Graben which is located between the Glynn Wye moraine and Manuka Creek localities.

Detailed field mapping and surveying of 1888 fault scarp profiles at the Glynn Wye moraine locality identified an increase

in the amount of vertical displacement (and by implication a reduction in lateral displacement) in the vicinity of a 15-20° constraining bend in the fault, at the NE corner of Poplars Graben.

14. The implication of this internal or secondary segmentation of the Hope Fault and the observed change in lateral slip at a segment boundary during the 1888 earthquake, is that slip-rate estimates derived from measurement of displacement at a single locality are likely to be unique to that locality. Only estimates from locations unaffected by jogs or bends at segment boundaries can be extrapolated beyond the individual locality.

15 The different displacements at the Glynn Wye moraine locality show that spatial variations in lateral slip distribution occur over long ($10^5$ yr) time intervals. These cumulative spatial variations in lateral slip emphasise the persistence of the causative fault bends and jogs over similar periods of time. The spatial variations in lateral slip across these structures expressed at the surface are inferred to be distributed within basement rocks at depth, throughout anastomosing domains of cataclastic shear which extend several hundred metres beyond either side of the fault.

16. Near Manuka Creek a slip-rate of 10.6 ±0.3 mm/yr is obtained from a Late Holocene degradational terrace riser offset by the Hope Fault. A comparison of this rate with the Late Pleistocene incremental slip-rate at the Glynn Wye moraine indicates an <u>apparent</u> decrease in lateral slip-rate on the Hope Fault between the Late Pleistocene and Late Holocene. However, I do not believe that it is possible

to infer temporal variations in slip-rate from displacements measured at localities on either side of the secondary segment boundaries and I conclude that apparent temporal variations in lateral slip are more likely to be spatial variations in disguise.

In this case the decrease in lateral slip across Lake Glynn Wye Graben during the 1888 earthquake is equivalent to the ratio between the Late Quaternary slip-rate estimated at Glynn Wye moraine and the Late Holocene slip-rate near Manuka Creek.

17. Corroborative evidence of a relatively constant rate of slip during the Late Holocene is indicated by evidence for the last five earthquakes (including the 1888 event) in Raupo Swamp near Manuka Creek, on the Hope River Segment of the Hope Fault. Four silt horizons coincide with expected datum stratigraphic features compatible with evidence of the paleo-earthquakes, based on an average Late Holocene recurrence interval of 141 ±3 years calculated from the dated terrace offset at Manuka Creek, divided by the inferred 1.5 m displacement at this locality during the 1888 earthquake. The predicted location of the silt horizons within the peat is based on an average peat accumulation rate of 2.2 ±0.2 mm/yr which was calculated utilizing a $^{14}C$ date near the base of the peat. Further $^{14}C$ dating is required to refine this estimate, but coincidence between the predicted horizons and the silt layers is good. Pollen analysis of the peat column also provided evidence of an ecological reponse to ground disturbance coincident with two of the silt layers.

18. The internal consistency between the historic, inferred pre-historic and geologic rates of lateral slip indicates that the Hope River segment of the Hope Fault ruptures with characteristic magnitude, and with similar point-specific displacement in successive earthquakes.

19. Results from the trenching studies at Manuka Creek indicate that the Hope River Segment of the Hope Fault has ruptured repeatedly during the past 800 years, during earthquakes of characteristic recurrence and magnitude. Evidence at Raupo Swamp for the last five earthquakes (including the 1888 event) indicates a tentative average recurrence interval between earthquakes of 134 ±27 years.

20. The 1888 earthquake and its associated effects is interpreted as a characteristic event for this segment of the fault. It may also be inferred to represent an average upper-bound magnitude for earthquakes on strike-slip faults centred in Amuri District, because the Hope Fault is the largest strike-slip fault in the region.

21. On this basis a characteristic earthquake model will provide a more realistic expression of earthquake recurrence than an exponential magnitude distribution derived from historical (instrumental) seismicity, but until similar detailed studies of other active faults in the region have been completed, the continued use of regional seismicity parameters to calculate the overall hazard is justified.

22. As a first step in the process of evaluating site specific response in earthquakes in Amuri District, the 1888 earthquake (and its revised magnitude of M = 6.5 to 6.8) is adopted as representative of future large events on the Hope Fault and other strike-slip faults the region. The revised magnitude estimate, combined with the strong motion attenuation expression of Katayama et.al. (1978) may be used to predict the acceleration response at sites on different ground types for a range of epicentral distances. The results indicate that on bedrock sites at short (<20 km) epicentral distances, accelerations of between 0.23 g and 0.34 g may be anticipated. The predicted response 100 km away at Christchurch is between 0.1 g and 0.13 g. These values are slightly lower than equivalent previous estimates of seismic risk in northern Canterbury which have been based on larger predicted earthquake magnitudes and intensities, and regional instrumental seismicity.

23. Predicted seismic effects in the Amuri District during future earthquakes on the Hope River Segment of the Hope Fault may be inferred from the distribution of intensities in the 1888 earthquake. The highest intensities are anticipated in the Glynn Wye area, but beyond the immediate vicinity of the fault (>200 m) intensities and associated property damage may depend greatly on local site effects. Extreme variations in felt intensity over very short distances was an important characteristic of the distribution of seismic effects during the 1888 earthquake, emphasizing the importance and complexity of local ground conditions in determining site response to an earthquake of given magnitude.

## Recommendations for Future Work

1. A paleoseismic site investigation at Horseshoe Lake, involving the coring of lake bottom sediments to obtain a continuous record of sedimentation since the formation of the lake c.3500 yr BP. Textural differences within the cores may be compared with potential ecological responses to earthquakes on the Hope Fault, recorded by floral and benthic faunal indices.

2. Trenching across the Kakapo Fault at Dismal Valley is recommended as the next step in establishing the recent displacement history. A number of potential trenching sites on the fault are located between the Glynn Wye outwash surface and the youngest surfaces above the active floodplain of Kakapo Brook.

3. A detailed basement rock structural analysis along the lower reaches of Kakapo Brook, Manuka Creek and Gorge Stream may indicate to what extent the active Late Quaternary shear zones along and between the Hope and Kakapo Faults are inherited structures. As a small-scale analog this study might provide clues about the Upper Cenozoic structural evolution of the Marlborough Transform System. development Fault segmentation study

4. An intermediate-field (approximately 1-5 km) geodetic network should be established to monitor detectable short-term ground deformation across the Hope and Kakapo Faults at Glynn Wye. The network should extend well beyond the currently recognisable limits of coseismic fault displacement so as to gain a realistic

impression of the total strain across the fault zone.

5. A seismograph network (incorporating a strong motion recording capability) is recommended for the Hope Valley-Hanmer Plains area, in view of the high probability of a magnitude M = 6.5 to 6.8 event occurring on the Hope River Segment of the Hope Fault within the next 60 years.

## REFERENCES

Aki, K., (1984). Asperities, barriers and characteristic earthquakes. Journal of Geophysical Research v. 89, p. 5867-5872.

Anderson, H.J., (1987). A Gravity Survey of the Hanmer Depression, North Canterbury. DSIR Research Report No.214, p.4-20.

Aydin, A., and Nur, A., (1982). Evolution of Pull-Apart Basins and Their Scale Independence. Tectonics v. 1, p. 95-105

Barka, A.A., and Kadinsky-Cade, K., (1988). Strike-slip fault geometry in Turkey and its influence on earthquake activity. Tectonics, v.7, No.3, p.663-684.

Bath, M., (1979). Introduction to Seismology. Birkhauser Verlag, Basel. 428 p.

Berryman, K.R., (1984). Late Quaternary Tectonics of New Zealand In: An Introduction to the Recent Crustal Movements of New Zealand. The Royal Society of New Zealand Miscellaneous Series 7, p. 91-107.

Bibby, H.M., (1981). Geodetically determined strain across the southern end of the Tonga-Kermadec-Hikurangi subduction zone. Geophysical Journal of the Royal Astronomical Society, v.66, p. 513-533.

Bradshaw, J.D., and Andrews, P.B., In Weaver, S.W., and Lewis, D.W., (eds.) (1980). Field Excursions Guide Book, Christchurch Conference, November 24th-27th, 1980. Geological Society of New Zealand Inc., C1-C12.

Bradshaw, J.D.; Adams, C.J., and Andrews, P.B., (1981). Carboniferous to Cretaceous on the Pacific margin of Gondwana: the Rangitata phase of New Zealand, In Cresswell, M.M., and Vella, P. (eds.) Gondwana Five: Proceedings of the Fifth International Gondwana Symposium. A.A. Balkema, Rotterdam, p. 217-221.

Brown, L.J.; Wilson, D.D.; Moar, N.T., and Mildenhall, D.C. (1988). Stratigraphy of the late Quaternary deposits of the northern Canterbury Plains, New Zealand. New Zealand Journal of Geology and Geophysics, v. 31, p.305-335.

Bull, W.B., (1984). Tectonic Geomorphology. J. Geol. Education, v. 32, p. 310-324.

Bull, W.B., and Knuepfer, P.L.K., (1987). Adjustments by the Charwell River, New Zealand, to uplift and climatic changes. Geomorphology, v. 1, p.15-32.

Burrows, C.J., In Burrows, C.J. (ed.), (1974). Handbook to the Arthur's Pass National Park. Arthur's Pass National Park Board. 104 p.

---------- (1988). Late Otiran and early Aranuian radiocarbon dates from South Island localities. New Zealand Natural Sciences, v. 15, p. 25-36.

Canterbury Times, (1888). September 7 - October 25. Held at Canterbury Public Library, Christchurch.

Chinn, T.J.H., (1981). Use of rock weathering-rind thickness for Holocene absolute age-dating in New Zealand. Arctic and Alpine Research, v. 13, p. 33-45.

Clayton, L., (1965). Late Pleistocene geology of the Waiau Valleys, North Canterbury, New Zealand. Unpublished PhD Thesis, Illinois University.

Clayton, L., (1966). Tectonic Depressions along the Hope Fault, a Transcurrent Fault in North Canterbury, New Zealand. N.Z. Journal of Geology and Geophysics v.9 (1-12), p.95-104.

---------- (1968). Late Pleistocene Glaciations of the Waiau Valleys, North Canterbury. N.Z. Journal of Geology and Geophysics, v.11, No.3, p.753-767.

Cornell, C.A., (1968). Engineering seismic risk analysis. Bulletin of the Seismological Society of America, v. 58, No.5, p. 1583-1606.

Cotton, C.A., (1947). The Hanmer Plain and the Hope Fault. N.Z. Journal of Science & Technology, B29, p.10-17.

Dibble, R.R.; Ansell, J.H., and Berrill, J.B., (1980). Report on a study of seismic risk for B.P. New Zealand Ltd sites at Woolston and Lyttleton. Report to B.P. New Zealand Ltd, (J. Berrill pers.comm.).

Eiby, G.A., (1966). The Modified Mercalli scale of intensity and its use in New Zealand. New Zealand Journal of Geology and Geophysics, v. 9, p. 122-129.

Eiby, G.A., (1968). An annotated list of New Zealand earthquakes, 1460-1965. New Zealand Journal of Geology and Geophysics, v.11, No.3, p.630-647.

Ellis, P.J.; Thomas, I.L., and McDonnell, M.J., (1978). Landsat II over New Zealand: Monitoring our resources from space. Physics and Engineering Laboratory, DSIR Bulletin 221.

Esteva, L., (1976). Seismicity, In Lomnitz, C., and Rosenblueth, E. (eds.): Seismic Risk and Engineering Decisions. Elsevier, Amsterdam. p.179-222.

Fellows, D.L., (1986). Prefeasibility study of the seismotectonic hazards for the proposed Waiau (Canterbury) hydro development. New Zealand Geological Survey Report EDS 108. 61 p.

Freund, R., (1971). The Hope Fault: A Strike-Slip Fault in New Zealand. N.Z. Geological Survey, Bulletin 86. 49pp

Grapes, R., and Wellman, H., (1988). The Waiarapa Fault. Geology Board of Studies Publication No.4, Research School of Earth Sciences, Victoria University of Wellington. 55p.

Gregg, D.R., (1964). Geological Map of New Zealand 1:250,000. Sheet 18, "Hurunui". D.S.I.R., Wellington.

Gutenburg, B. and Richter, C.F., (1954). Seismicity of the Earth. (2nd ed.), Princeton University Press.

Hanks, T.C., and Kanamori, H., (1979). A moment magnitude scale. Journal of Geophysical Research, v. 84, No.20, p.2981-2987.

Hardy, E.F., and Wellman, H.W., (1984). The Alpine, Wairau, and Hope Faults. V.U.W. Geology Dept. Publication No.27. 15 pp

Harland, W.B., (1971). Tectonic transpression in Caledonian Spitzbergen. Geological Magazine 108, p. 27-42.

Hatherton, T., (1980). Shallow Seismicity in New Zealand 1956-75. Journal of the Royal Society of New Zealand, v.10, No.1, p. 19-25. Hayes, R.C., (1953). Some aspects of earthquake activity in the New Zealand region. Proceedings of the 7th Pacific Science Congress 2, p. 629-636.

Hogben, G., (1890). The Determination of the Origin of the Earthquake of the 5th December, 1881, felt at Christchurch and other Places. Transactions and Proceedings of the New Zealand Institute, v. XXIII, p.465-470.

-------- (1891). The Earthquakes of New Zealand. Australasian Association for the Advancement of Science, v. III, p.37-57.

Hutton, F.W., (1888). The Earthquake in the Amuri. Transactions of the New Zealand Institute, 21, p. 269-293.

Jones, E., (1933). Autobiography of an early settler in New Zealand. Coulls Somerville Wilkie Ltd, Wellington. 179 p.

Kanamori, H., (1977). The energy release in great earthquakes. Journal of Geophysical Research, v.82, p. 2981-2987.

Kasahara, K., (1981. Earthquake Mechanics. Cambridge University Press, Cambridge. 248 p.

Katayama, T.; Iwasaki, T.; Saeki, M. (1978) Statistical analysis of earthquake acceleration response spectra. Transactions of the Japanese Society of Civil Engineering, v. 10, p. 311-313.

Keller, E.A., (1986). Investigation of active tectonics: Use of surficial earth processes, In Active Tectonics: Studies in Geophysics. Nat. Acad. Press. 136-147.

King, G., and Yielding, G., (1984). The evolution of a thrust fault system: processes of rupture initiation, propagation and termination in the 1980 El Asnam (Algeria) earthquake. Geophysical Journal of the Royal Astronomical Society, v.77, p.915-933.

Knuepfer, P.L.K., (1984). Tectonic Geomorphology and Present Day Tectonics of the Alpine Shear System, South Island, New Zealand. Unpublished PhD Thesis, The University of Arizona. 489 p.

Krinitzsky, E.L., and Marcuson, W.F., (1983). Principles for selecting earthquake motions in engineering design. Bulletin of the Association of Engineering Geologists, v. 20, No.3, p.253-265.

Lensen, G.J., (1963). Geological Map of New Zealand, 1:250,000. Sheet 16, "Kaikoura". D.S.I.R., Wellington.

Lensen, G.J., (1964). The general case of progressive fault displacement of flights of degradational terraces. New Zealand Journal of Geology and Geophysics, v. 7, p. 864-870.

Lensen, G.J., (1968). Analysis of progressive fault displacement during down-cutting at the Branch River Terraces, South Island, N.Z.. Bulletin of the Geological Society of America v.79, p. 545-556.

Lyttleton Times, (1888). September 3 - September 11. Held at Canterbury Public Library.

Mabin, M.C.G., (1983). Late Otiran sedimentation and glacial chronology in the Warwick Valley, southeast Nelson. New Zealand Journal of Geology and Geophysics, v.26, p. 189-195.

MacKinnon, T.C., (1983). Origin of the Torlesse terrane and coeval rocks, South Island, New Zealand. Geological Society of America Bulletin, v. 94, p. 967-985.

Madariaga, R., (1983). High frequency radiation from dynamic fault models. Annales Geophysicae v.1, p. 17-23.

◄—— Mann, P.; Hempton, M.R.; Bradley, D.C., and Burke, K., (1983). Development of Pull-Apart Basins. Journal of Geology, v. 91, p. 529-554.

McKay, A., (1888). Remarks on the earthquakes in the Amuri. Transactions of the New Zealand Institute, v. 21, p.508-509.

-------- (1890). On the Earthquakes of September 1888, in the Amuri and Marlborough districts of the South Island. New Zealand Geological Survey Report of Geological Explorations, v.20, p.1-16

-------- (1902). Report on the Recent Seismic Disturbances within Cheviot County in Northern Canterbury and the Amuri District of Nelson, New Zealand. Government Printer, Wellington. 80 p.

Matuschka, T., (1980). Assessment of seismic hazards in New Zealand. Dept. of Civil Engineering Research Report No. 222, University of Auckland, New Zealand.

Medvedev, (1962). Engineering Seismology. Moscow, Akademia Nauk Press.

Mulholland, M., (1982). Estimation of design earthquake motions for New Zealand. Unpublished M.E. Thesis, University of Canterbury, New Zealand. 97 p.

Naylor, M.A.; Mandl, G., and Siypestieyn, C.H.K., (1986). Fault geometries in basement-induced wrench faulting under different initial stress states. Journal of Structural Geology, v.8, p. 737-752.

Newmark, N.M., Blume, J.A., and Kapur, K.K., (1973). Seismic design spectra for nuclear power plants. Journal Power Division Proceedings. ASCE, 99 (PO2), p. 287-303.

New Zealand Seismological Observatory, (1988). New Zealand earthquakes 1460-1986. Seismological Observatory, Geophysics Division, DSIR, Wellington.

Oborn, L.E., and Suggate, R.P., (1959). Sheet 21 - Christchurch. Geological Map of New Zealand 1:250 000. DSIR, Wellington.

Peek, R., (1980). Estimation of seismic risk for New Zealand. Dept. of Civil Engineering Research Report 80-21, University of Canterbury, New Zealand.

Peek, R.; Berrill, J.B.; Davis, R.O., (1980). A seismicity model for New Zealand. Bulletin of the National Society for Earthquake Engineering, v. 13, No.4, p. 355-364.

Pierce, K.L., (1986). Dating Methods, In Active Tectonics: Studies in Geophysics. National Academy Press, Washington D.C. p. 195-214.

Richter, C.F., (1958). Elementary Seismology. W.H. Freeman & Co., San Fransisco. 768 p.

Rodgers, D.A., In Sylvester (ed.), (1984). Wrench Fault Tectonics. American Association of Petroleum Geologists Reprint Series No. 28, p.345-359.

Rynn, J.M.W., and Scholz, C.H., (1978). Seismotectonics of the Arthur's Pass region, South Island, New Zealand. Geological Society of America Bulletin, v. 89, p. 1373-1388.

Schwartz, D.P., and Coppersmith, K.J., (1984). Fault behaviour and characteristic earthquakes: Examples from Wasatch and San Andreas Faults. Journal of Geophysical Research, v. 89, p. 5681-5698.

Schwartz, D.P.; Coppersmith, K.J., and Swan, F.H., (1984). Methods for estimating maximum earthquake magnitudes. Proceedings of the 8th World Conference on Earthquake Engineering, San Fransisco, v. 1, p. 279-285.

Schwartz, D.P., and Coppersmith, K.J., (1986). Seismic hazards: New trends in analysis using geologic data, In Active Tectonics: Studies in Geophysics. National Academy Press, Washington D.C. p. 215-230.

Segall, P., and Pollard, D.D., (1980). Mechanics of discontinuous faults. Journal of Geophysical Research v. 85, p. 4337-4350.

Sibson, R.H., (1985). Stopping of earthquake ruptures at dilational fault jogs. Nature, v. 316, p. 248-251.

Sibson, R.H., (1986). Rupture Interaction with Fault Jogs In Das, S.; Boatwright, J., and Scholz, C.H. (eds): Earthquake Source Mechanics. Geophysical Monograph 37, Maurice Ewing Volume 6, p. 157-167.

Sieh, K.E., (1984). Lateral offsets and revised dates of large prehistoric earthquakes at Pallett Creek, Southern California. Journal of Geophysical Research, v. 89, No.B9, p. 7641-7670.

Sieh, K.E., and Jahns, R.H., (1984). Holocene activity of the San Andreas Fault at Wallace Creek, California. Geological Society of America Bulletin v. 45, p. 883-896.

Silberling, N.J.; Nichols, K.M.; Bradshaw, J.D., and Blome, C.D., (1988). Limestone and chert in tectonic blocks from the Esk Head subterrane, South Island, New Zealand. Geological Society of America Bulletin, v. 100, p. 1213-1223.

Slemmons, D.B., (1982). Determination of design earthquake magnitudes for microzonation. Proceedings of the Third International Earthquake Microzonation Conference, v.1, p. 119-130.

Smith, W.D., (1978). Spatial distribution of felt intensities for New Zealand earthquakes. N.Z. Journal of Geology and Geophysics, v. 21, No.3, p. 293-311.

Smith, W.D., and Berryman, K.R., (1983). Revised estimates of earthquake hazard in New Zealand. Bulletin of the N.Z. National Society for Earthquake Engineering, v. 16, No.4, p. 259-272.

Smith, W.D., and Berryman, K.R., (1986). Earthquake hazard in New Zealand: inferences from seismology and geology. Royal Society of New Zealand Bulletin 24, p. 223-242.

Speight, R., (1933). The Arthur's Pass earthquake of 9th March, 1929. New Zealand Journal of Science and Technology, v. XV, No.3, p. 173-182.

Sporli, K.B., (1978). Mesozoic tectonics, North Island, New Zealand. Geological Society of America Bulletin, v. 89, p. 415-425.

Stevens, G.R., (1974). Rugged Landscape: The Geology of Central New Zealand. Reed, Wellington, 286p.

Suggate, R.P., (1965). Late Pleistocene Geology of the Northern Part of the South Island, New Zealand. N.Z. Geological Survey Bulletin, 77. 92 p.

Suggate, R.P.; Stevens, G.R., and Te Punga, M.T., (eds) (1978). The Geology of New Zealand. Government Printer, Wellington, 2 vols., 820 pp.

---------- (1988). Quaternary deposition and deformation in the Buller and tributary valleys. New Zealand Geological Survey Record, 25, 51 p.

Sylvester, A.G., (1986). Nearfield Tectonic Geodesy, In Active Tectonics: Studies in Geophysics. National Academy Press, Washington D.C. p. 164-180.

The Press, (1888). September 3 - September 18. Held at Canterbury Public Library.

Van Dissen, R., (1987). Neotectonics of the Kaikoura area, southeastern Marlborough. Unpublished Report to Earth Deformation Section, New Zealand Geological Survey.

Vita-Finzi, C., (1986). Recent Earth Movements: An Introduction to Neotectonics. Academic Press Inc., London. 226 p.

Walcott, R.I., (1978). Present Tectonics and Late Cenozoic evolution of New Zealand. Geophysical Journal of the Royal Astronomical Society, v. 52, p. 137-164.

Walcott, R.I., (1979). Plate motion and shear strain rates in the vicinity of the Southern Alps, In Walcott, R.I., and Cresswell, M.M., (eds.): The Origin of the Southern Alps. Royal Society of New Zealand, Bulletin 18, p.5-12.

Walcott, R.I.; Christoffel, D.A., and Mumme, T.C., (1981). Bending within the axial tectonic belt of New Zealand in the last 9 myr from paleomagnetic data. Earth and Planetary Science Letters, v. 52, p. 427-434.

Walcott, R.I., (1984). The major structural elements of New Zealand, In Walcott, R.I. (ed): An Introduction to the Recent Crustal Movements of New Zealand. Royal Soc. N.Z. Misc. Series Publication 7, p. 1-6

Warren, G., (1967). Geological Map of New Zealand, 1:250,000. Sheet 17, "Hokitika". D.S.I.R., Wellington.

Wellman, H.W., In Benson, W.N. (1952). Meeting of the Geological Division of the Pacific Science Congress in New Zealand, February 1949. Interim Proceedings of the Geological Society of America, 1950.

Wellman, H.W., (1953). Data for the Study of Recent and Late Pleistocene Faulting in the South Island of New Zealand. N.Z. Journal of Science & Technology, B34, p. 270-288.

---------- (1985). Rate of Dextral Faulting in the Central Part of New Zealand from Weathering Rind Ages. Unpublished Draft Report, Dept. of Geology, Research School of Earth Sciences, V.U.W., Wellington.

Wesnousky, S.G.; Scholz, C.H.; Shimazaki, K., and Matsuda, T., (1983). Earthquake frequency distribution and the mechanics of faulting. Journal of Geophysical Research v. 88, No. B11: p. 9331-9340.

Whitehouse, I.E.; McSaveney, M.J.; Knuepfer, P.L.K., and Chinn, T.J.H., (1986). Growth of weathering rinds on Torlesse sandstone. In Colman and Delthier (eds.): Rates of chemical weathering of rocks and minerals. Academic Press.

Wood, P.R., (1984). Guidebook to the South Island Scientific Excursions. International Symposium on Recent Crustal Movements of the Pacific Region, Wellington, N.Z., Feb. 1984. The Royal Society of New Zealand Miscellaneous Series 9, p. 39-53.

Woodcock, N.H., and Fisher, M., (1986). Strike-slip duplexes. Journal of Structural Geology, v. 8, No. 7, p. 725-735.

Wyss, M., (1979). Estimating maximum expectable magnitude of earthquakes from fault dimensions. Geology, v. 7, No.7, p. 336-340.

Youngs, R.R., and Coppersmith, K.J., (1985). Implications of fault slip rates and earthquake recurrence models to probabilistic seismic hazard estimates. Bulletin of the Seismological Society of America, v. 75, No.4, p. 939-964.

APPENDIX 1. Radiocarbon Age Determinations.

D S I R Department of Scientific and Industrial Research

Institute of Nuclear Sciences
P O Box 31 312
Lower Hutt
New Zealand

RADIOCARBON LABORATORY

Report on age determination by gas counting

17 November 1988

Submitted by : H. Cowan,
Department of Geology,
University of Canterbury

Sample :
Identifier M32/f12
Description Peat
Project Hope Fault

Results :
Reference for publication NZ 7586
Conventional radiocarbon age 554, + 43 - 43 yr BP

| | | | | |
|---|---|---|---|---|
| $D^{14}C$ | 66.7 | ± | 4.9 | ‰ |
| pM | 93.3 | ± | 0.5 | % |
| $\delta^{13}C$ | 26.6 | ± | 0.1 | ‰ |

Notes :
INS reference number R 11646/3
Pretreatment Hot water + $H_3PO_4$.
Counting run 1500 min. Counter C6372

Corrected age (68% confidence interval):

| | | | |
|---|---|---|---|
| 1394 | - | 1436 | CAL AD ( 60 %) |
| 1326 | - | 1337 | CAL AD ( 9 %) |

Marine corr. factor, delta R =

Comments

Terms and definitions conform with those published by Stuiver and Polach, Radiocarbon (1977) 19 353-363

Corrected age uses the Stuiver and Pearson calibration curves Radiocarbon (1986) 28.2B

Limit age and limit pM are based on a 3 σ criterion. For 1 σ, add 8800 yr to the limit age and divide limit pM by 3.

Enquiries on this sample : Telephone (04) 690 107, FAX (04) 690 657

D S I R Department of Scientific and Industrial Research

Institute of Nuclear Sciences
P O Box 31 312
Lower Hutt
New Zealand

RADIOCARBON LABORATORY

Report on age determination by gas counting

17 November 1988

Submitted by : H. Cowan,
Department of Geology,
University of Canterbury

Sample :
Identifier M32/f14
Description Small branches
Project Hope Fault - swamp date

Results :
Reference for publication NZ 7588
Conventional radiocarbon age 565, + 60 - 60 yr BP

| | | | | |
|---|---|---|---|---|
| $D^{14}C$ | 68.0 | ± | 7.0 | °/₀₀ |
| pM | 93.2 | ± | 0.7 | % |
| $\delta^{13}C$ | 26.7 | ± | 0.1 | °/₀₀ |

Notes :
INS reference number R 11646/5
Pretreatment Hot water + $H_3PO_4$.
Counting run 2000 min. Counter B7759

Corrected age (68% confidence interval):

| | | | |
|---|---|---|---|
| 1387 | - | 1436 | CAL AD ( 43 %) |
| 1315 | - | 1350 | CAL AD ( 25 %) |

Marine corr. factor, delta R =

Comments

Terms and definitions conform with those published by Stuiver and Polach, Radiocarbon (1977) 19 353-363

Corrected age uses the Stuiver and Pearson calibration curves Radiocarbon (1986) 28.2B

Limit age and limit pM are based on a 3 σ criterion. For 1 σ, add 8800 yr to the limit age and divide limit pM by 3.

Enquiries on this sample : Telephone (04) 690 107, FAX (04) 690 657

D S I R Department of Scientific and Industrial Research

Institute of Nuclear Sciences
P O Box 31 312
Lower Hutt
New Zealand

RADIOCARBON LABORATORY

Report on age determination by gas counting

17 November 1988

Submitted by : H. Cowan,
Department of Geology,
University of Canterbury

Sample : Identifier M32/f15
Description Wood - charcoal
Project Kakapo Fault dating

Results : Reference for publication NZ 7589
Conventional radiocarbon age <250, + - , yr BP

| | | | | |
|---|---|---|---|---|
| $D^{14}C$ | 8.4 | ± | 6.2 | °/₀₀ |
| pM | 99.2 | ± | 0.6 | % |
| $\delta^{13}C$ | 26.0 | ± | 0.1 | °/₀₀ |

Notes : INS reference number R 11646/6
Pretreatment Hot water + $H_3PO_4$.
Counting run 1000 min. Counter C6390

Corrected age (68% confidence interval):
>1700 - CAL AD ( %)
- CAL ( %)

Marine corr. factor, delta R =

Comments

Terms and definitions conform with those published by Stuiver and Polach, Radiocarbon (1977) 19 353-363

Corrected age uses the Stuiver and Pearson calibration curves Radiocarbon (1986) 28.2B

Limit age and limit pM are based on a 3 σ criterion. For 1 σ, add 8800 yr to the limit age and divide limit pM by 3.

Enquiries on this sample : Telephone (04) 690 107, FAX (04) 690 657

D S I R Department of Scientific and Industrial Research

Institute of Nuclear Sciences
P O Box 31 312
Lower Hutt
New Zealand

RADIOCARBON LABORATORY

Report on age determination by gas counting

17 November 1988

Submitted by : H. Cowan,
Department of Geology,
University of Canterbury

Sample : Identifier M32/f10
Description Peat
Project Sedimentation rate

Results : Reference for publication NZ 7584
Conventional radiocarbon age 550, + 45 - 45 yr BP

| | | | | |
|---|---|---|---|---|
| $D^{14}C$ | 66.2 | ± | 5.2 | °/₀₀ |
| pM | 93.4 | ± | 0.5 | % |
| $\delta^{13}C$ | 28.6 | ± | 0.1 | °/₀₀ |

Notes : INS reference number R 11646/1
Pretreatment Extraction with hot water + $H_3PO_4$
Counting run 2000 min. Counter C6381

Corrected age (68% confidence interval):

| | | | |
|---|---|---|---|
| 1394 | - | 1438 | CAL AD ( 61 %) |
| 1327 | - | 1336 | CAL AD ( 7 %) |

Marine corr. factor, delta R =

Comments

Terms and definitions conform with those published by Stuiver and Polach, Radiocarbon (1977) 19 353-363

Corrected age uses the Stuiver and Pearson calibration curves Radiocarbon (1986) 28.2B

Limit age and limit pM are based on a 3 σ criterion. For 1 σ, add 8800 yr to the limit age and divide limit pM by 3.

Enquiries on this sample : Telephone (04) 690 107, FAX (04) 690 657

D S I R Department of Scientific and Industrial Research

Institute of Nuclear Sciences
P O Box 31 312
Lower Hutt
New Zealand

RADIOCARBON LABORATORY

Report on age determination by gas counting

17 November 1988

Submitted by : H. Cowan,
Department of Geology,
University of Canterbury

Sample :
Identifier M32/f17
Description tree trunk
Project Hope Fault - dating

Results :
Reference for publication NZ 7591
Conventional radiocarbon age 3280, + 60 - 60 yr BP

| | | | | |
|---|---|---|---|---|
| $D^{14}C$ | 334.9 | ± | 5.0 | °/₀₀ |
| pM | 66.5 | ± | 0.5 | % |
| $\delta^{13}C$ | 25.5 | ± | 0.1 | °/₀₀ |

Notes :
INS reference number R 11646/8
Pretreatment Hot water + $H_3PO_4$
Counting run 1000 min. Counter C6389

Corrected age (68% confidence interval):
1611 - 1456 CAL BC ( %)
- CAL ( %)

Marine corr. factor, delta R =

Comments

Terms and definitions conform with those published by Stuiver and Polach, Radiocarbon (1977) 19 353-363

Corrected age uses the Stuiver and Pearson calibration curves Radiocarbon (1986) 28.2B

Limit age and limit pM are based on a 3 σ criterion. For 1 σ, add 8800 yr to the limit age and divide limit pM by 3.

Enquiries on this sample : Telephone (04) 690 107, FAX (04) 690 657

D S I R Department of Scientific and Industrial Research

Institute of Nuclear Sciences
P O Box 31 312
Lower Hutt
New Zealand

RADIOCARBON LABORATORY

Report on age determination by gas counting

17 November 1988

Submitted by : H. Cowan,
Department of Geology,
University of Canterbury

Sample :
Identifier M32/f11
Description Small branches
Project Age of landslide

Results :
Reference for publication NZ 7585
Conventional radiocarbon age 3336, + 65 - 65 yr BP

| | | | | |
|---|---|---|---|---|
| $D^{14}C$ | 339.8 | ± | 5.4 | °/₀₀ |
| pM | 66.0 | ± | 0.5 | % |
| $\delta^{13}C$ | 24.8 | ± | 0.1 | °/₀₀ |

Notes :
INS reference number R 11646/2
Pretreatment Hot water + $H_3PO_4$.
Counting run 1000 min. Counter C6394

Corrected age (68% confidence interval):
1671 - 1525 CAL BC ( %)
- CAL ( %)

Marine corr. factor, delta R =

Comments

Terms and definitions conform with those published by Stuiver and Polach, Radiocarbon (1977) 19 353-363

Corrected age uses the Stuiver and Pearson calibration curves Radiocarbon (1986) 28.2B

Limit age and limit pM are based on a 3 σ criterion. For 1 σ, add 8800 yr to the limit age and divide limit pM by 3.

Enquiries on this sample : Telephone (04) 690 107, FAX (04) 690 657

D S I R Department of Scientific and Industrial Research

Institute of Nuclear Sciences
P O Box 31 312
Lower Hutt
New Zealand

RADIOCARBON LABORATORY

Report on age determination by gas counting

17 November 1988

Submitted by : H. Cowan,
Department of Geology,
University of Canterbury

Sample : Identifier M32/f13
Description Small branches
Project Hope Fault - sedimentation rates

Results : Reference for publication NZ 7587
Conventional radiocarbon age 3220, + 65 - 65 yr BP

| | | | | |
|---|---|---|---|---|
| $D^{14}C$ | 330.0 | ± | 5.4 | °/₀₀ |
| pM | 67.0 | ± | 0.5 | % |
| $\delta^{13}C$ | 27.6 | ± | 0.1 | °/₀₀ |

Notes : INS reference number R 11646/4
Pretreatment Hot water + $H_3PO_4$ .
Counting run 1000 min. Counter C6395

Corrected age (68% confidence interval):
1527 - 1406 CAL BC ( %)
- CAL ( %)

Marine corr. factor, delta R =

Comments

Terms and definitions conform with those published by Stuiver and Polach, Radiocarbon (1977) 19 353-363

Corrected age uses the Stuiver and Pearson calibration curves Radiocarbon (1986) 28.2B

Limit age and limit pM are based on a 3 σ criterion. For 1 σ, add 8800 yr to the limit age and divide limit pM by 3.

Enquiries on this sample : Telephone (04) 690 107, FAX (04) 690 657

APPENDIX 2. River Downcutting by the Buller and Charwell Rivers. From Knuepfer (1984).

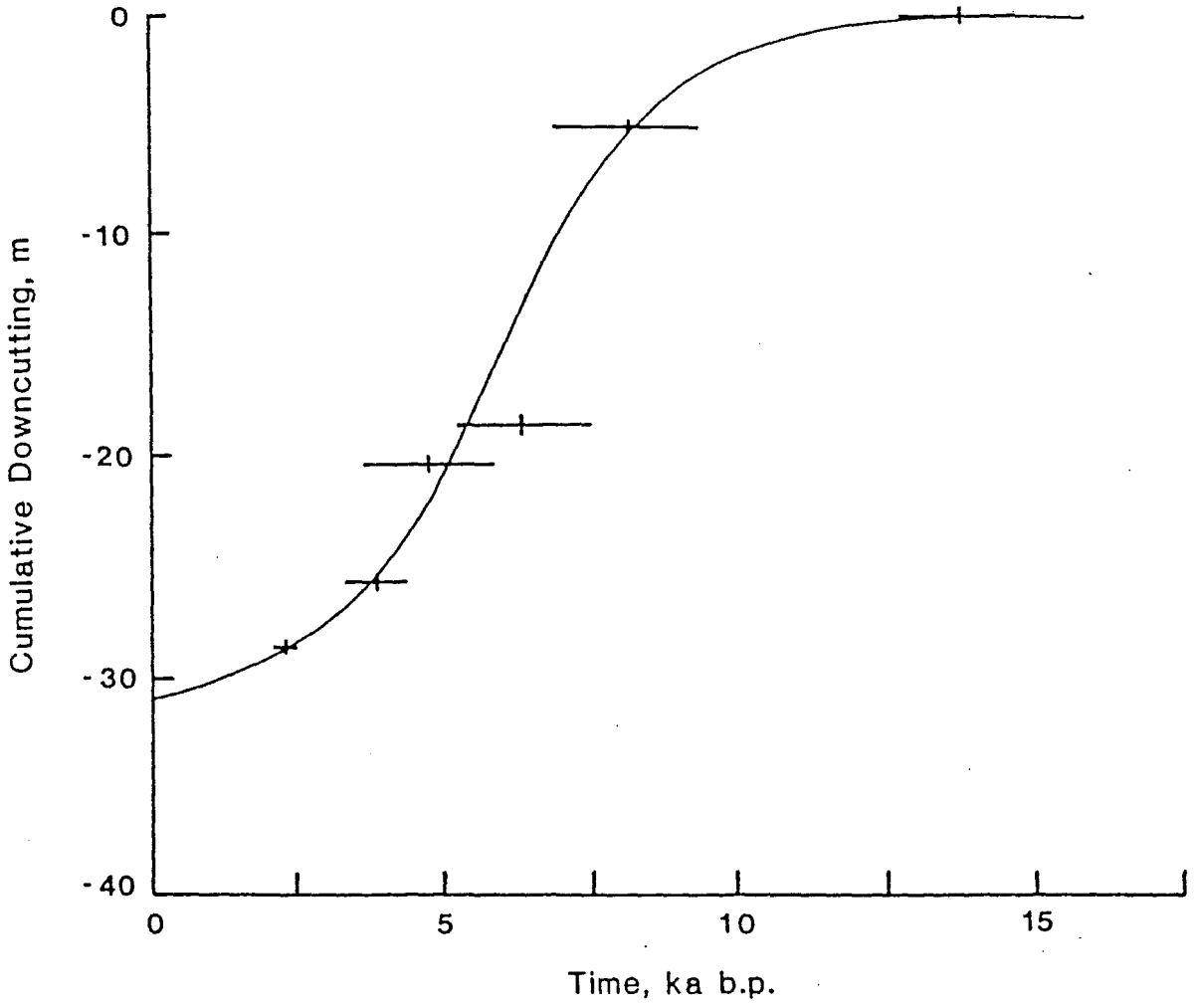


2a) Down-cutting history of the Buller River. Crosses show uncertainties in ages of terrace surfaces and their distance below the surface. Smooth curve reflects "average" rates of down-cutting; a true down-cutting curve would be a jagged, saw-tooth-shaped line reflecting down-cutting, pauses, and deposition of lag deposits. From Knuepfer (1984).

2b) Down-cutting history of the Charwell River, see 2a) for explanation.

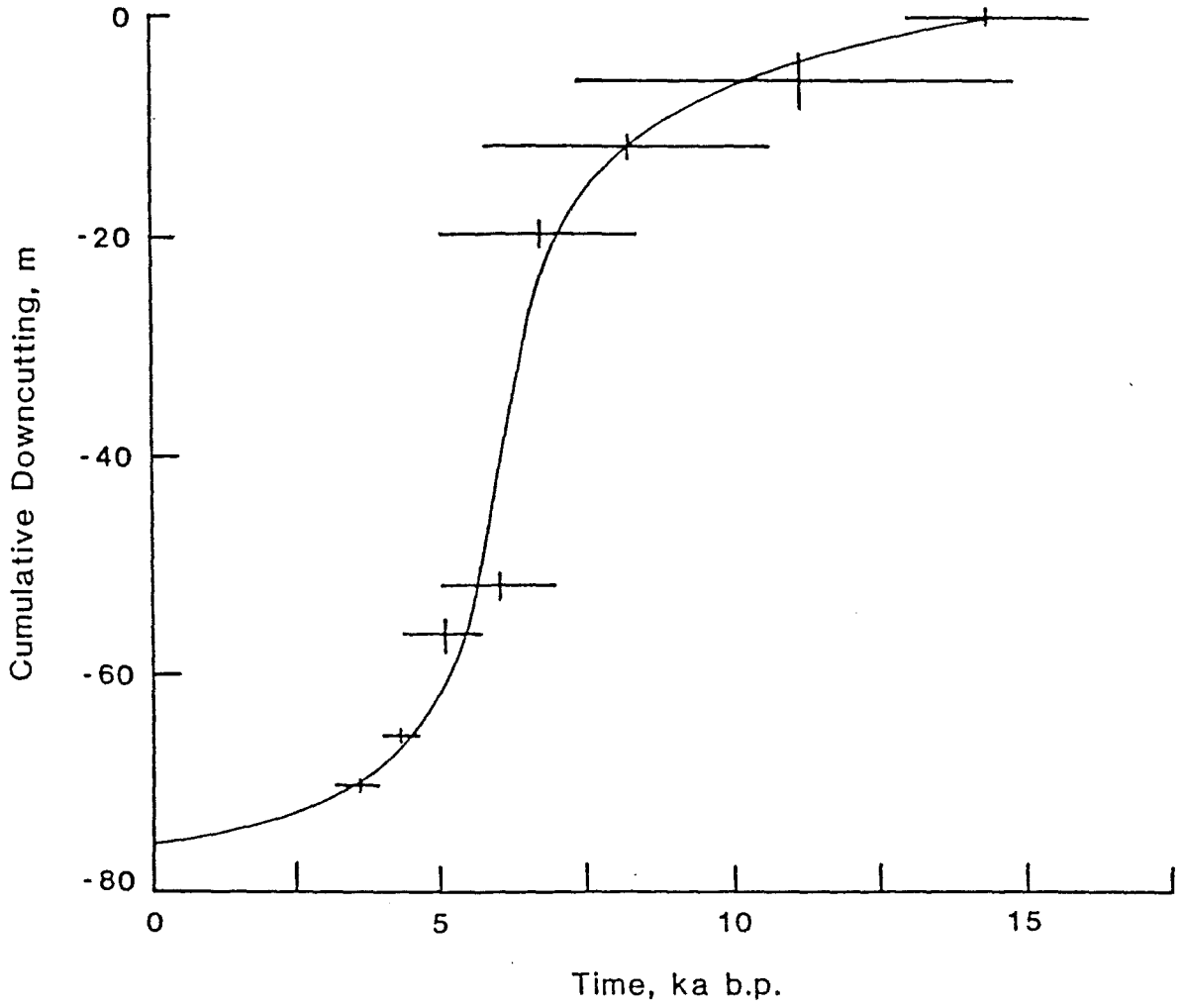

# THE MODIFIED MERCALLI SCALE OF EARTHQUAKE INTENSITY AND ITS USE IN NEW ZEALAND

G. A. EIBY

Seismological Observatory, Geophysics Division, Department of Scientific and Industrial Research, Wellington

*(Received for publication 9 August 1965)*

ABSTRACT

The nature and use of the Modified Mercalli intensity scale is explained, and the degrees of the scale redefined in terms capable of direct application in New Zealand.

## INTRODUCTION

Classification of earthquake effects according to the degrees of an intensity scale makes it simpler to compare the effects of one earthquake with those of another, and to study the different effects of a particular earthquake in different places. Many national differences are apparent in the scales now in use, but those most frequently used are similar enough to have given rise to proposals for a single universal scale to be used by seismologists everywhere. A scale based upon the work of Rossi and Forel was presented to the Second International Seismological Conference in Strassburg (Cancani, 1904). It greatly influenced European practice and is the basis of Sieberg's (1923) scale. From this, in turn, Wood and Neumann's (1931) Modified Mercalli scale, used in America and New Zealand, was derived. Unfortunately Cancani's original proposals contained ambiguities and misconceptions that were not resolved in the later modifications, and attempts to obtain international agreement upon a single scale have recently been renewed (Anon., 1964).

Eiby (1965) has discussed the concept of felt intensity and the requirements of a satisfactory scale in a longer paper. He concludes that attempts to define a universal scale are both undesirable and destined to fail. The maximum number of degrees of intensity that can be satisfactorily distinguished is about twelve. Provided that the scales set up in different countries contain this number of degrees, a broad and useful correspondence between them will inevitably result. This is apparent from the table of correlations established by Gorshkov and Shenkareva (1958).

## DEFECTS OF SOME EXISTING SCALES

The Modified Mercalli scale of Wood and Neumann was originally published in two forms, one being an abridged version "adapted for the use of those who desire simply an outline of the principal features". This abridged version has so often been published without qualification as *the* Modified Mercalli scale that many seismologists and most engineers seem unaware that the full version exists. As Richter (1958) points out, the two versions conflict in some important details. He gives an improved statement of the abridged scale, adding a clarification of the types of building involved. This he terms the "1956 version". It still suffers from abridgement, and carries over the verbal infelicities of Wood and Neumann, which apparently arose from too literal translation of Sieberg's German.

The "international" scale proposed by Medvedev, Sponheuer, and Kárník (1963), though better than either of Wood and Neumann's versions taken alone, has defects that were avoided by Richter. Their classification of structures has been heavily influenced by the constructional practices of eastern Europe and the Soviet Union, making truly international use difficult. The rigid "definitions of quantity" to be applied in assessing the proportion of buildings damaged are inappropriate in rural areas and other regions where the number of examples available is necessarily small. The number of occurrences of a given type of failure does not always increase from "a few" though "many" to "all" as the intensity increases. For example, a small proportion of toilet fixtures and corrugated-iron tanks have defects of construction or installation that cause them to fail at low intensities, but most of them will remain intact until much more general damage is observed. It is also doubtful whether all the groupings of effects supposed to represent a single degree of this intensity scale are valid.

Of existing intensity scales, the Sieberg scale, the "1956 version" of the Modified Mercalli scale, and Kawasumi's (1951) scale are the most satisfactory. None of them is suitable for use in all countries, and it may be considered a merit of Kawasumi's scale that it contains explicit reference to structures that are characteristically Japanese. Wood and Neumann fail to appreciate the differences between American and European buildings, and to allow for the fact that the "ordinary well constructed building" of today is very different from those considered by Cancani, Rossi, and Forel, with whom the description originated.

## NEW ZEALAND INTENSITY ASSESSMENTS

Before 1943, the Seismological Observatory, Wellington, published all its intensity data in terms of the Rossi-Forel scale. Since then, it has used a Modified Mercalli scale intended to be that of Wood and Neumann. Until recently, members of the Observatory staff assessing questionnaires or the information in their field notes have used the abridged version of the scale most of the time, going to the full one only when it became necessary to clarify some uncertainty. In 1960, the system of collecting intensity data was reorganised, and it became apparent that a more consistent method of assessing intensities was needed. It was decided not to issue "interpretations" of the categories of Wood and Neumann, but to rewrite the scale in terms directly applicable in New Zealand. The first draft of this New Zealand version was introduced in 1963.

The scale presented below is not intended to be a new one, but merely

a clarification of the old. It leans heavily upon Richter, but restores some of the effects he omits, and adds a few phenomena commonly seen in New Zealand but not included in other scales, grouping them in such a way that the essential differences between the degrees can be more clearly appreciated. Definitions of the four classes of masonry buildings and of other types of structure mentioned in the scale follow the list of effects. Appropriate allowance should be made for the deterioration of old buildings that have not been regularly maintained.

## MODIFIED MERCALLI SCALE (N.Z. VERSION, 1965)

MM 1 Not felt by humans, except in especially favourable circumstances, but birds and animals may be disturbed.
Reported mainly from the upper floors of buildings more than 10 storeys high.
Dizziness or nausea may be experienced.

Branches of trees, chandeliers, doors, and other suspended systems of long natural period may be seen to move slowly.
Water in ponds, lakes, reservoirs, etc., may be set into seiche oscillation.

MM 2 Felt by a few persons at rest indoors, especially by those on upper floors or otherwise favourably placed.

The long-period effects listed under MM 1 may be more noticeable.

MM 3 Felt indoors, but not identified as an earthquake by everyone.
Vibration may be likened to the passing of light traffic.

It may be possible to estimate the duration, but not the direction.
Hanging objects may swing slightly.
Standing motorcars may rock slightly.

MM 4 Generally noticed indoors, but not outside.
Very light sleepers may be wakened.
Vibration may be likened to the passing of heavy traffic, or to the jolt of a heavy object falling or striking the building.

Walls and frame of buildings are heard to creak.
Doors and windows rattle.
Glassware and crockery rattles.
Liquids in open vessels may be slightly disturbed.
Standing motorcars may rock, and the shock can be felt by their occupants.



MM 5 Generally felt outside, and by almost everyone indoors.
Most sleepers awakened.
A few people frightened.

Direction of motion can be estimated.
Small unstable objects are displaced or upset.
Some glassware and crockery may be broken.
Some windows cracked.
A few earthenware toilet fixtures cracked.
Hanging pictures move.
Doors and shutters may swing.
Pendulum clocks stop, start, or change rate.

MM 6 Felt by all.
People and animals alarmed.
Many run outside.
Difficulty experienced in walking steadily.

Slight damage to Masonry D.
Some plaster cracks or falls.
Isolated cases of chimney damage.

Windows, glassware, and crockery broken.
Objects fall from shelves, and pictures from walls.
Heavy furniture moved. Unstable furniture overturned.

Small church and school bells ring.
Trees and bushes shake, or are heard to rustle.
Loose material may be dislodged from existing slips, talus slopes, or shingle slides.

MM 7 General alarm.
Difficulty experienced in standing.
Noticed by drivers of motorcars.
Trees and bushes strongly shaken.
Large bells ring.

Masonry D cracked and damaged.
A few instances of damage to Masonry C.

Loose brickwork and tiles dislodged.
Unbraced parapets and architectural ornaments may fall.
Stone walls cracked.
Weak chimneys broken, usually at the roof-line.
Domestic water tanks burst.
Concrete irrigation ditches damaged.

Waves seen on ponds and lakes.
Water made turbid by stirred-up mud.
Small slips, and caving-in of sand and gravel banks.

MM 8 Alarm may approach panic.
Steering of motorcars affected.

Masonry C damaged, with partial collapse.
Masonry B damaged in some cases.
Masonry A undamaged.

Chimneys, factory stacks, monuments, towers, and elevated tanks twisted or brought down.
Panel walls thrown out of frame structures.
Some brick veneers damaged.
Decayed wooden piles broken.
Frame houses not secured to the foundation may move.

Cracks appear on steep slopes and in wet ground.
Landslips in roadside cuttings and unsupported excavations.
Some tree branches may be broken off.

Changes in the flow or temperature of springs and wells may occur.
Small earthquake fountains.

MM 9 General panic.

Masonry D destroyed.
Masonry C heavily damaged, sometimes collapsing completely.
Masonry B seriously damaged.
Frame structures racked and distorted.

Damage to foundations general.
Frame houses not secured to the foundations shifted off.
Brick veneers fall and expose frames.

Cracking of the ground conspicuous.
Minor damage to paths and roadways.
Sand and mud ejected in alluviated areas, with the formation of earthquake fountains and sand craters.
Underground pipes broken.
Serious damage to reservoirs.

MM 10 Most masonry structures destroyed, together with their foundations.
Some well built wooden buildings and bridges seriously damaged.
Dams, dykes, and embankments seriously damaged.
Railway lines slightly bent.
Cement and asphalt roads and pavements badly cracked or thrown into waves.

Large landslides on river banks and steep coasts.

Sand and mud on beaches and flat land moved horizontally.
Large and spectacular sand and mud fountains.
Water from rivers, lakes, and canals thrown up on the banks.



MM 11 Wooden frame structures destroyed.
Great damage to railway lines.
Great damage to underground pipes.

MM 12 Damage virtually total. Practically all works of construction destroyed or greatly damaged.

Large rock masses displaced.
Lines of sight and level distorted.
Visible wave-motion of the ground surface reported.
Objects thrown upwards into the air.

*Categories of Non-wooden Construction*

Masonry A. Structures designed to resist lateral forces of about 9·1/g, such as those satisfying the New Zealand Model Building Bylaw, 1955. Typical buildings of this kind are well reinforced by means of steel or ferro-concrete bands, or are wholly of ferro-concrete construction. All mortar is of good quality and the design and workmanship is good. Few buildings erected prior to 1935 can be regarded as in category A.

Masonry B. Reinforced buildings of good workmanship and with sound mortar, but not designed in detail to resist lateral forces.

Masonry C. Buildings of ordinary workmanship, with mortar of average quality. No extreme weakness, such as inadequate bonding of the corners, but neither designed nor reinforced to resist lateral forces.

Masonry D. Buildings with low standards of workmanship, poor mortar, or constructed of weak materials like mud brick and rammed earth. Weak horizontally.

*Windows*

Window breakage depends greatly upon the nature of the frame and its orientation with respect to the earthquake source. Windows cracked at MM 5 are usually either large display windows, or windows tightly fitted to metal frames.

*Chimneys*

The "weak chimneys" listed under MM 7 are unreinforced domestic chimneys of brick, concrete block, or poured concrete.

*Water tanks*

The "domestic water tanks" listed under MM 7 are of the cylindrical corrugated-iron type common in New Zealand rural areas. If these are only partly full, movement of the water may burst soldered and riveted seams.

Hot-water cylinders constrained only by supply and delivery pipes may move sufficiently to break the pipes at about the same intensity.

## ASSIGNING INTENSITIES

When assigning an intensity it is important that the observer should note not only what damage has occurred, but the condition and situation of the object or structure affected. An intensity rating must not be based upon a single happening, even in regions where data are scarce, except perhaps when it is certain that the object affected is a typical member of its class. Most effects extend over several degrees of the scale, and it is only by observing the whole complex of events and the characteristic effects of adjacent degrees that a just assessment can be made.

It will be found necessary to consider what has not occurred, as well as what has. For example, an earthquake that damages a sound chimney could not have been overlooked by the occupants of the house, or have been unaccompanied by the disturbance of other material objects. It is often helpful to approach the proposed rating from both the higher and the lower sides, satisfying oneself that a higher rating would undoubtedly be too high, and a lower one too low. The temptation to assign intensities between the degrees of the scale should be resisted: it is doubtful whether more than 12 categories of effects can be adequately defined. In a few cases it may be necessary to state 4 *or* 5, but never 4½ or *between* 4 and 5.

Special care is needed at the lowest intensities, and also with those above MM 8. The waves responsible for the slight shaking experienced in the outer parts of the felt area of a large earthquake are of much longer period than those of a small earthquake close at hand, and the effects observed differ correspondingly. In most cases, the approximate distance of the epicentre is known, and proper allowance is easy to make.

The time of day should also be considered. Only insomniacs will report an earthquake of intensity MM 3 at 1 or 2 a.m.; and at any time, the MM 4 region will contain many people who remain unaware of the shock.

Usually where the intensity exceeds MM 8, the area will be visited by qualified assessors. However, it is necessary to issue a warning that the behaviour of buildings incorporating anti-seismic precautions (Masonry A) is usually too complex to make buildings of this kind good indicators of intensity on their own. Similarly, damage that results from contact of two buildings of very different dimensions or mechanical properties, while of great interest to the engineer, does not depend in any simple way upon the intensity, and is more informative when the intensity can be found independently.

Similar caution is needed when dealing with geological phenomena like ground uplift and faulting. These are not observed at low intensities, but they are not in themselves indicators of the degree of shaking. It is particularly important that an area should not be mapped as that of greatest intensity solely on the grounds that it is traversed by fresh breakage along a fault (Louderback, 1942).





## ACKNOWLEDGMENTS

Thanks are due to many people who have examined and discussed drafts of this scale, in particular to Mr J. R. Bennett, Secretary of the Earthquake and War Damage Commission, and to Mr D. J. McArthur of his staff; to Mr R. R. Dibble of the Geology Department, Victoria University of Wellington; to a number of architects and engineers, and to colleagues in the Geophysics Division, D.S.I.R. Their help has been invaluable, but they will not necessarily agree with this final version.

## REFERENCES

ANON. 1964: Intergovernmental Meeting on Seismology and Earthquake Engineering. *Chronique de l'UGGI, 55*: 147–57.

CANCANI, A. 1904: Sur l'Emploi d'une Double Échelle Sismique des Intensités. Empirique et Absolue. *Gerlands Beitr. z. Geophys., Erganzungsband 2*: 281–3.

EIBY, G. A. 1965: The Assessment of Earthquake Felt Intensities. *Proc. 3rd World Conf. on Earthq. Engng. Paper III/E/10.*

GORSHKOV, G. P.; SHENKAREVA, G. A. 1958: O Korrelyatsii Seismicheskikh Shkal. *Trudy Inst. Fiz. Zem. 1 (168)*: 44–64.

KAWASUMI, H. 1951: Measures of Earthquake Danger and Expectancy of Maximum Intensity Throughout Japan as Inferred from the Seismic Activity in Historical Times. *Bull. Earthq. Res. Inst., Tokyo 29*: 469–81. (*See* p. 481.)

LOUDERBACK, G. D. 1942: Faults and Earthquakes. *Bull. Seismol. Soc. Amer. 32*: 305–30.

MEDVEDEV, S.; SPONHEUER, W.; KARNÍK, V. 1963: "Seismische Skala." Inst. für Bodendynamik und Erdbebenforschung, Jena. 6 pp.

RICHTER, C. F. 1958: "Elementary Seismology." Freeman, San Francisco. 768 pp. (*See* pp. 136–8.)

SIEBERG, A. 1923: "Erdbebenkunde." Gustav Fischer, Jena. 572 pp.

WOOD, H. O.; NEUMANN, F. 1931: Modified Mercalli Intensity Scale of 1931. *Bull. Seismol. Soc. Amer. 21*: 277–83.

## APPENDIX 4. REGIONAL FELT INTENSITIES IN THE 1888 AMURI EARTHQUAKE

### Explanatory Notes

I have compiled this list of local and regional felt intensities and damage in the 1888 earthquake to provide a credible basis for my re-evaluation of Modified Mercalli Intensities and estimates of earthquake magnitude. Previous estimates of felt intensity and magnitude of the Amuri earthquake have been too high, and convey an excessively conservative impression of the event and its consequences.

The sources for this information are Hutton (1888), McKay (1888) and (1890), the Canterbury Times (Sept 7-Oct 25, 1888); the Lyttleton Times (Sept 3-Sept 11, 1888); The Press (Sept 3-Sept 18, 1888); and an autobiographical account of the earthquake: Jones (1933).

Following the description of seismic effects at each locality is an estimate of the Modified Mercalli Intensity at the site (see Appendix 2 for discussion on the application of the Modified Mercalli Scale in New Zealand).

### Felt Intensities and Damage Reports for the 1888 Amuri Earthquake

#### Amuri District

**Glynn Wye** The manager's wooden house was distorted and tilted eastward, but remained on its foundations; the chimneys were thrown down. A small wooden cottage remained intact, but was shifted bodily 0.4m to the north. The 40m long woolshed suffered foundation damage and partial collapse, and a masonry sheep-dip was totally wrecked. The stable, workshop and storehouse were not much damaged. Large landslides on surrounding hillslopes, especially between Gorge Stream and Horseshoe Lake. Fault displacements of up to 2.6m. **MM9**

**Hopefield** Chimneys thrown down and roof twisted out of shape, but walls and foundations intact. **MM8 or MM9**

**Upper Waiau** Cob huts and stone woolshed destroyed (the woolshed was built on the fault). Wooden house suffered partial foundation collapse but was otherwise undamaged. **MM8 or MM9**

**Woodbank** Old brick portion of the homestead collapsed, but a recent addition in wood was only slightly damaged. Chimneys and a cob hut collapsed. **MM8**

**Hot Springs** No damage was done, minor changes in spring flow and temperature. **MM6?**

**Jack's Pass Hotel** No damage and very little breakage of glass. **MM4, possibly MM5**

**St. James'** Chimney tops cracked, no other damage. **MM6**

**Jollies Pass Hotel** No damage done, and very little breakage of glass. **MM4 possibly MM5**

**Clarence Accommodation House** Slight chimney damage. **MM6**

**Tarndale** Sleepers woken, but no damage. **MM5**

**St. Helen's** Chimneys thrown down; glass and furniture damage. **MM7 to MM8**

**Ferry Hotel** An old cob building, but only slightly damaged. **MM6 to MM7**

**Marble Point** Opposite Marble Point, hillside north of Waiau River failed in large landslide. **MM7 to MM8**

**Tekoa** A brick house. The upper portions of the walls fell. Large landslides in surrounding mountains. **MM7 to MM8**

**Balmoral** No damage reported. **MM4 to MM5?**

**Culverden** No damage at the township. Minor chimney damage at the Culverden Station. **MM6**

**Pahau Pastures** Chimney moved, objects thrown from shelves. No damage. **MM6**

**Montrose** Minor chimney damage. **MM6**

**Leslie Hills** A stone building. Walls were cracked and chimneys thrown down. Cob huts nearby were undamaged. **MM7**

**St Leonards** Several chimneys down. **MM7**

**Lyndon** One chimney fell. **MM6**

**Waiau Township** Several chimneys down, and a monument in the cemetery overturned. **MM7**

**Highfield** Chimneys broken off at the roof-line. **MM7**

**Kaikoura** A few chimney tops thrown down and others cracked. **MM6**

## Canterbury District

**Waikari** Two chimneys down. **MM6**

**Amberley** No damage reported. **MM4?**

**Rangiora** Minor damage to one chimney, and some crockery broken. **MM5**

**Kaiapoi** The tops of two or three very old chimneys were thrown down. The woollen factory chimney was undamaged. **MM5**

**Ohoka** A few clocks stopped. No damage. **MM5**

**Belfast** Strongly felt, but no damage. Meat works chimney unscathed. **MM5**

**Christchurch** The upper 8m of the cathedral spire was destroyed. Chimney damage mostly in eastern Christchurch; slight damage to some buildings. Very little, if any, glass or crockery broken. **MM6 to possibly MM7.**

**Lyttleton** No damage done. The water in the harbour was not disturbed.

**Prebbleton** Strongly felt and minor crockery damage. **MM6**

**Leeston** Strongly felt, but no damage. **MM5**

**Southbridge** Strongly felt, but no damage. **MM5**

**Akaroa** Strongly felt but no damage done. **MM5**

**Springfield** All sleepers woken, heavy shaking but no damage. **MM5**

**Bealey-Arthurs Pass** Large landslides, about 1 week to clear road. **MM7 possibly MM8**

**Selwyn** Most sleepers woken. Railway clock stopped. No Damage. **MM5.**

**Kirwee** Most sleepers woken. No damage. **MM5.**

**Glentunnel** Strongly felt, but no damage. **MM5.**

**Ashburton** Isolated cracking of plaster. **MM6**

**Rakaia** Strongly felt but no damage done. **MM5**

**Geraldine** Strongly felt but no damage done. **MM5**

**Timaru** Strongly felt but no damage done. **MM5**

<u>Nelson and Westland</u>

**Nelson** Most sleepers wakened but no damage. **MM5**

**Blenheim** Felt by some, shake of long duration but not very violent. **MM4**

**Lyell** Strongly felt but no damage. **MM5**

**Westport** Isolated cracking of chimneys, and some glass and crockery damage. **MM5 possibly MM6**

**Boatman's** Strongly felt but no damage. **MM5**

**Reefton** No chimney damage, but minor glass and crockery breakage. **MM5**

**Greymouth** Old and badly built chimneys fell, and there was considerable glass and crockery damage. Heavy furniture overturned. **MM6**

**Hokitika** Chimneys thrown down and others cracked. **MM6**

Other Districts

**Wellington** Shake of long duration, felt by few people. **MM4**

**Masterton** Shake of long duration, felt by few people. **MM4**

**Napier** Not felt.

**New Plymouth** Shake of long duration, felt by few people. **MM4**

**Dunedin** Slight shock of long duration. **MM4**

**Invercargill** Pronounced shock, but no damage. **MM5**

## APPENDIX 5. EARTHQUAKES FELT IN AMURI DISTRICT DURING OCTOBER, 1888.

### Explanatory Notes

Three earthquakes felt in the Amuri District during October, 1888 were the subject of a telegram from an Amuri runholder to A. McKay, Assistant Geologist. McKay (1890), and recently Knuepfer (1984) interpreted these shocks to represent strong aftershocks or a second main shock to the Sept 1, 1888 event, extending surface rupture along the Hope Fault to the east of Hanmer Basin.

-------- *** --------

Copy of Telegram from Mr D. Rutherford to Mr A. McKay, dated Culverden, 29th October, 1888.

Earthquake-shock on Tuesday, the 23rd instant, at 8.17 p.m., direction west to east, with loud rumbling noise and undulating motion. On Friday 26th, at 12.48 a.m., similar shock to that of Tuesday, but lasting longer, with undulating motion. On Sunday, the 28th, at 7.22 a.m., a sharp jerky shock, no noise, direction west to east, lasting only two or three seconds. The general opinion is that the first two shocks did not originate at Hanmer Plains.*

---

* This is probable. The shocks appear to have been felt at Kaikoura more strongly than elsewhere, showing that the old fracture line is being opened afresh in that direction.-A. McKAY."

(McKay 1890 p.16).

APPENDIX 6. Observed isoseismals for the May 23, 1968, Inangahua Earthquake (M = 7.1). From Smith (1978).

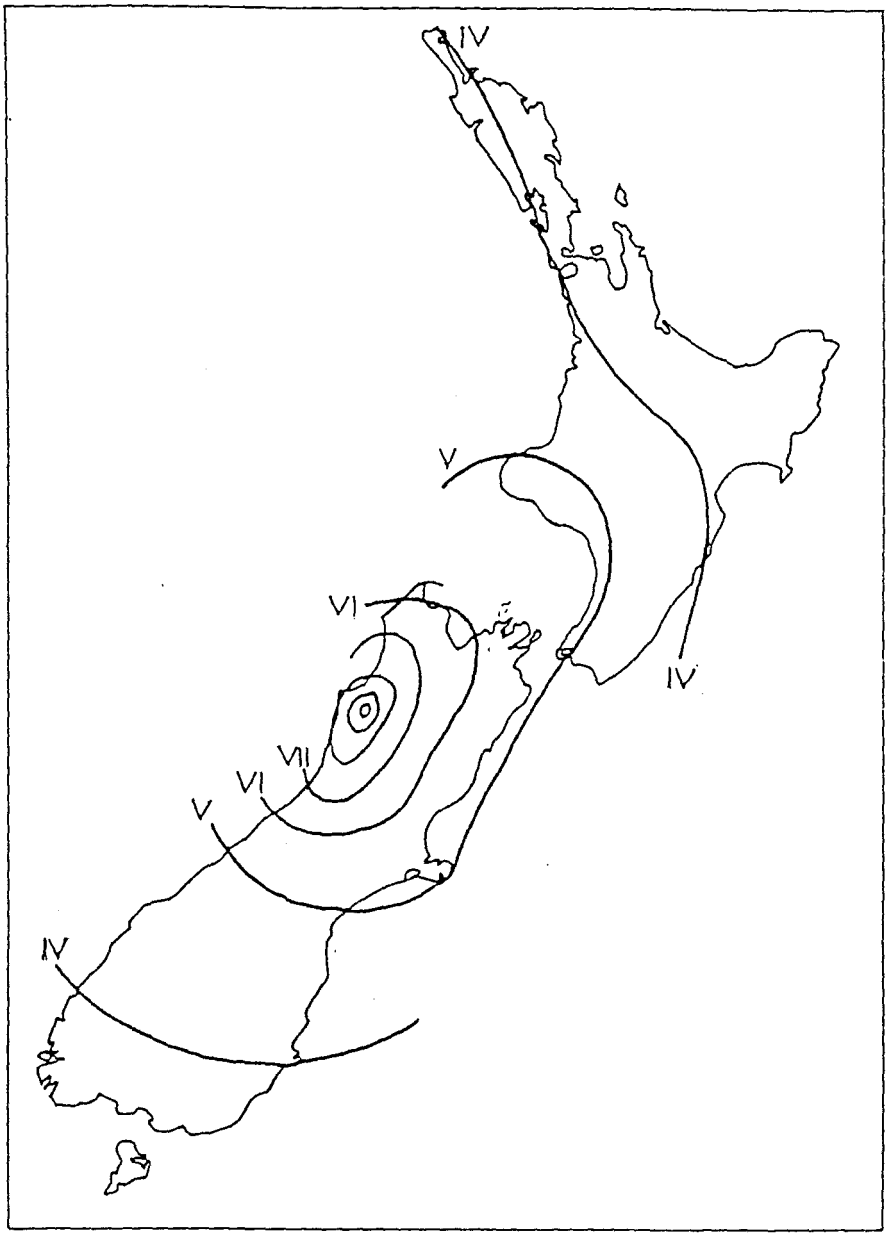

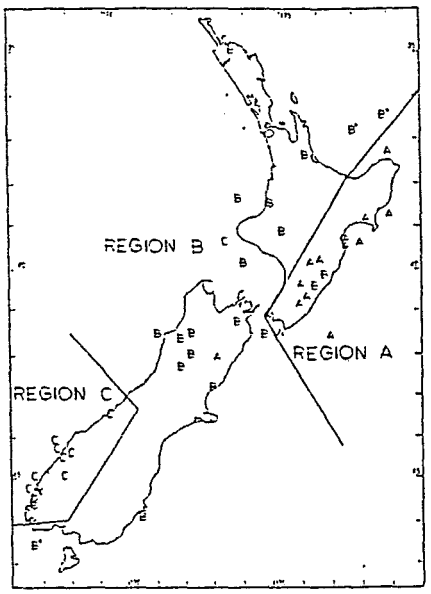


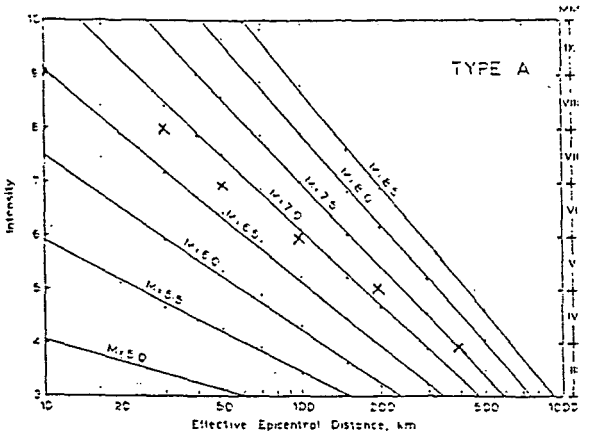


Fig. 9—Intensity as a function of magnitude and distance for earthquakes of type A. See text for explanation. Parameters are given in Table 2.

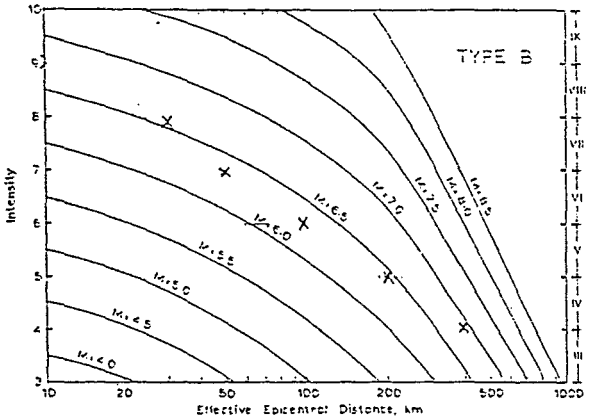


Fig. 10—Intensity curves for type B earthquakes. Parameters are given in Table 3.

APPENDIX 7. Classification of shallow (<40 km) earthquakes (Smith, 1978), and intensity attenuation for the 1888 Amuri Earthquake. Using the intensity curves of Smith (1978).

## APPENDIX 8. LIST OF EARTHQUAKES FELT STRONGLY IN NORTH CANTERBURY, BETWEEN 1860 AND 1965.

Explanatory Notes

Information in Appendix 1 is taken from Eiby (1968) and Fellows (1986).

For the pre-instrumental period (prior to about 1930) the provisional magnitude categories of the "Descriptive Catalogue" are used. Shocks in Class A are believed to have had magnitudes of >7.5, and those in Class B, magnitudes of 6-7.5. Class C shocks were probably above magnitude 5 (Eiby 1968).

For the early instrumental period, the cited magnitudes are teleseismic values reported by Gutenburg & Richter (1954), or the International Seismological Summary (ISS). All other instrumentally recorded magnitudes were originally taken from NZ Seismological Bulletins.

| Date | Provisional Epicentre | Magnitude Class |
|---|---|---|
| 1869 June 5 | Banks Peninsula | C |

Intensity in Christchurch about MM7

| | | |
|---|---|---|
| 1870 Aug 31 | Banks Peninsula | C |

Apparently some property damage in Christchurch. Felt Banks Peninsula, Mid-Canterbury, Greymouth, and Dunedin.

| | | |
|---|---|---|
| 1881 Dec 5 | North Canterbury | B |

Christchurch cathedral spire slightly damaged. Felt over most of South Island. Hogben (1891) assigns epicenter to Lake Sumner.

| | | |
|---|---|---|
| 1888 Sept 1 | North Canterbury | B |

Intensities of MM8 or more were experienced in Christchurch and much of North Canterbury. Felt area includes most of South Island and southern North Island. Faulting at GlynnWye.

**Note: The detailed review of the Amuri earthquake in this study, revises felt intensities in the Christchurch area down to about MM6-MM7.**

1888 Oct 23 North Canterbury B

Felt from Taupo to Timaru. Possibly an aftershock of Sept. 1. **Note: The distribution of felt reports indicate a northern South Island or North Island origin for this earthquake, not the Hope Fault. See discussion in text (section 3.5).**

1888 Dec 27 North Canterbury C

Possibly an after-shock of Sept.1. Felt in Christchurch about MM6, and southwards to Dunedin. **Note: This MM Intensity estimate has not been evaluated and may be too high.**

1895 Aug 4 Mid-Canterbury C

Felt Christchurch to Dunedin. Two chimneys fell in Christchurch.

1901 Nov 16 Cheviot B

Intensity MM9 at Cheviot. Felt New Plymouth to Dunedin, but not apparently in Hawke's Bay, Wairarpa, or in Westland. One death.

1922 Dec 25 North Canterbury B

ISS give an epicentre at 43.0°S, 173.0°E. Intensity about MM7 at Rangiora. Felt Taranaki to Dunedin.

1929 Mar 9 Arthur's Pass B

ISS epicentre at 42.5°S, 172.0°E. Gutenburg and Richter give M=6.9. Felt over the whole country except Northland Peninsula. Maximum intensities above MM8 in mountainous country.

1943 Aug 23 Arthur's Pass M = 5.5-6

Felt Nelson, Marlborough, Canterbury and Westland. Intensity MM7 in epicentral region. Epicentre 42.8°S, 171.7°E.

1945 Aug 30 Waiau M = 5.4

Intensity MM6 in epicentral region.

1946 Jun 26 Upper Rakaia M = 6

Felt over most of the South Island. Intensities above MM7 in Lake Coleridge area. Many after-shocks. Epicentre 43.2°S, 171.5°E

1946 Jun 28 Upper Rakaia M = 5.5-6

Felt over northern and central parts of the South Island. Intensity about MM6 in Lake Coleridge region. Epicentre 43.2°S, 171.4°E. This was the largest after-shock of 1946 Jun 26.

1948 May 22 Waiau M = 6.4

Intensity about MM8 in the epicentral region. Felt over the northern half of the South Island. A foreshock of M=5.9, and at least four after-shocks of M>5.5 Main shock epicentre, 42.5°S, 173.0°E.

1951 Jan 10 Cheviot M = 5.6

Felt from Cook Strait to Banks Peninsula. Intensity MM7-MM8 in Cheviot area. Epicentre 42.8°S, 173.2°E. Several after-shocks of M>5.0.

1955 Seaward Kaikouras M = 5.1

Minor damage in the Cheviot district. Intensity about MM6. Felt over the northern half of the South Island. Epicentre 42.8°S, 173.3°E.

1973 Apr 22 Marlborough M = 5.2

Epicentre 42.32°S, 172.99°E, possibly associated with the Clarence Fault. Minor (mm) lateral displacement was reported (Wood 1973); maximum intensity of MM7 in epicentral region.

APPENDIX 9. Ground acceleration estimates for Modified Mercalli Scale Intensities, VI-X in North Canterbury-South Marlborough. From Fellows (1986).

| Earthquake intensity | Average Peak (1) Ground acceleration (mean) | Average peak ground (2) acceleration | Mean Return periods |
|---|---|---|---|
| VI | 0.04 - 0.17 g | 0.25 - 0.05 g | 6 years (3) |
| VII | 0.10 - 0.19 g | 0.05 - 0.10 g | 20 years (3) |
| VIII | 0.15 - 0.25 g | 0.10 - 0. 2 g | 69 years (4) |
| IX | 0.25 - 0.47 g | 0. 2 - 0. 4 g | 245 years (4) |
| X | 0.31 - 0.95 g | - | 1000 years (4) |

NOTES: (1) Range of Average Peak ground acceleration derived from Krinitzsky - Chang curves. (Table 7, Figure 15a).

(2) Range of average peak ground accelerations based on the intensity - acceleration relations of Medvedev (1962). (Figure 15b).

(3) Mean return periods for earthquakes at Kaikoura, based on Smith & Berryman (1983) estimates using both historic seismicity and active fault data.

(4) Mean Return periods based on the estimates in Section 6.2 of Fellows (1986).

# APPENDIX 10. The attenuation expression of Katayama et.al. (1978).

## Statistical Analysis of Earthquake Acceleration Response Spectra

Tsuneo KATAYAMA*, Toshio IWASAKI** and Mitsuaki SAEKI***

*Published in the Proc. of JSCE, No. 275, July 1978, pp. 29-40 (In Japanese).*
**Associate Professor, Institute of Industrial Science, University of Tokyo, Tokyo*
***Head, Ground Vibration Section, Earthquake Disaster Prevention Division, Public Works Research Institute, Ministry of Construction*
****Chief Research Engineer, Japan Engineering Consultants Co., Ltd.*

Statistical analysis was made for 277 acceleration response spectral amplitudes at each of the 18 natural periods of a SDOF system in terms of earthquake magnitude, epicentral distance and recording-site ground conditions. The accelerograms used for analysis were the horizontal components of 67 earthquakes recorded at various places in Japan during 1956 and 1974.

Magnitude, distance and site condition were divided into several discrete categories as shown in Table 1, and the following form of prediction formula was assumed:

$$\overline{SA}(T,h)=f_M(T,h)*f_\Delta(T,h)*f_{GC}(T,h)$$

where

$\overline{SA}(T,h)$ = Predicted absolute acceleration response spectral amplitude for given $T$ and $h$,
$T$ = Natural period of SDOF system(s),
$h=0.05$ = Damping factor of SDOF system,
$f_M(T,h)$ = Weighting factor for each magnitude category in Table 1,
$f_\Delta(T,h)$ = Weighting factor for each distance category in Table 1,
$f_{GC}(T,h)$ = Weighting factor for each ground conditions category in Table 1.

The values of the weighting factors were so determined that the predicted spectral amplitudes best agree with the measured spectral amplitudes. The results obtained for each of the 18 natural periods are summarized in Table 2. For example, the absolute acceleration spectral amplitude for $T=0.5$ s and $h=0.05$ that would be obtained from the ground motion recorded on Type III ground and caused by an earthquake with $M=6.1$–$6.7$ and $\Delta=20$–$59$ km is predicted as

$$\overline{SA}(0.5,\ 0.05)=0.309\times 2.91\times 140=126\ (\mathrm{cm/s^2})$$

Examples of predicted acceleration response spectra are shown in Fig. 1. It is clearly demonstrated by Fig. 1 that not only the intensity but also the frequency characteristics of ground motion is dependent on earthquake magnitude and epicentral distance.

Table 1 Items and categories used for quantification analysis.

| Item | Category | Mean of the Data in Each Category |
|---|---|---|
| Earthquake Magnitude ($M$) | $M$=4.5~5.3 | 4.96 |
| | $M$=5.4~6.0 | 5.75 |
| | $M$=6.1~6.7 | 6.30 |
| | $M$=6.8~7.4 | 7.06 |
| | $M$=7.5~7.9 | 7.65 |
| Epicentral Distance ($\Delta$ : km) | $\Delta$=6~19 | 11.7 |
| | $\Delta$=20~59 | 38.2 |
| | $\Delta$=60~119 | 82.9 |
| | $\Delta$=120~199 | 158.7 |
| | $\Delta$=200~405 | 271.3 |
| Ground Condition at Recording Site | Type I: Tertiary or Older Rock (Defined as Bedrock), or Diluvium with $H^*<10$ m | |
| | Type II: Diluvium with $H\geqq 10$ m or Alluvium with $H<10$ m | |
| | Type III: Alluvium with $H<25$ m Including Soft Layer** with Thickness Less than 5 m | |
| | Type VI: Other than the above, Usually Soft Alluvium or Reclaimed Land | |

* Depth to Bedrock.
** Sand Layer Vulnerable to Liquefaction or Extremely Soft Cohesive Soil Layer.

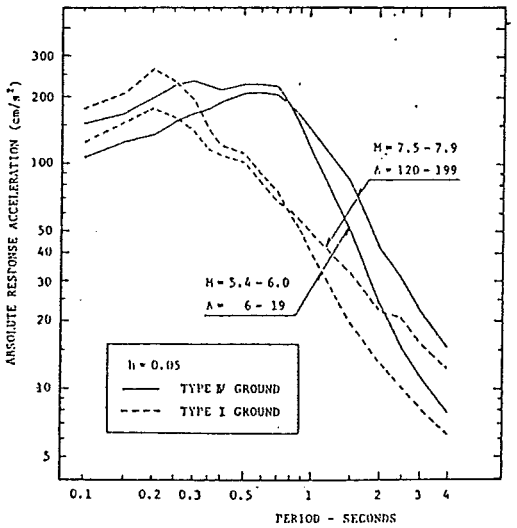


Fig. 1 Examples of predicted acceleration spectra.

Table 2 Weighting coefficients obtained from quantification analysis.

| $T$* | $\rho$** | $f_M$ ($T$, 0.05) Magnitude ($M$) | | | | | $f_D$ ($T$, 0.05) Epicentral Distance ($\Delta$ : km) | | | | | $f_{GC}$ ($T$, 0.05) Ground Condition ($GC$) | | | |
|---|---|---|---|---|---|---|---|---|---|---|---|---|---|---|---|
| | | 4.5~5.3 | 5.4~6.0 | 6.1~6.7 | 6.8~7.4 | 7.5~7.9 | 6~19 | 20~59 | 60~119 | 120~199 | 200~405 | Type I | Type II | Type III | Type IV |
| 0.10 | 0.56 | 0.218 | 0.278 | 0.296 | 0.399 | 1.00 | 5.10 | 2.67 | 2.05 | 0.994 | 1.00 | 126 | 107 | 120 | 106 |
| 0.15 | 0.53 | 0.225 | 0.274 | 0.297 | 0.448 | 1.00 | 4.85 | 3.01 | 2.15 | 1.00 | 1.00 | 155 | 130 | 141 | 125 |
| 0.20 | 0.54 | 0.185 | 0.280 | 0.288 | 0.499 | 1.00 | 5.48 | 3.24 | 2.07 | 1.05 | 1.00 | 169 | 149 | 161 | 129 |
| 0.25 | 0.55 | 0.171 | 0.254 | 0.283 | 0.534 | 1.00 | 6.86 | 3.65 | 2.33 | 1.21 | 1.00 | 135 | 129 | 143 | 129 |
| 0.30 | 0.56 | 0.164 | 0.269 | 0.280 | 0.548 | 1.00 | 6.59 | 3.51 | 2.25 | 1.27 | 1.00 | 109 | 130 | 147 | 131 |
| 0.35 | 0.55 | 0.161 | 0.274 | 0.302 | 0.588 | 1.00 | 5.74 | 3.05 | 2.13 | 1.24 | 1.00 | 92.8 | 126 | 149 | 142 |
| 0.40 | 0.57 | 0.152 | 0.268 | 0.311 | 0.557 | 1.00 | 5.45 | 3.01 | 1.92 | 1.33 | 1.00 | 83.0 | 122 | 145 | 144 |
| 0.50 | 0.63 | 0.108 | 0.237 | 0.309 | 0.593 | 1.00 | 6.35 | 2.91 | 1.60 | 1.36 | 1.00 | 76.6 | 113 | 140 | 156 |
| 0.60 | 0.67 | 0.0889 | 0.246 | 0.321 | 0.618 | 1.00 | 5.88 | 2.79 | 1.46 | 1.32 | 1.00 | 62.1 | 101 | 134 | 159 |
| 0.70 | 0.70 | 0.0730 | 0.222 | 0.315 | 0.644 | 1.00 | 6.77 | 2.96 | 1.56 | 1.37 | 1.00 | 50.0 | 88.8 | 118 | 148 |
| 0.80 | 0.68 | 0.0683 | 0.214 | 0.294 | 0.595 | 1.00 | 5.89 | 2.73 | 1.54 | 1.28 | 1.00 | 47.9 | 91.0 | 115 | 145 |
| 0.90 | 0.67 | 0.0672 | 0.214 | 0.285 | 0.581 | 1.00 | 5.13 | 2.38 | 1.48 | 1.20 | 1.00 | 46.4 | 90.5 | 113 | 136 |
| 1.00 | 0.67 | 0.0653 | 0.204 | 0.284 | 0.636 | 1.00 | 4.62 | 2.15 | 1.40 | 1.16 | 1.00 | 43.3 | 89.3 | 107 | 125 |
| 1.50 | 0.72 | 0.0503 | 0.138 | 0.204 | 0.534 | 1.00 | 4.40 | 2.20 | 1.44 | 1.00 | 1.00 | 33.0 | 56.5 | 68.5 | 84.6 |
| 2.00 | 0.71 | 0.0605 | 0.148 | 0.215 | 0.585 | 1.00 | 3.66 | 1.99 | 1.29 | 0.924 | 1.00 | 24.7 | 36.8 | 44.1 | 46.2 |
| 2.50 | 0.70 | 0.0587 | 0.136 | 0.183 | 0.405 | 1.00 | 3.50 | 1.95 | 1.34 | 0.947 | 1.00 | 21.9 | 32.7 | 35.8 | 33.0 |
| 3.00 | 0.69 | 0.0660 | 0.138 | 0.194 | 0.391 | 1.00 | 3.26 | 1.79 | 1.35 | 0.867 | 1.00 | 18.8 | 26.6 | 28.5 | 26.6 |
| 4.00 | 0.68 | 0.0704 | 0.144 | 0.187 | 0.395 | 1.00 | 2.81 | 1.61 | 1.27 | 0.788 | 1.00 | 15.7 | 20.3 | 24.1 | 19.1 |

* $T$=Period (Seconds), ** $\rho$=Correlation coefficient

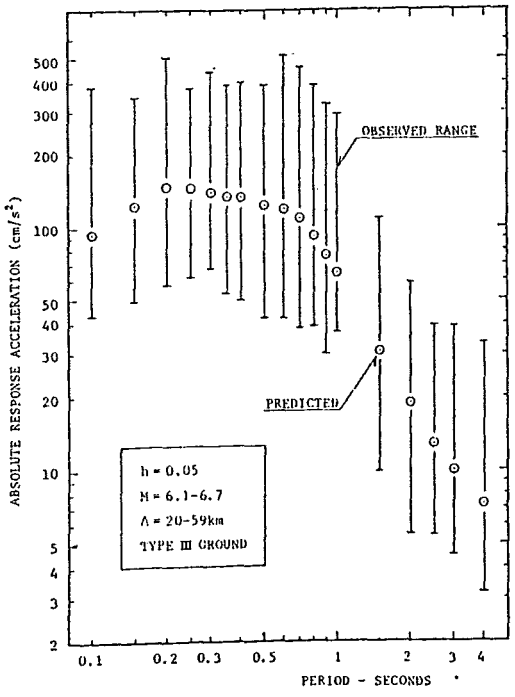


Fig. 2 An example of observed range and predicted value of acceleration spectral amplitude.

By using the results shown in Table 2, the effects of magnitude, distance and site conditions on the acceleration response spectrum were studied in quantitative terms. The effect of earthquake magnitude was found most noticeable in the period range longer than about 0.7 s, in which the increase in spectral amplitude due to the increase in magnitude is more notable than in shorter-period range. The increase in spectral amplitude due to the decrease in epicentral distance is most pronouncedly found in the shorter-period range less than about 0.8 s. The effect of site ground conditions is well demonstrated in the period range between 0.5 s and 2.0 s, in which the spectral amplitude generally increases as the soil becomes softer. These characteristics are in accordance with those qualitatively discussed by a number of previous investigators.

As is seen in the values of correlation coefficients in Table 2, correlation between predicted values $\overline{SA}$ and observed values $SA$ is not very high. This indicates that, although the formula gives a single predicted spectrum for a certain combination of magnitude, distance and ground conditions, observed spectra computed from accelerograms obtained for the same combination of categories exhibit considerable deviations from the predicted spectrum. Figure 2 shows the ranges of observed spectral amplitudes of 32 accelerograms recorded for the combination of $M$=6.1-6.7, $\Delta$=20-59 km and Type III ground together with the predicted spectrum.

In order to examine the degree of uncertainty of the prediction formula, the distribution of the ratios between the observed and the predicted amplitudes was investigated at each of the 18

natural periods of the SDOF system. Let this ratio be denoted by $\alpha$, i.e. $\alpha=SA/\overline{SA}$. There are 277 $\alpha$-values available at each natural period. The distribution of $\alpha$ was found to be not in significant contradiction to the log-normal model at the 5% significance level. Furthermore, the probability density functions of $\alpha$ at the 18 periods were found to be expressed by a single equation for most practical purposes. The predicted spectrum computed by the aforementioned formula corresponds to the spectrum with a probability of being exceeded $p=0.5$. Approximate acceleration response spectra with $p=0.05$, 0.1, 0.2, 0.3 and 0.4 were found to be obtained by multiplying the predicted spectrum by factors of 3.2, 2.4, 1.8, 1.4, and 1.2, respectively.

Although the results shown above seem to find wide application in earthquake engineering problems, care should be taken with respect to the following two points: (1) The data used for analysis are far from sufficient in number nor uniform in distribution. There is a serious shortage of accelerograms of large earthquakes, especially recorded at short epicentral distances. (2) Magnitude and distance categories shown in Table 1 have relatively wide ranges and the classification of ground conditions involves considerable ambiguity.